CONSTRUCTION MATERIALS CONSULTANTS, INC.

Laboratory Investigation Of A Reinforced Concrete Anaerobic Digester In A Wastewater Treatment Plant

Waynesville Wastewater Treatment Plant
Anaerobic Digester Assessment
Waynesville, North Carolina

May 24, 2021
CMC 0321112

TABLE OF CONTENTS

Executive Summary 1
Introduction 5
Background and Field Photographs 5
Purpose 5
Methodologies 12
Petrographic Examinations 12
Analyses of Water-Soluble Anion Contents 13
Scanning Electron Microscopy and X-Ray Microanalyses 14
X-Ray Diffraction 15
X-Ray Fluorescence Spectroscopy 16
Thermal Analyses 17
Samples 18
Petrographic Examinations 28
Lapped Cross Sections 28
Micrographs of Lapped Cross Section 50
Thin Sections 67
Micrographs of Thin Sections 73
SEM-EDS Analyses of Altered Zone in Core 1 88
Coarse Aggregates 89
Fine Aggregates 89
Paste 90
Air 91
X-Ray Diffraction Studies of Altered and Unaltered Zones 92
X-Ray Fluorescence Studies of Altered and Unaltered Zones 93
Water-Soluble Anion Contents 94
Thermal Analyses of Altered and Unaltered Zones 97
Discussions 100
Limited Depths of Alteration of Concrete at the Interior Tank Wall 100
Noticeable Depths of Carbonation of Concrete at the Exterior Tank Wall 100
Sound Interior Concrete of The Tank Wall 100
Future Serviceability of the Tank 101
References 101

EXECUTIVE SUMMARY

The present investigation is for a 60 foot diameter, 27 foot tall reinforced concrete anaerobic digester located at the Waynesville Wastewater Treatment facility reportedly constructed around 1982. The digester roof was removed and contents were mostly drained for plans to operate the digester for a different purpose. It is believed that no protective coatings have been used on the interior surfaces, whereas, the exterior surface was coated. The tank is being evaluated for repairs and possible protective coatings on the interior and exterior of the tank for future use.

The interior wall of the tank showed: (a) a cover (depth of steel) thickness estimated about 1-1/2″ to 2-1/2″ from the surface; (b) vertical lines of segregated coarse aggregates; (c) visible cracking; (d) surface films; (e) variable conditions vertically at the two drops. The exterior of the tank wall showed: (a) visible cracking with efflorescence indicating water migration through the cracks; (b) orange staining at some cracks suggesting corrosion; (c) failing or failed coatings; (d) a few delamination as cracking subparallel to the surface detected from sounding with a hammer at selected areas; and (d) cover (depth of steel) was estimated to be about 1-1/8″ to 2-1/2″ from the interior surface.

Upper area of the tank is: (a) approx. 5 ft. from the top, (b) grey with exposed coarse aggregate from surface deterioration; (c) area with most atmospheric exposure; and (d) relatively harder exposed surface from that already deteriorated (~1/16″ to 1/8″ with nail scratching). Middle area of the tank is: (a) approx. 5 ft. to 17 ft.; (b) primarily orange (upper) /red (lower) in color; (c) waterline reportedly usually at approximately 5-10 ft. below surface; and (d) variably softer surface (~1/8″ to 1/4″ or more with nail scratching). Lower area of the tank is: (a) approx. 20 feet to bottom; (b) tan in color; (c) relatively harder surface (~1/16″ to 1/8″ with nail scratching).

Issues or concerns are: (a) potential materials-related distress, deterioration and contamination, as it may relate to: (a) future performance of the concrete, (b) impact on installation of new coatings, including depth of surface deterioration, depth of chemically or physically altered surfaces, and (c) corrosion of embedded metals.

Purposes of laboratory investigations are to determine: (a) the quality of the surface concrete and concrete within the body of the cores, as it may impact future performance in WWTP and exterior freezing and thawing exposures; (b) any current materials-related distress or the presence of conditions in the concrete that may promote future materials-related distress; and, (c) depth of carbonation and presence of ions at the surface and within the body of cores that may promote corrosion or future distress.

As a result, four concrete cores, identified as C1 through C4 were retrieved at successively higher elevations. The waterline in the WWTP is reportedly between 5 and 10 ft. from the tank top. Core C1, taken at about 15′ depth from the tank top, is from an area that is continuously below the waterline. Core C4, taken at about 3′ from the tank top at the highest elevation of all four cores is from the aerated zone continuously above the waterline. Cores C2 and C3 were taken at about 7 to 11 ft. from the tank top, which are from middle transitional zone of intermittent submersions.

Concrete in the interior surface of tank was subjected to chemicals from the containment solutions as well as air-born gases from moisture to carbon dioxide to other gas residues of the chemicals from containment solutions, whereas the

exterior surface of the tank was primarily exposed to atmospheric carbon dioxide. For the interior wall, concrete at the middle and lower zones were exposed to the intermittent and continuously submerged conditions of the containment solution at and below the waterline, respectively, where the waterline is reportedly between 5 and 10 ft. from the tank top.

Exposed coarse aggregate particles in otherwise gray toned surface are seen at the top aerated portion of the interior surface of the tank wall, whereas orange to brown discoloration is observed in the middle and lower zones where concrete was in contact with the containment solution. Darkest reddish-brown discoloration of the interior surface occurred in the middle zone of interior surface whereas lighter brown discoloration occurred at the lower zone of interior wall concrete. In fact, there is a distinct color zoning of the interior tank wall surface from cement gray at the very top to orange, dark reddish-brown to lighter brown/orange zones of discolored concrete found at the successively deeper levels with relatively sharp contact between the color zones. Such color zoning is the result of interaction of concrete with the chemicals in the containment solution of tank along with differential drying of the chemical-soaked concrete in the aerated portions. The very top cement gray zone is probably not contaminated with the chemicals to bring the distinct discolorations seen in the lower zones even though concrete in the gray zone showed deterioration as leaching and loss of cement paste around coarse aggregate particles to expose long streaks of coarse aggregate particles similar to the situations where a Portland cement concrete is exposed to an acidic solution.

Compared to the concrete-chemical interactions and resultant discolorations, alterations, etc. in the interior wall, the exterior tank surface is relatively sound, with its characteristic cement gray color tone not only from the concrete but also from the thin protective cementitious coating applied, except only a few isolated areas of sheet-like spalling of the protective coats. The exterior surface ends of Cores C1, C3, and C4 showed this protective cementitious coating of less than a millimeter thickness.

Depths of carbonation of concrete are found to be always greater from the exterior surface of the tank than the depths measured from the interior surface. For example, depths of carbonation of cores measured from exterior surface ends varied from 48 mm in Core C1 to 56 mm in Core C2 to only 14 mm in Core C4, whereas corresponding carbonation depths from the interior surfaces are only 5 mm in Core C1, 10 mm in Core C2, and 7 mm in Core C4 which are associated with the zones of chemical alteration of concrete from the interior surfaces.

Cores C1 and C2 taken from the 15 ft. and 11 ft. depths from the tank top, respectively, showed significantly deeper atmospheric carbonation from the exterior surfaces, measured to be 48 mm and 56 mm, respectively, whereas Core C4 from the aerated portion of the tank taken from only 3 ft. depth from the tank top showed only 14 mm deep carbonation from the exterior surface. Therefore, depths of carbonation of concrete at the exterior surface of tank are deeper at the lower and middle zones, but noticeably shallower at the top aerated zone.

Interior tank surfaces show black discoloration of concrete in Cores C1 and C2 taken from 15 ft. and 11 ft. depths from the tank top whereas no such black discoloration, only carbonation in Core C4 taken from the aerated portion of interior wall above the water line.

Along with deep carbonation of concrete from the exterior tank wall surface from the middle and lower zones, Core C2 shows some softening, and short, discontinuous cracking of concrete within the top 56 mm of carbonated zone from the

exterior surface which is judged to be related not only to atmospheric carbonation but distress due to cyclic freezing and thawing at critically saturated conditions. Core C2 was taken from a portion that has intermittent submersion and exposures to moisture which if permeates through the tank wall to the exterior surface end and freezes can develop such near-exterior-surface cracks from cyclic freezing and thawing.

Coarse aggregate particles in all four cores are compositionally similar crushed schist and gneiss having nominal maximum sizes of $^{3}/_{4}$ in. (19 mm). Particles are dense, hard, angular, equidimensional to elongated, well-graded-, and well-distributed across the thickness of the tank wall (i.e., the depths of the cores). A few crushed stone particles show dark weathering rims that are not indicative of any deleterious reactions in the particles but rather innocuous interactions during storage in the aggregate stockpile. Particles show characteristic parallel alignment of quartzo-feldspathic and micaceous minerals defining the schistose and banded (gneissose) textures. There is no evidence of any deleterious reactions of coarse aggregate particles found in the cores even in the interior ends of the tank wall where chemical alterations of paste have occurred to the point of exposing the near-surface aggregate particles.

Fine aggregates are compositionally similar natural siliceous sands of nominal maximum sizes $^{3}/_{8}$ in. (9.5 mm) consisting of major amounts of quartz and quartzite and subordinate amounts of granite, feldspar, and other siliceous rocks. Fine aggregate particles are angular (due to some light crushing) to subangular to subrounded, dense, hard, equidimensional to elongated, unaltered, uncoated, and uncracked. There is no evidence of alkali-aggregate reactions or any other potentially deleterious reactions except a few brown opaline chert particles that have shown internal microcracking.

Paste is compositionally similar moderately dense, and moderately hard in the interior bodies except visible discoloration and alteration at the interior surface ends to depths of less than 5 mm to 10 mm consisting of a black altered zone at the exposed interior wall surface followed by a mixed oxidized (stained) and carbonated brown discolored zone and a gray discolored zone followed by a carbonated zone. Paste at the exterior surface ends of the cores show deep carbonation due to interaction with atmospheric carbon dioxide, which are measured to be 48 mm in Core C1 to 56 mm in Core C2 to only 14 mm in Core C4, whereas corresponding carbonation depths from the interior surfaces are only 5 mm in Core C1, 10 mm in Core C2, and 7 mm in Core C4. Freshly fractured surfaces have subvitreous lusters and subconchoidal textures. Residual and relict Portland cement particles are present and estimated to constitute 10 to 12 percent of the paste volumes in the interior bodies. Distributed throughout the paste are a few fine, spherical, clear, dark brown to black glassy particles of fly ash having the fineness of Portland cement. Hydration of Portland cement is normal. Lining the walls of some entrapped air voids especially towards the interior surface ends are secondary ettringite deposits that are indicative of the prolonged presence of moisture in the concrete during service due to penetration of containment solutions from the interior tank wall. The textural and compositional features of pastes are indicative of cementitious materials contents estimated to be equivalent to 6 to $6^{1}/_{2}$ bags of Portland cement per cubic yard of which 10 to 15 percent is estimated to be fly ash and water-cementitious materials ratios similar to all four cores and estimated to be 0.45 to 0.50.

Concrete in all four cores are non-air-entrained having air contents estimated to be 1 to 2 percent.

In summary, the interior tank wall surface in the four cores show clear evidence of alterations due to interactions with tank's containment solutions. Such interactions have created discoloration, softening of paste, sometimes microcracking,

carbonation, leaching, oxidation (staining), etc., which are often present as bands of discolored altered pastes from black paste at the interior wall surface to reddish-brown oxidized and carbonated zone to gray and beige carbonated zone. Interfaces between the zones and between the altered and interior unaltered zones are sharp. Depths of alteration of such zones, however, are shallow in all four cores, measured to be: (a) 5 to 7 mm in Core C1 occurring as a dark gray to black altered layer sometimes with an inner brown layer at the interior wall; (b) 7 to 8 mm in Core C2 again occurring as a black to dark gray altered layer in the interior wall often with thin brown layer at the interior wall; and (c) 7 mm from interior wall of Core C4 where instead of a black altered layer mostly beige to brown carbonated layer is seen. Evidence of interaction of containment solution with the altered zones in the interior tank wall is also reflected in chemical analyses where altered zones showed enrichment in sulfate both in XRF studies and in ion chromatography of water-soluble sulfates from the altered zones. Concrete beyond these 10 mm of the altered interior surfaces of tank wall in Cores C1, C2, and C4 are sound and present in good conditions without any alteration.

By contrast the exterior tank wall surface represented in Cores C1, C2, and C4 show noticeable depths of carbonation, despite the presence of a thin (< 1 mm thickness) protective cementitious coating, indicating prolonged interaction of the tank's exterior wall with the atmospheric carbon dioxide prior to the installation of the protective cementitious coat. Paste at the exterior surface ends of the cores show deep carbonation due to interaction with atmospheric carbon dioxide, which are measured to be 48 mm in Core C1 to 56 mm in Core C2 to only 14 mm in Core C4, whereas corresponding carbonation depths from the interior surfaces are only 5 mm in Core C1, 10 mm in Core C2, and 7 mm in Core C4.

Sandwiched between the 10 mm altered interior tank wall and almost 56 mm carbonated exterior tank wall, the interior bodies of concrete in Cores C1, C2, and C4 are all present in sound and serviceable condition. Lack of air entrainment can cause some freezing-related issues, which is, however, absent probably due to the vertical orientation of the structure preventing any moisture saturation during freezing. Evidence of secondary ettringite deposits in air voids, however, indicate prolonged presence of moisture in the concrete from penetration of containment solutions of tanks, which has not introduced any freezing-related deterioration of the non-air-entrained concrete in the tank wall.

Based on detailed petrographic examinations, determination of shallow depths of alterations of concrete from the interior tank wall especially for cores drilled from deeper locations, which were in contact with the containment solutions, relatively sound conditions of concrete towards the exterior wall surface even in the carbonated exteriors, sound conditions of unaltered interior concrete, the tank wall is judged to be serviceable for its future intended purpose. Perhaps removal of the altered, discolored portions of interior wall with a fresh new repair coat will extend its life. The exterior cementitious coating is only 1 mm in thickness, with some peeling at some locations in the field photos, but is important to mitigate future access of atmospheric carbonation especially since the concrete showed extensive carbonation from the exterior wall end, which has occurred prior to the placement of the protective coating. Deep carbonation from the exterior end can cause carbonation-induced corrosion of steel in concrete, where the importance of having such a protective coating as seen and its well adherence to the concrete wall are paramount. Except for discolorations, aggregate exposure at the higher elevation, banded discolored interior surface, etc. as seen in the field photos, the determined inherent well-consolidated nature of concrete in the tank wall has prevented deeper migration of potentially deleterious chemicals from the containment solution along the interior wall.

INTRODUCTION

Reported herein are the results of detailed laboratory studies of a reinforced concrete anaerobic digester at the Waynesville Wastewater Treatment facility located in Waynesville, North Carolina.

BACKGROUND AND FIELD PHOTOGRAPHS

The 60 foot diameter, 27 foot tall reinforced concrete anaerobic digester (Figure 1) at the Waynesville Wastewater Treatment facility was reportedly constructed around 1982. The digester roof was recently removed and contents were mostly drained. There are plans to operate the digester in an alternative mode. It is believed that no protective coatings have been used on the interior surfaces in the past. The exterior, however, is coated. The tank is being evaluated for repairs and possible protective coatings on the interior and exterior of the tank for future use.

The interior wall of the tank showed (Figures 2 and 3): (a) a cover (depth of steel) thickness estimated about 1-1/2" to 2-1/2" from the surface; (b) vertical lines of segregated coarse aggregates; (c) visible cracking; (d) surface films; (e) variable conditions vertically at the two drops. The exterior of the tank wall showed (Figures 4 and 5): (a) visible cracking with efflorescence indicating water migration through the cracks; (b) orange staining at some cracks suggesting corrosion; (c) failing or failed coatings; (d) a few delamination as cracking subparallel to the surface detected from sounding with a hammer at selected areas; and (d) cover (depth of steel) was estimated to be about 1-1/8" to 2-1/2" from the interior surface.

Upper area of the tank is: (a) approx. 5 ft. from the top, (b) grey with exposed coarse aggregate from surface deterioration; (c) area with most atmospheric exposure; and (d) relatively harder exposed surface that already deteriorated (~1/16" to 1/8" with nail scratching). Middle area of the tank is: (a) approx. 5 ft. to 17 ft.; (b) primarily orange (upper) /red (lower) in color; (c) waterline reportedly usually at approximately 5-10 ft. below surface; and (d) variably softer surface (~1/8" to 1/4" or more with nail scratching). Lower area of the tank is: (a) approx. 20 feet to bottom; (b) tan in color; (c) relatively harder surface (~1/16" to 1/8" with nail scratching).

Issues or concerns are: (a) potential materials-related distress, deterioration and contamination, as it may relate to: (a) future performance of the concrete, (b) impact on installation of new coatings, including depth of surface deterioration, depth of chemically or physically altered surfaces, and (c) corrosion of embedded metals.

PURPOSE

Based on the above background information provided, purposes of laboratory investigations are to determine: (a) the quality of the surface concrete and concrete within the body of the cores, as it may impact future performance in WWTP and exterior freezing and thawing exposures; (b) any current materials-related distress or the presence of conditions in the concrete that may promote future materials-related distress; and, (c) depth of carbonation and presence of ions at the surface and within the body of cores that may promote corrosion or future distress.

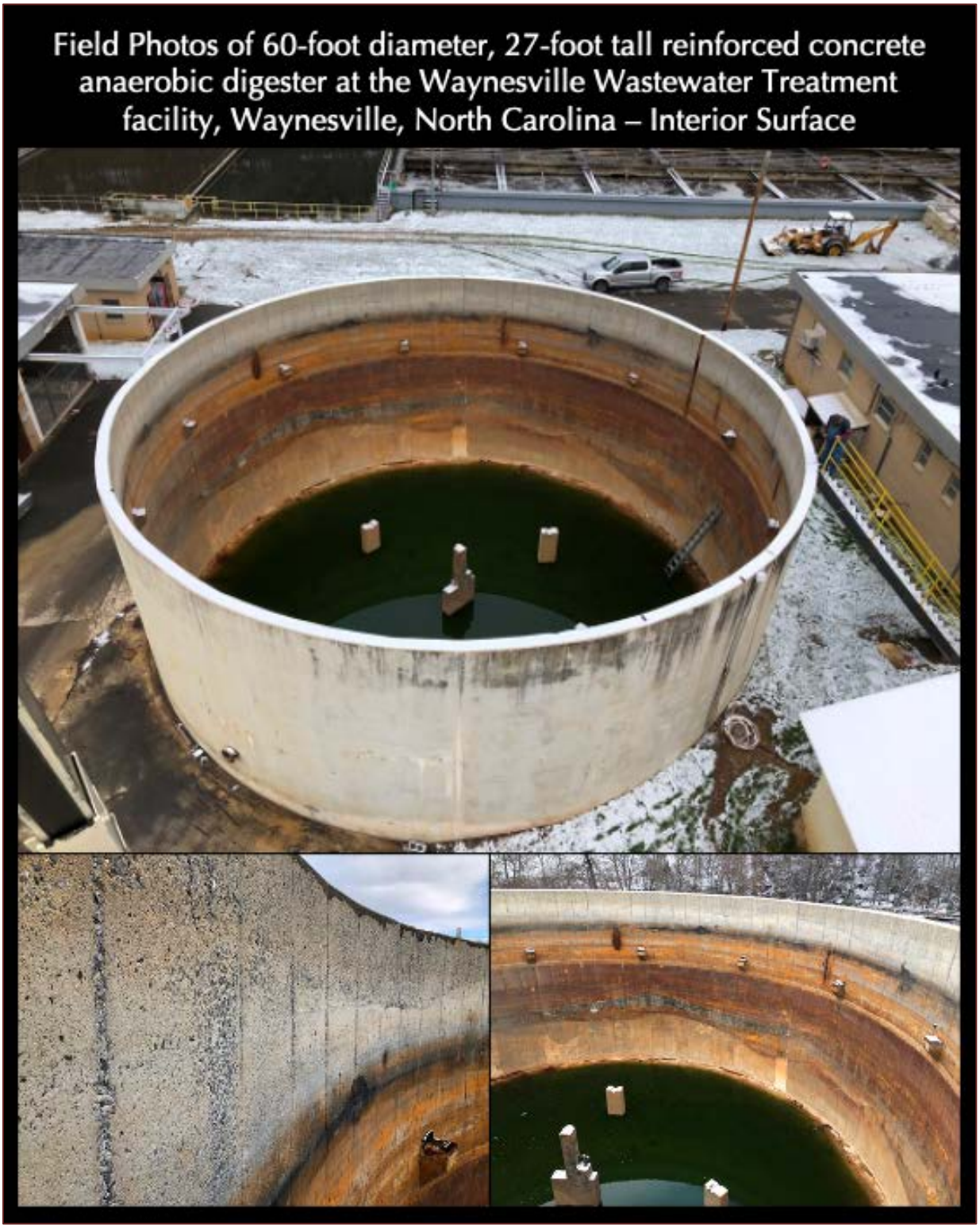

Figure 1: Field photo of the reinforced concrete digester at the Waynesville Wastewater Treatment facility where the interior surface of tank wall shows a cement gray toned surface at the very top with deteriorated exposed aggregate surface followed by various layers of discolored concrete surface and dark green colored containment solution at the bottom of tank.

Figure 2: Field photos of the interior surface of the digester wall showing loss of paste around aggregate particles at the cement gray toned very top portion of the wall with occasional cracks and parallel joints followed by layers of discolored concrete surface where other than discoloration the surface does not show any aggregate exposure as seen at the very top gray zone.

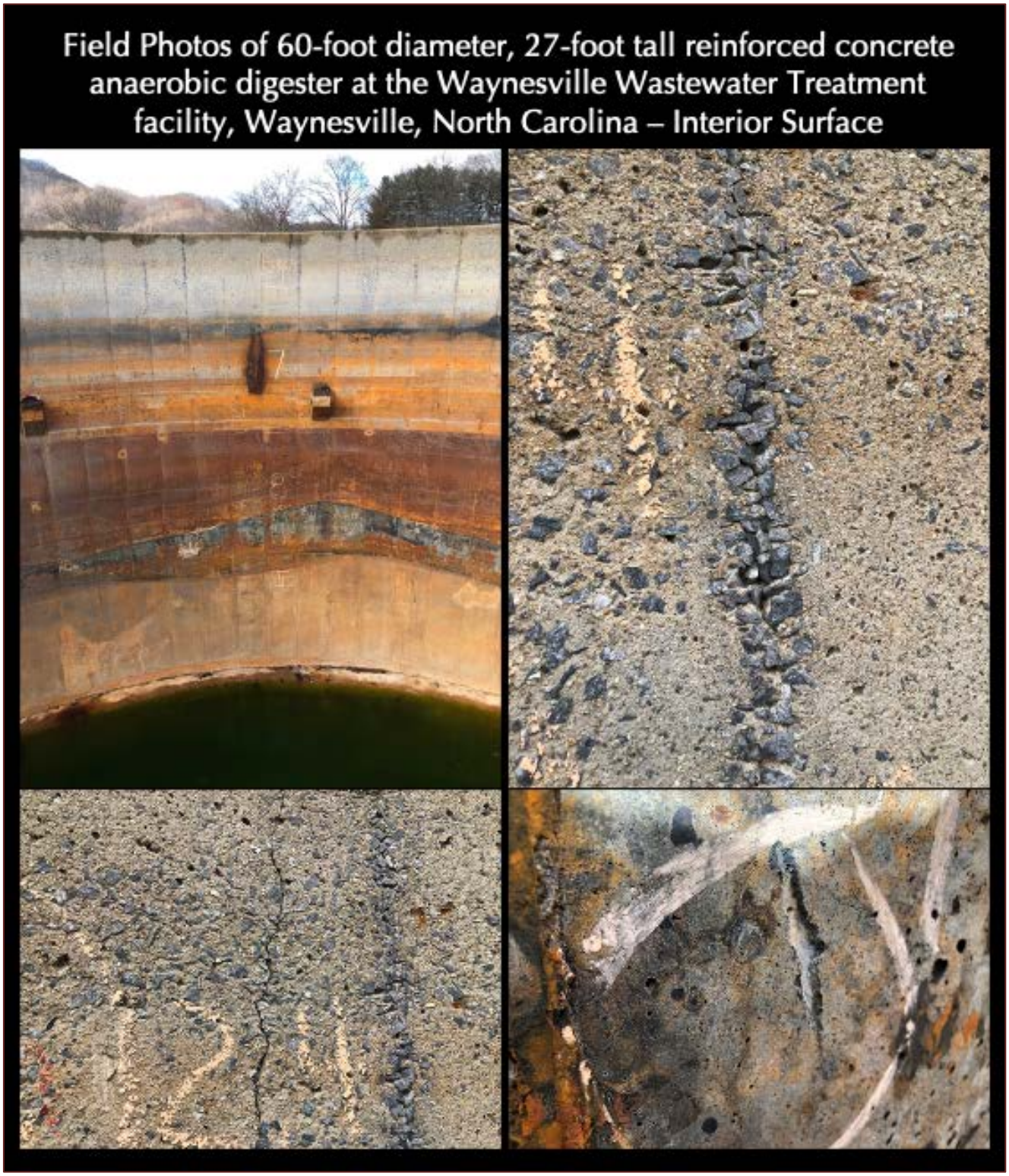

Figure 3: Interior digester wall surface showing layer-by-layer discoloration of the interior surface starting from cement gray very top zone where aggregate particles are exposed due to differential dissolution of paste relative to aggregates, which is followed by a narrow dark gray to black zone, an orange light brown zone, a dark reddish-brown rust-colored zone, and finally a lighter brown zone at the bottom before the containment solution.

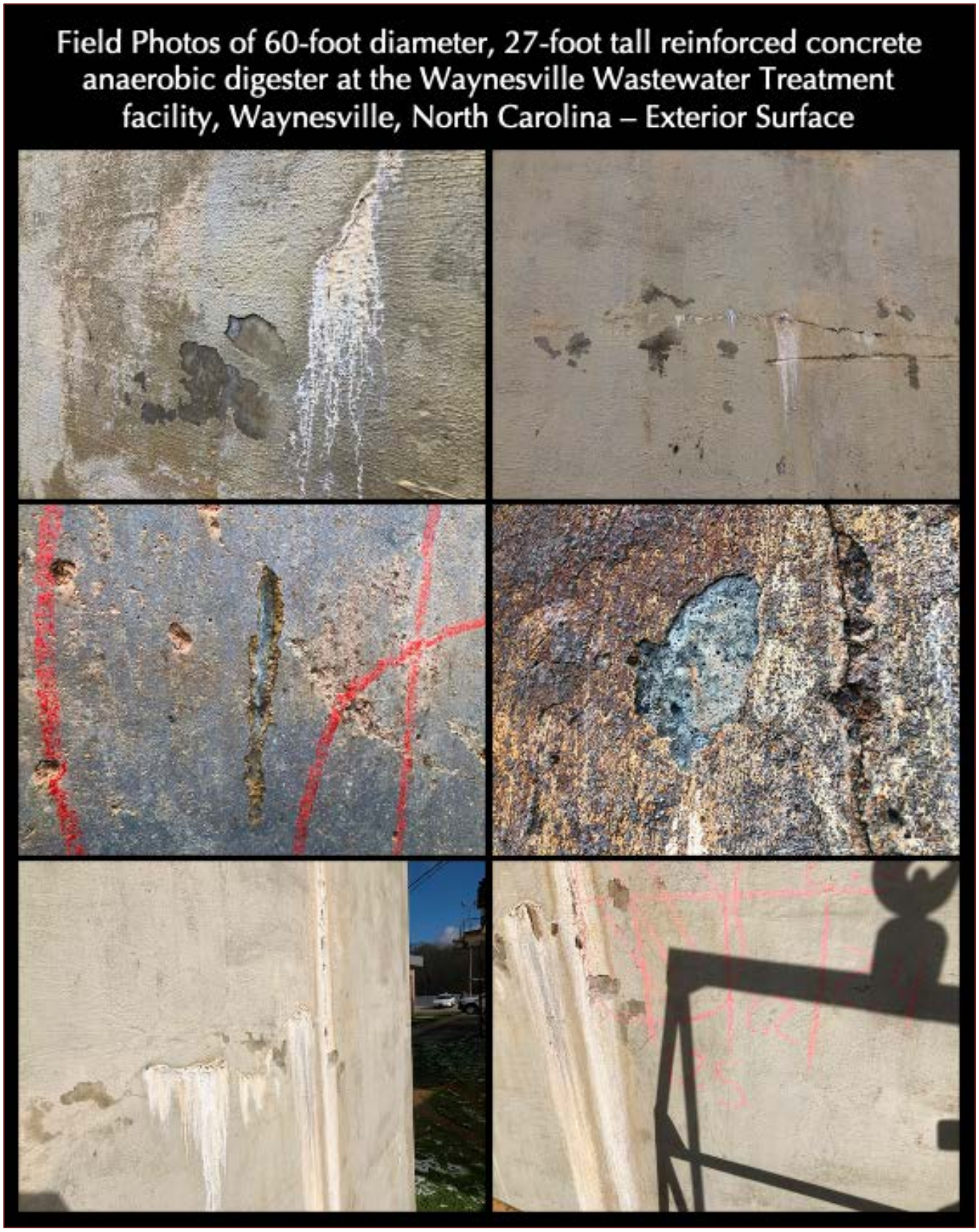

Figure 4: The exterior digester wall surface showing a thin cementitious protective coat, which in the cores received is measured to be less than 1 mm in thickness. A few areas show spalling of the coating.

Figure 5: A few localized areas showing spalling of the cementitious protective coating applied on the exterior surface of the digester.

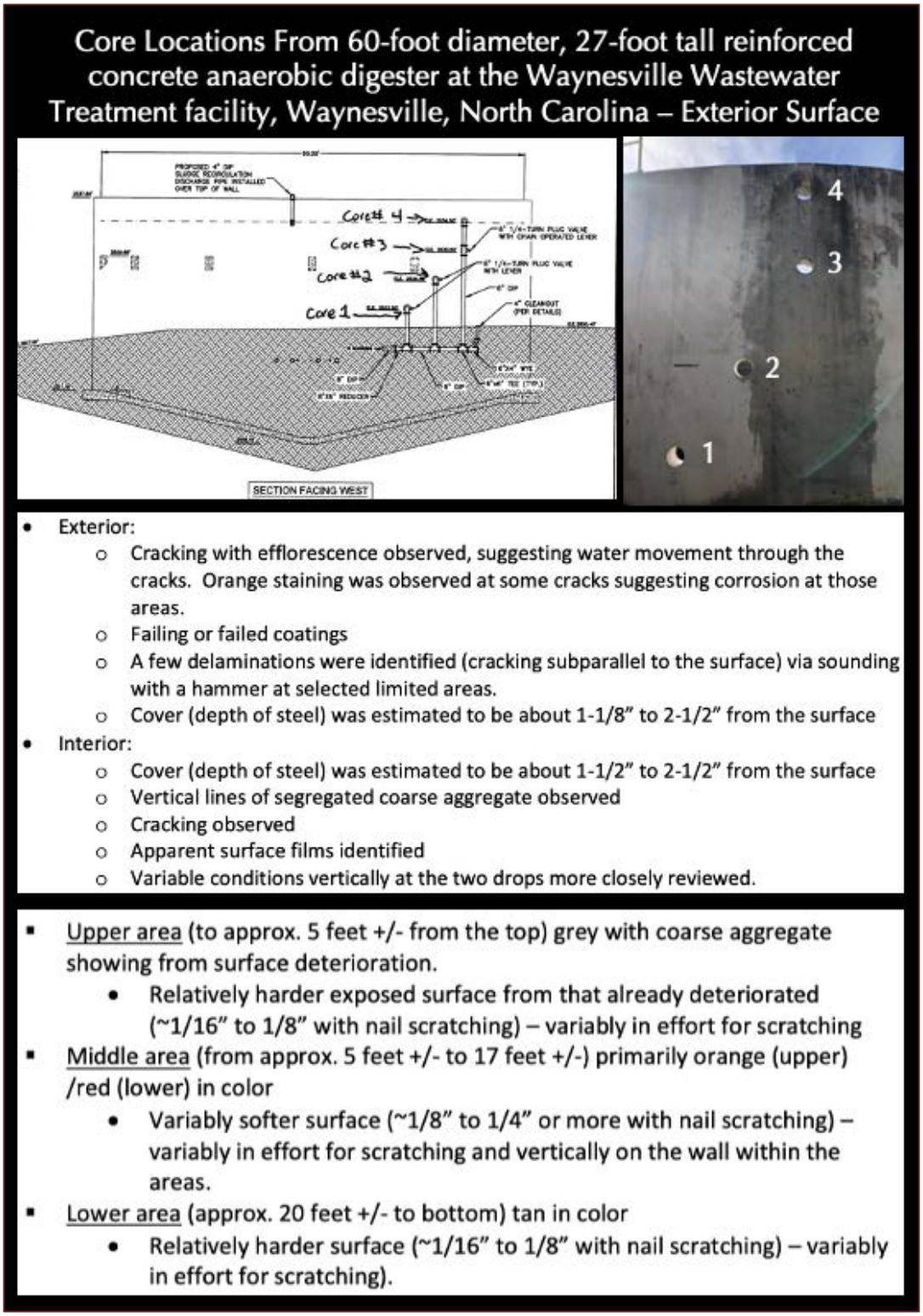

Figure 6: Locations of four cores collected from four levels of the tank starting with C1 from the very bottom and C4 at the very top. Shown are features observed during field investigation of the interior and exterior surfaces of digester.

METHODOLOGIES

PETROGRAPHIC EXAMINATIONS

The cores were examined using the methods and procedures of ASTM C 856 "Standard Practice for Petrographic Examination of Hardened Concrete." Details of concrete petrography, and sample preparation techniques for petrographic examinations of concrete are provided in Jana (2006).

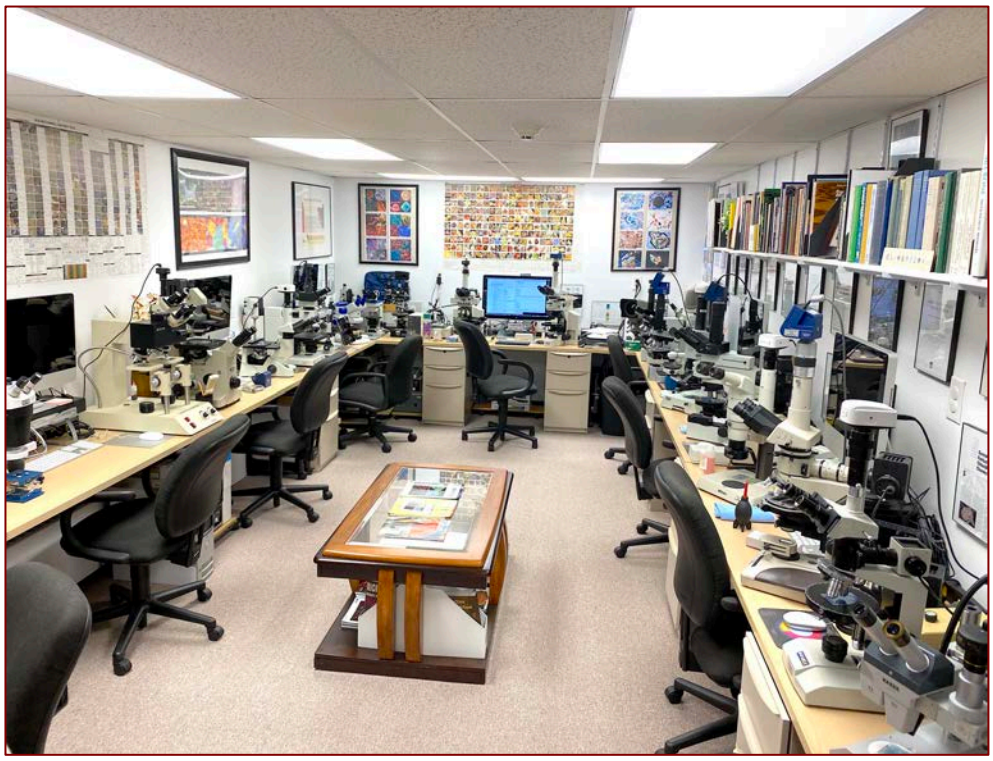

Figure 7: Some of the optical microscopes in the optical microscopy laboratory that were used for this investigation, e.g., from low-power stereo microscope, to high-power transmitted-light stereo-zoom microscope with plane and crossed-polarized light, to epi-fluorescent microscope for observations of florescent dye-mixed epoxy impregnated thin sections and petrographic microscopes for further observations of thin sections of concretes.

Briefly, the steps followed during petrographic examination of samples include:

i. Visual examinations of the concretes, as received, including adequate documentation of dimensions, measurements, condition, physical properties, integrity, etc.;
ii. Low-power stereo microscopical examinations of as-received, saw-cut and freshly fractured sections, and lapped cross sections of samples for evaluation of texture, air-void systems, and compositions;
iii. Examinations of oil immersion mounts in a petrographic microscope for mineralogical compositions of specific areas of interests;
iv. Examinations of fluorescent dye-mixed (to highlight open spaces, cracks, etc.) low-viscosity epoxy-impregnated large area (50 mm × 75 mm) thin sections of concretes in a petrographic microscope for detailed compositional and microstructural analyses;
v. Photographing the samples, as received and at various stages of preparation with a digital camera and a flatbed scanner; and,
vi. Photomicrographs of lapped sections and thin sections of concretes taken with stereomicroscope and petrographic microscope, respectively to provide detailed compositional and mineralogical information of concretes.

ANALYSES OF WATER-SOLUBLE ANION CONTENTS

Water-Soluble anion (e.g., chloride, sulfate) contents of interior surfaces and 80 mm inside from the interior ends of Cores C1 and C2 were determined by ion chromatography according to the procedures of ASTM D 4327. Analyses were done on the pulverized portions of saw-cut sections taken from the altered interior ends, and from 80 mm inside.

The sample preparation steps were similar to that of water-soluble chloride contents in concrete according to the methods of ASTM C 1218: "Standard Test Method for Water-Soluble Chloride in Mortar and Concrete."

Steps followed in water-soluble anion contents by ion chromatography are as follows:

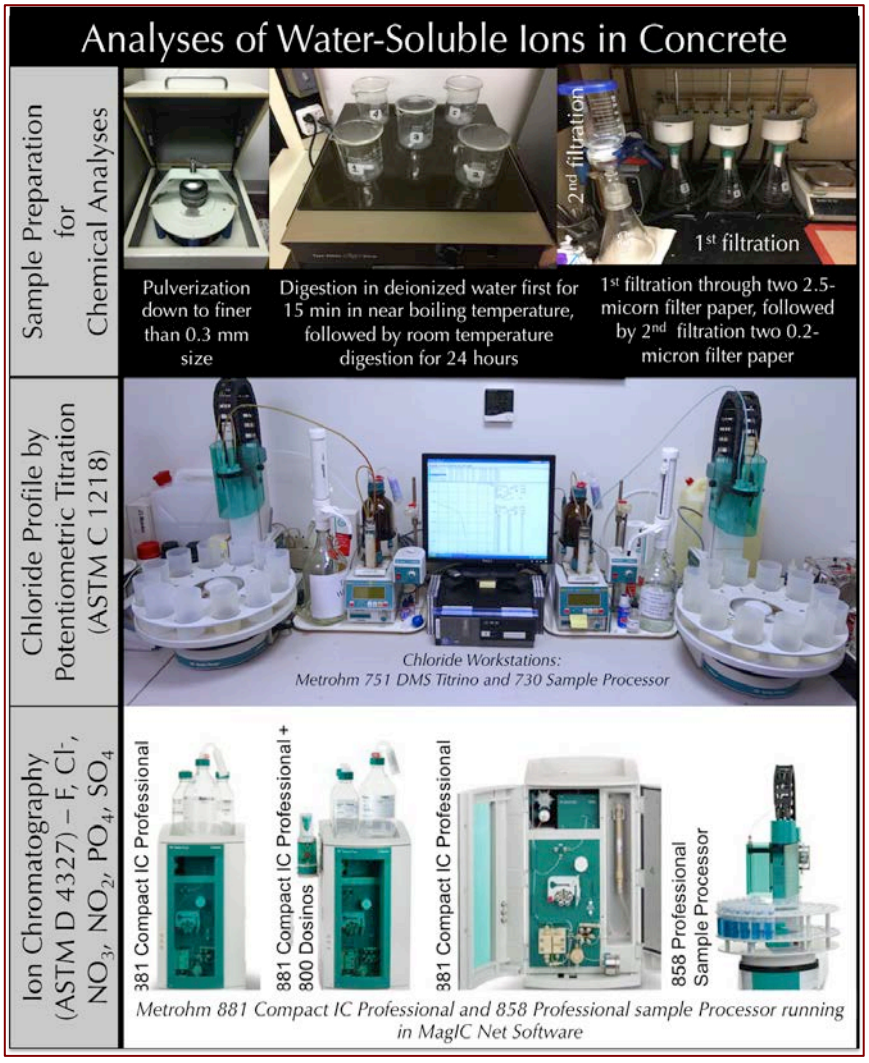

Figure 8: Sample preparation and analyses of water-soluble ions of by ion chromatography.

- Sample Selection and Sectioning – A representative portion of each core from the desired depth was sectioned and pulverized to fine powder passing US No. 50 sieve.
- Water Digestion – About 10±0.01 gm. of powder sample was measured and dispersed with 100-mL deionized water in a 250-mL beaker, stirring and breaking up any lumps with a glass rod.
- Further Digestion in Boiling Water – Covered the beaker from previous step with a watch glass, and heated rapidly to boiling, but not more than 10 minutes. Removed from hot plate.
- Filtration – Filtered the sample solution, under suction, through two 2.5 micron filter papers fitted to a Buchner funnel in a 500-mL filtration flask. Transferred the filtrate from the flask to the original beaker, which was already rinsed twice with water, along with the flask. Cooled the filtrate to room temperature. The final volume was 200-mL.
- Filtrates of water-digested samples were used for determination of various anions by ion chromatography (IC) by following the methods of ASTM D 4327 for anion chromatography, *a la* ASTM D 4327 for water-soluble fluoride, chloride, nitrate, nitrite, bromide, phosphate, and sulfate ions by using Metrohm 881 Compact IC Professional with attached 858 Professional Sample Processor with a sodium carbonate-bicarbonate eluent.
- In IC, ppm-chloride is converted to weight percent by weight% Cl = [(ppm-Cl from IC × Filtrate Volume 200 ml × Dilution Factor) / (Sample weight, 10 grams × 10,000)].

SCANNING ELECTRON MICROSCOPY AND X-RAY MICROANALYSES

Figure 9: CamScan Series 2 scanning electron microscope used for examination of alteration of interior surface of tank wall.

After optical microcopy, thin section examination was further carried out in a scanning electron microscope (Figure 9) for examination of alteration of interior surface of tank wall in one core. The microscope is equipped with a high-resolution column 40Å tungsten, 40 kV electron optics zoom condenser 75° focusing lens operating at 20 kV, equipped with a variable geometry secondary electron detector, backscatter electron detector, EDS detector for observations of microstructures at high-resolution, compositional analysis, and quantitative determinations of major element oxides from various areas of interest, respectively. Revolution 4Pi software is used for digital storage of secondary electron and backscatter electron images, elemental mapping, and analysis along a line, a point or an area of interest. A 50 mm × 75 mm thin section of the sample was polished, coated with a gold-palladium alloy, and used with a custom-made aluminum sample holder in the large multiported chamber with the eucentric 50 × 100 mm motorized stage.

X-RAY DIFFRACTION

Mineralogical compositions of altered interior surface end and 80 mm inside from the interior end of Core C2 were determined by X-ray diffraction (XRD) studies. Sectioned samples were pulverized to finer than 44-micron (US 325 sieve) particle size. The purpose of this study is to detect changes in mineralogical compositions of concrete due to alterations with containment solutions along the interior surface of tank wall.

X-ray diffraction was carried out in a Bruker D2 Phaser (2nd Generation, Figure 10) benchtop Powder diffractometer (Bragg-Brentano geometry) employing a Cu X-ray tube (Cu k-alpha radiation of 1.54 angstroms), a primary slit of 1 mm, a receiving slit of 3 mm, a position sensitive 1D Lynxeye XE-T detector. Generator settings used are 30 kV and 10mA (300 watt). Sample was placed in a zero background sample holder which is an optically polished 111 plane of silicon wafer attached to a stainless steel sample holder for use in the 6-position sample stage of D2 Phaser. Tests were scanned at 2θ from 8° to 64° with a step of 0.05° 2θ integrated at 0.05 sec. step^{-1} dwell time.

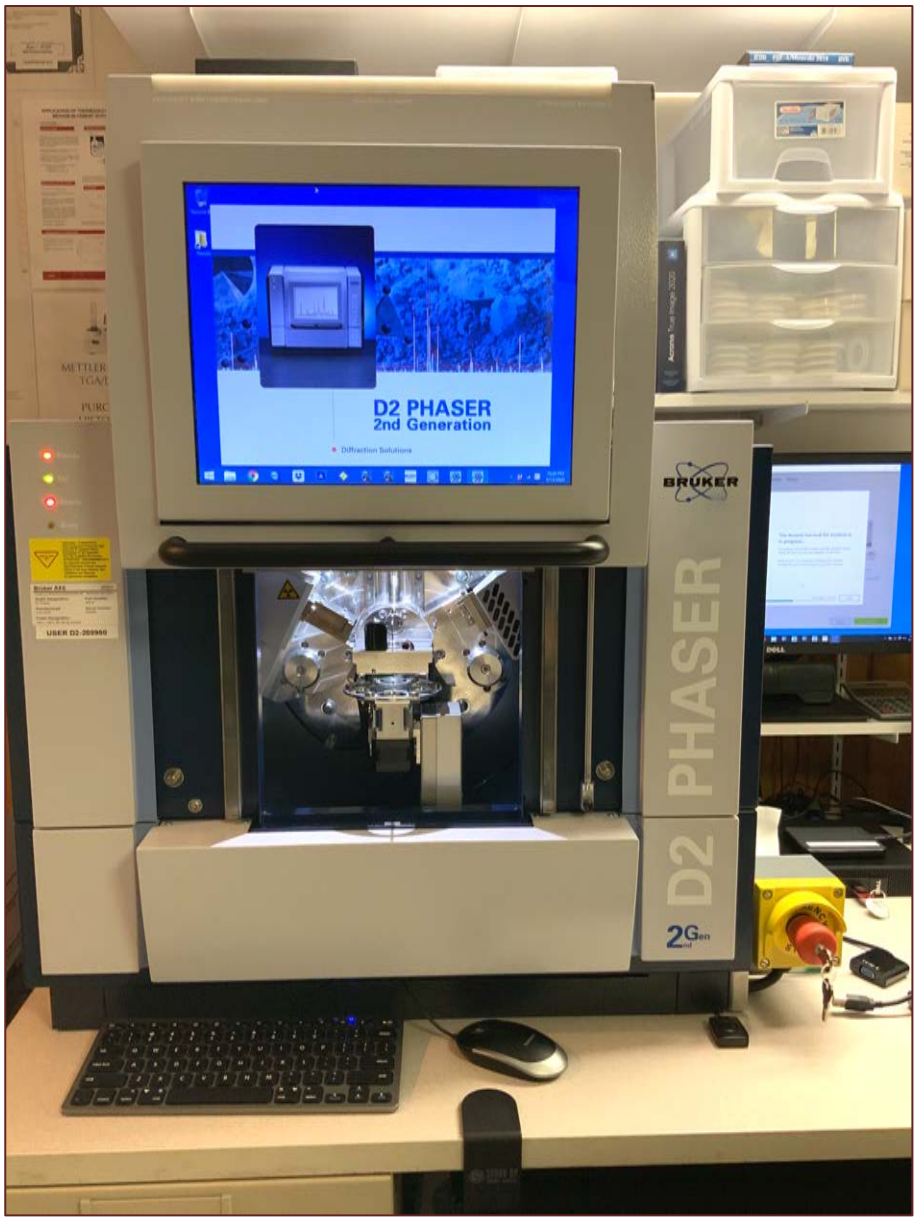

Figure 10: Bruker's D2 Phaser (2nd generation) benchtop X-ray powder diffractometer with Lynxeye 1D position sensitive detector used in X-ray diffraction studies of samples.

The resulting diffraction patterns were collected by Bruker's Diffrac.Measurement software. Phase identification was done with Bruker's Diffrac.EVA software with the search-match database from Crystallographic Open Database (COD).

X-RAY FLUORESCENCE SPECTROSCOPY

Major elemental oxide compositions of altered interior surface and 80 mm inside from the interior end of Core C2 were determined by X-ray fluorescence (XRF) studies. Sectioned samples were pulverized to finer than 44-micron (US 325 sieve) particle size. The purpose of this study is to detect changes in chemical compositions of concrete due to alterations with containment solutions along the interior surface of tank wall.

Figure 11: Rigaku NEX-CG in CMC, which can perform analyses of 9 pressed pellet or fused bead of sample. Samples are prepared either as pressed pellet (usually the one already prepared for XRD) or can also accommodate fused bead with proper calibration of standard beads.

A series of standards from Portland cements, lime, gypsum to various rocks, and masonry mortars of certified compositions (e.g., from USGS, GSA, NIST, CCRL, Brammer, or measured by ICP) are used to calibrate the instrument for various oxides and empirical calculations are done from such calibrations to determine oxide compositions of concrete.

An energy-dispersive bench-top X-ray fluorescence unit from Rigaku Americas Corporation (NEX-CG) was used (Figure 11). Rigaku NEX CG delivers rapid qualitative and quantitative determination of major and minor atomic elements in a wide variety of sample types with minimal standards. Unlike conventional EDXRF analyzers, the NEX CG was engineered with a unique close-coupled Cartesian Geometry (CG) optical kernel that dramatically increases signal-to-noise. By using monochromatic secondary target excitation, instead of conventional direct excitation, sensitivity is further improved. The resulting dramatic reduction in background noise, and simultaneous increase in element peaks, result in a spectrometer capable of routine trace element analysis even in difficult sample types. The instrument is calibrated by using various certified (CCRL, NIST, GSA, and Brammer) reference standards of cements and rocks.

THERMAL ANALYSES

Thermal analyses encompass: (1) thermogravimetric analysis (TGA), which measures the weight loss during heating related to decomposition of a phase of interest at a specific temperature that is characteristic of the phase from which both the phase composition and the abundance can be determined; (2) differential thermal analysis (DTA, or first derivative of TGA i.e. DTG) measuring temperature difference between the sample and an inert standard (Al_2O_3) both are heated at the same rate and time where endothermic peaks are recorded when the standard continues to increase in temperature during heating but the sample does not due to decompositions (e.g., dehydration of hydrous or decarbonation of carbonate phases); the endothermic or exothermic transitions are characteristic of particular phase, which can be identified and quantified using DTA (or DTG); and (3) differential scanning calorimetry (DSC), which follows the same basic principle as DTA, whereas temperature differences are measured in DTA, during heating using DSC energy is added to maintain the same and the reference material (Al_2O_3) at the same temperature; this energy use is recorded and used as a measure of the calorific value of the thermal transitions that the sample experiences; this is particularly useful for detection of quartz that undergoes polymorphic (α to β form) transitions and no weight loss.

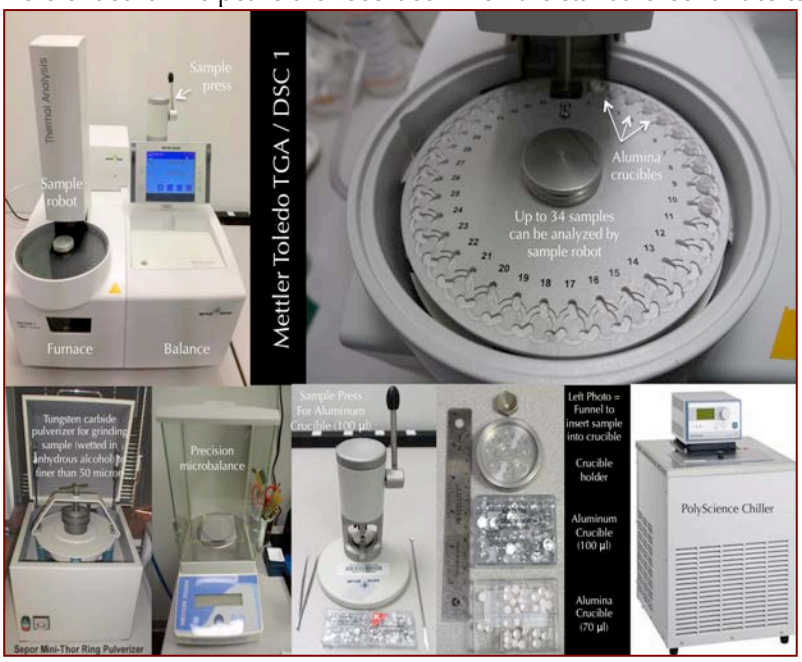

Figure 12: Mettler-Toledo simultaneous TGA/DSC1 unit in CMC that can accommodate 32 samples. The top left photo shows the TGA/DSC1 unit with sample robot for automation as well as the sample holder for pressing aluminum sample holders. Sample is pulverized in a ring pulverizer shown in the bottom left, then a small amount (usually 30-70 mg) is weighed in a precision balance (shown 2nd from left in bottom row) and taken in an alumina sample holder (without lid). For DSC measurements up to 600°C, sometimes sample is taken in an aluminum holder and pressed in sample press (3rd from left in bottom row) and pierced with a needle for release of volatiles from decomposition. A PolyScience chiller (rightmost one in the bottom row) is used to cool the furnace. An ultrapure nitrogen gas is purged through the system during analyses.

Simultaneous TGA and DSC analyses are done in a Mettler Toledo TGA/DSC 1 unit (Figure 12) on 30-70 mg of finely ground (<0.6 mm) sample in alumina crucible (70 µl, no lid) from 30°C to 1100°C at a heating rate of 10°C/min with high purity nitrogen as purge gas at a flow rate of 75.0 ml/min.

Thermal analyses were done on the altered interior surfaces and 80 mm inside from the interior ends of Cores C1 and C2. The purpose of this study is to determine the variations in phase compositions of altered and sound unaltered interior concrete from variations in decompositions of various hydrous, sulfate, and carbonate phases.

SAMPLES

Preliminary descriptions of four concrete cores, Cores C1 through C4 drilled from four different depths of tank wall, as received, are listed in the following Table 1 and in subsequent Figures 13 through 21 (Figures show first the original 9½ in. diameter cores and subsequently of smaller diameter (4 in.) ones drilled out from the original cores for better handling during sample preparation steps.

Core ID & Depth	Diameter	Length	Interior Surface	Exterior Surface	Cracking	Reinforcing Steel	Core Condition
C1 (~15 ft. from tank top) continuously submersed	9½ in. (240 mm)	11¾ in. (296 mm)	Weathered, altered reddish-brown (Figure 13)	Cementitious coat on concrete, fine hairline cracks, fine broom-finished (Figure 15)	Visible crack extending from the exterior surface to 6 in.	No. 5 reinforcing steel at 1¾ in., 2½ in., 8¾ in., and 9¼ in. depths from interior surface end	Intact, Dry, Ring
C2 (~11 ft. from tank top) at the waterline transition zone	9½ in. (240 mm)	11¾ in. (296 mm)	Weathered, altered reddish-brown (Figure 13)	Cementitious coat on concrete, fine broom-finished (Figure 15)	Visible crack extending from the exterior surface to 5 in.	No. 2 reinforcing steel at 2½ in. and No. 5 at 3 in. and 9 in., wire mesh at 4 in. and 9¼ in. depths from interior surface end	Intact, Dry, Ring
C3 (~7 ft. from tank top) at the waterline transition zone	9½ in. (240 mm)	11¾ in. (296 mm)	Weathered, rough, altered reddish-brown (Figure 13)	Cementitious coat on concrete; fine crack at joint, fine broom-finished (Figure 15)	Construction joint to a depth of ¾ in.; gray plastic at 5½ in. depth	No. 5 reinforcing steel at 2 in., 2½ in., 7½ in., 7¾ in., and 9 in. depths and wire mesh at 6⅛ in. depth from interior surface end	Intact, Dry, Ring
C4 (~3 ft. from tank top) at the aerated zone above the waterline	9½ in. (240 mm)	11¾ in. (296 mm)	Weathered, gray, coarse aggregate exposures (Figure 13)	Cementitious coat on concrete, fine broom-finished (Figure 15)	Construction joint to a depth of ¾ in.; gray plastic at 5½ in. depth	No. 5 reinforcing steel at 2½ in., 2⅞ in., 7½ in., 8 in., and 8¾ in. and wire mesh at 2½ in. depths from interior surface end	Intact, Dry, Ring

Table 1: Detailed preliminary descriptions and dimensions of four cores, as received from four depths of tank wall. The waterline is reportedly between 5 and 10 ft. from the tank top. Core C1 (15′ from tank top) is from an area that is continuously below the waterline, and Core C4 (3′ from tank top) is from the aerated zone continuously above the waterline; Cores C2 and C3 (7 to 11 ft. from tank top) are from middle transitional zone of intermittent submersions.

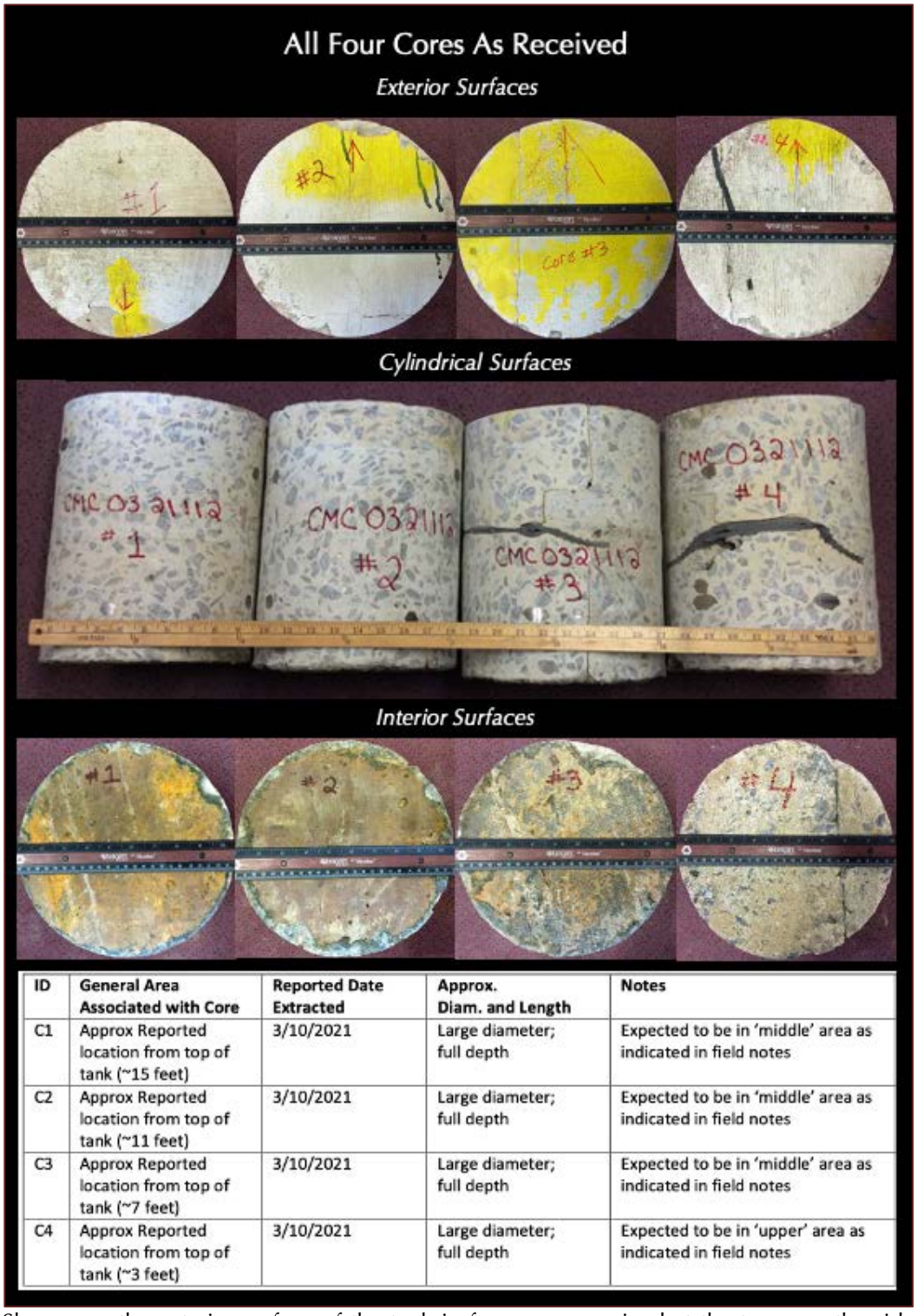

ID	General Area Associated with Core	Reported Date Extracted	Approx. Diam. and Length	Notes
C1	Approx Reported location from top of tank (~15 feet)	3/10/2021	Large diameter; full depth	Expected to be in 'middle' area as indicated in field notes
C2	Approx Reported location from top of tank (~11 feet)	3/10/2021	Large diameter; full depth	Expected to be in 'middle' area as indicated in field notes
C3	Approx Reported location from top of tank (~7 feet)	3/10/2021	Large diameter; full depth	Expected to be in 'middle' area as indicated in field notes
C4	Approx Reported location from top of tank (~3 feet)	3/10/2021	Large diameter; full depth	Expected to be in 'upper' area as indicated in field notes

Figure 13: Shown are the exterior surface of the tank in four cores received at the top row, the side cylindrical surfaces of cores in the 2nd row from top, the weathered discolored brown interior surface of tank wall in the four cores in the 3rd row from top, and locations and depths of retrieval of four cores in the table in the bottom row. Core C1 was taken from the lowest level which was probably continuously submerged in containment solution during operations whereas Core C4 was taken from the uppermost level probably from the aerated zone where concrete surface was not in direct contact with the containment solution, but the surface shows exposures of coarse aggregate particles relative to paste. Cores C2 and C3 were taken from intermediate zones where surface may have been in contact with the solution to cause discoloration.

Figure 14: Shown are the exterior surface of tank wall in four cores received where some edge spalling of the protective cementitious coat is seen in some cores.

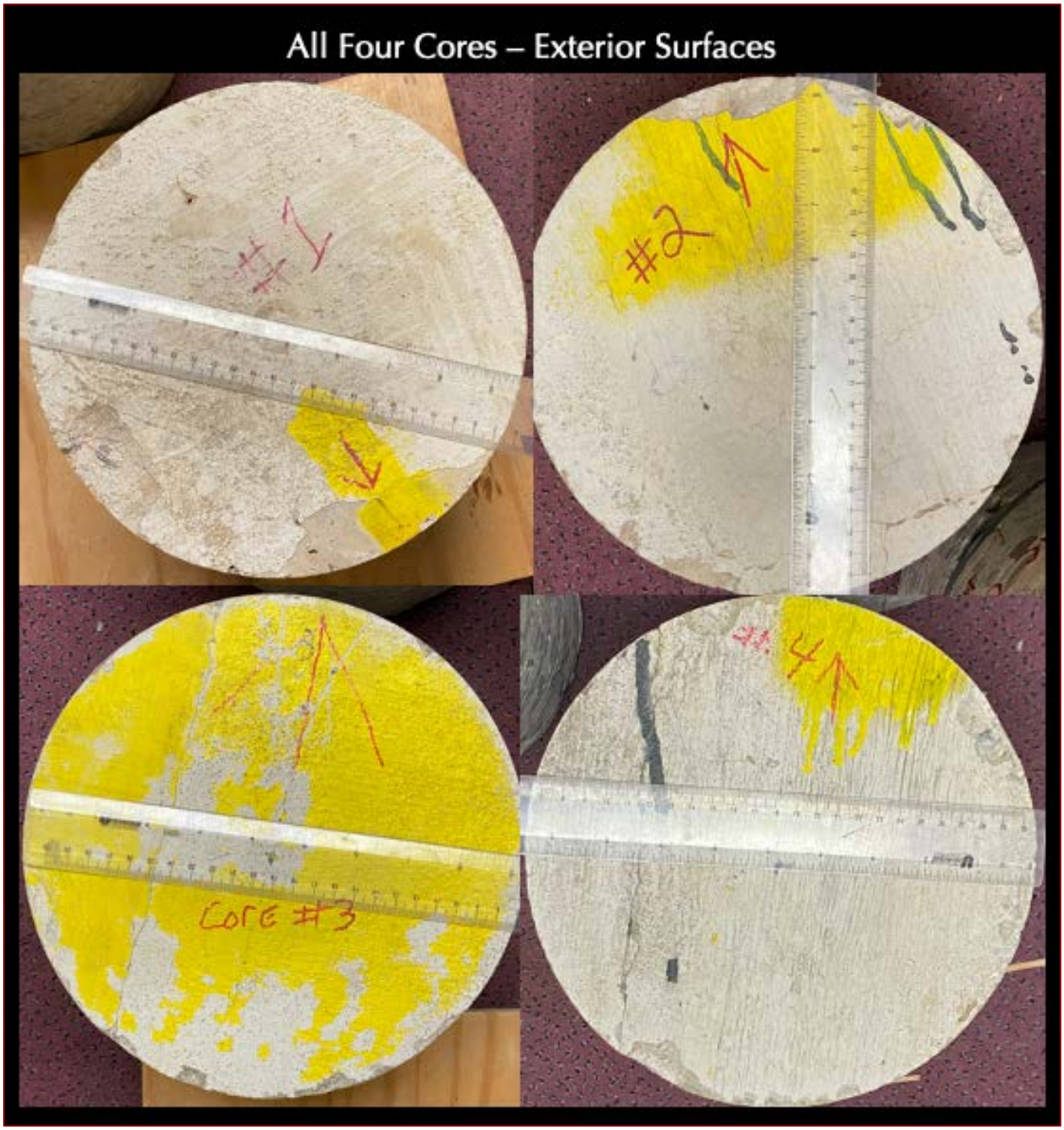

Figure 15: Shown are the exterior surface of tank wall in four cores received where some edge spalling of the protective cementitious coat is seen in some cores.

Figure 16: Shown are the exterior surface of tank wall in four cores received where some edge spalling of the protective cementitious coat is seen in some cores.

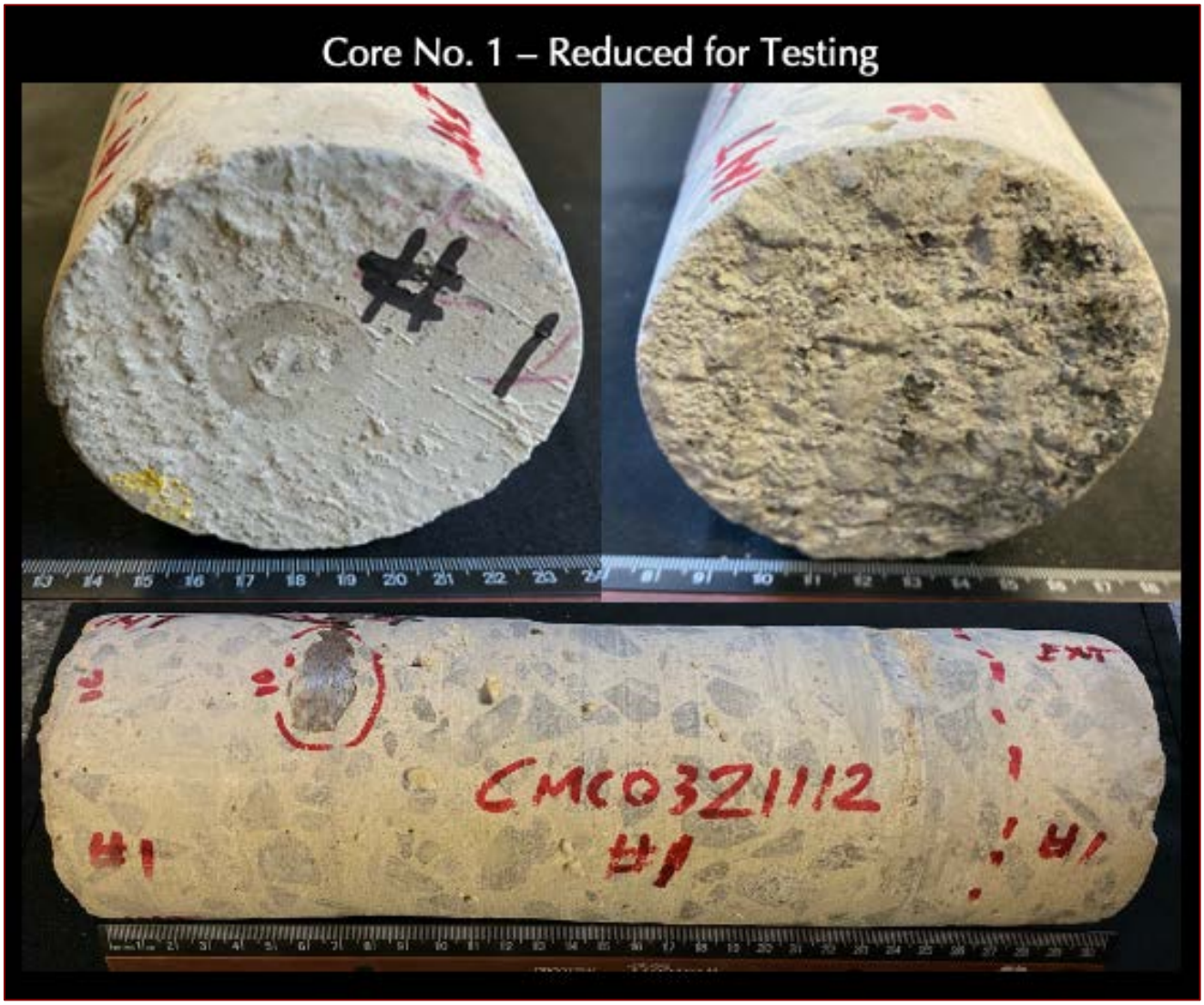

Figure 17: Core C1 reduced in diameter from the original 9½-in. diameter to 4-in. diameter for sample processing, showing the exterior and interior surfaces of tank wall at the opposite ends due to through-depth retrieval of the original core from the entire thickness of the tank wall. Steel reinforcement is circled, and directions of exterior and interior surfaces are marked as 'ext' and 'int,' respectively.

Figure 18: Core C2 reduced in diameter from the original 9½-in. diameter to 4-in. diameter for sample processing, showing the exterior and interior surfaces of tank wall at the opposite ends due to through-depth retrieval of the original core from the entire thickness of the tank wall. Steel reinforcement is circled, and directions of exterior and interior surfaces are marked as 'ext' and 'int,' respectively.

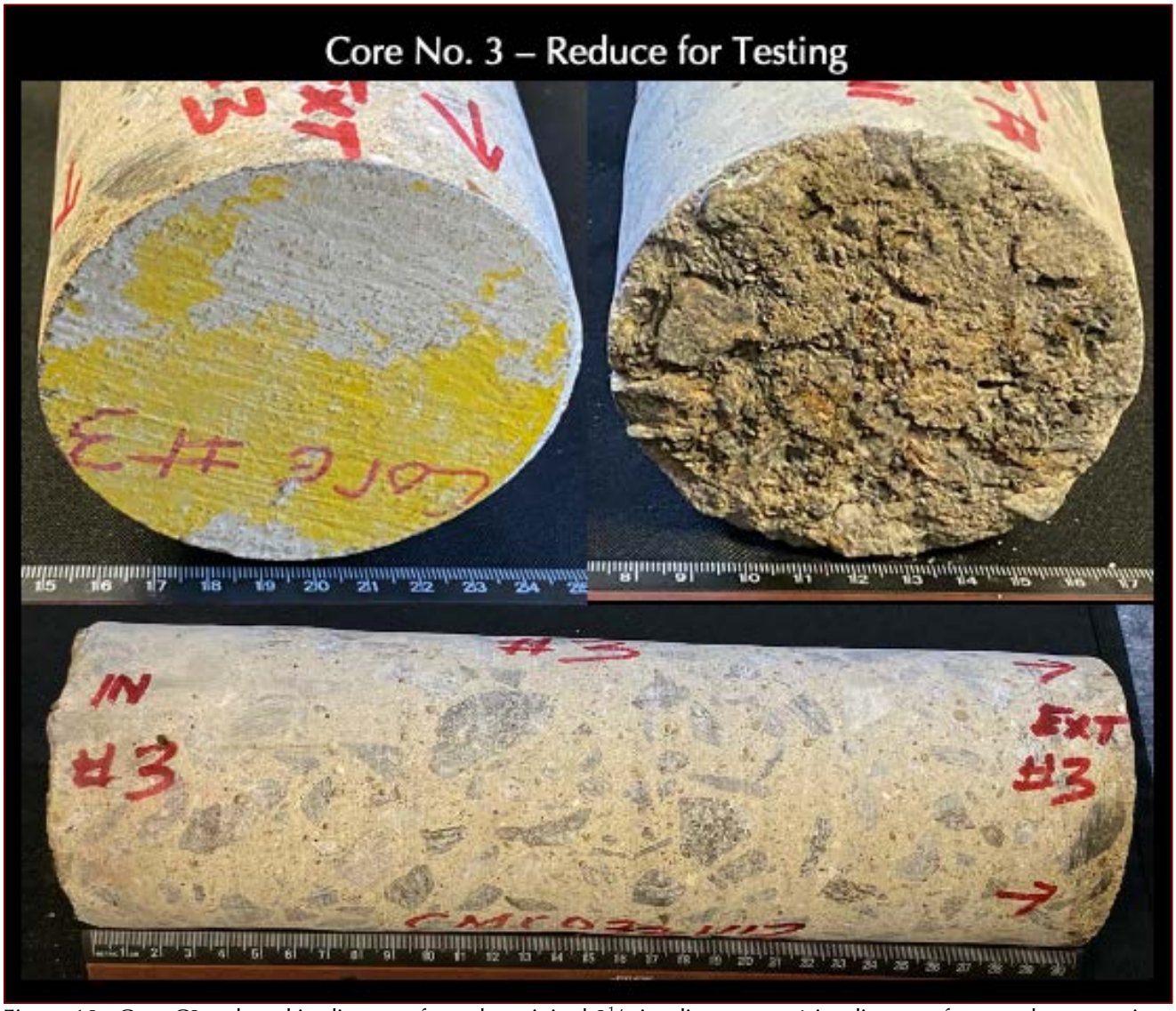

Figure 19: Core C3 reduced in diameter from the original 9½-in. diameter to 4-in. diameter for sample processing, showing the exterior and interior surfaces of tank wall at the opposite ends due to through-depth retrieval of the original core from the entire thickness of the tank wall. Directions of exterior and interior surfaces are marked as 'ext' and 'int,' respectively.

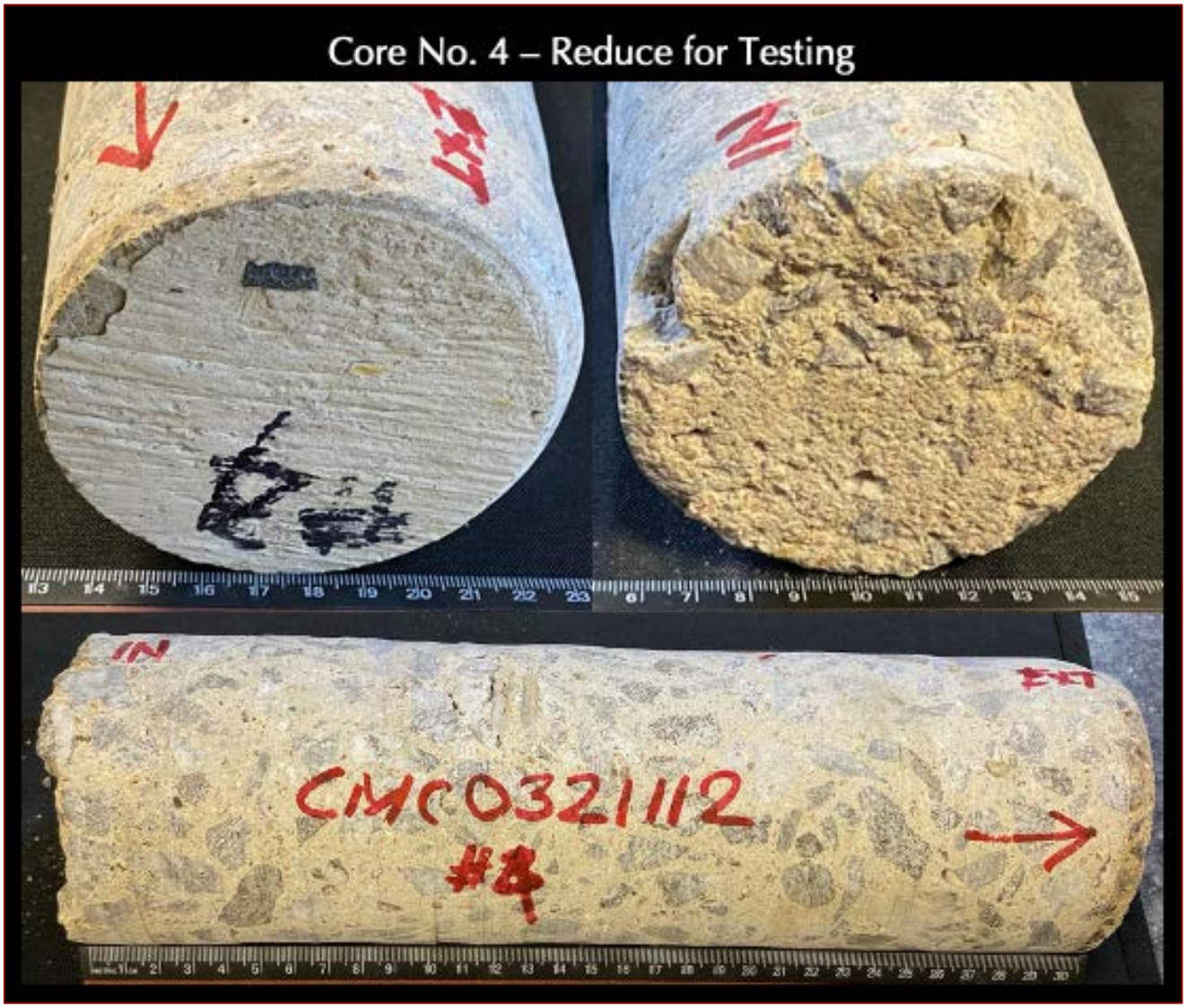

Figure 20: Core C4 reduced in diameter from the original $9^{1}/_{2}$-in. diameter to 4-in. diameter for sample processing showing the exterior, and interior surfaces of tank wall at the opposite ends due to through-depth retrieval of the original core from the entire thickness of the tank wall. Notice some spalling of protective cementitious coat on the exterior tank wall surface in the top left photo. Directions of exterior and interior surfaces are marked as 'ext' and 'int,' respectively.

Figure 21: Shown are the cement gray color of the exterior surface of tank wall surface on one (exterior tank wall) end of all four cores at the right, locations where cores were drilled in the center, and discolored and distressed concrete surfaces at the opposite (interior tank wall) ends of four cores in the left.

The waterline is reportedly between 5 and 10 ft. from the tank top. Core C1 (15' from tank top) is from an area that is continuously below the waterline, and Core C4 (3' from tank top) is from the aerated zone continuously above the waterline; Cores C2 and C3 (7 to 11 ft. from tank top) are from middle transitional zone of intermittent submersions.

PETROGRAPHIC EXAMINATIONS

LAPPED CROSS SECTIONS

Figure 22: Lapped cross section of Core C1 from the exterior surface end showing: (a) beige discoloration of concrete at the exterior surface end due to atmospheric carbonation to a depth of 48 mm where the carbonated zone is separated from the interior non-carbonated concrete by the dashed white line; (b) a vertical crack at one edge of the core from the exterior surface end marked with arrows; (c) crushed schist and gneiss coarse aggregate particles many with dark rims where particles are angular, dense, hard, medium gray and white, well-graded, and well-distributed; and (d) sound interstitial mortar fraction of concrete made using Portland cement paste and fine siliceous sand.

Figure 23: Lapped cross section of Core C1 from the exterior surface end showing before (left) and after (right) treatment with phenolphthalein alcoholic solutions to show carbonated zone at the exterior end where the concrete maintained its original beige discolored zone from interaction with atmospheric carbon dioxide, whereas pink discoloration of paste in the interior non-carbonated concrete. The depth of carbonation is measured to be 48 mm from the exterior end despite having a protective cementitious coating indicating prolonged interaction of the exterior tank wall surface with air prior to the placement of protecive coating.

Figure 24: Lapped cross section of Core C1 from the interior surface end showing: (a) layered black and brown discoloration of concrete at the interior surface end due to chemical alterations by interaction with the containment solution of tank to a depth of 5 to 7 mm where the altered zone (boxed) is separated from the interior sound unaltered concrete by a sharp boundary; (b) crushed schist and gneiss coarse aggregate particles many with dark rims where particles are angular, dense, hard, medium gray and white, well-graded, and well-distributed; and (c) sound interstitial mortar fraction of concrete made using Portland cement paste and fine siliceous sand.

Figure 25: Lapped cross section of Core C1 from the interior surface end showing: (a) layered black and brown discoloration of concrete at the interior surface end due to chemical alterations by interaction with the containment solution of tank to a depth of 5 mm where the altered zone (boxed) is separated from the interior sound unaltered concrete by a sharp boundary; (b) crushed schist and gneiss coarse aggregate particles many with dark rims where particles are angular, dense, hard, medium gray and white, well-graded, and well-distributed; and (c) sound interstitial mortar fraction of concrete made using Portland cement paste and fine siliceous sand.

Figure 26: Lapped cross section of Core C1 from the interior surface end showing before (left) and after (right) treatment with phenolphthalein alcoholic solutions to show carbonated zone at the interior end where the concrete maintained its original black discolored zone from interaction with atmospheric carbon dioxide whereas pink discoloration of paste in the interior non-carbonated concrete. The depth of carbonation is measured to be 5 mm from the interior end, which is noticeably lower than the carbonation depth measured from the exterior end.

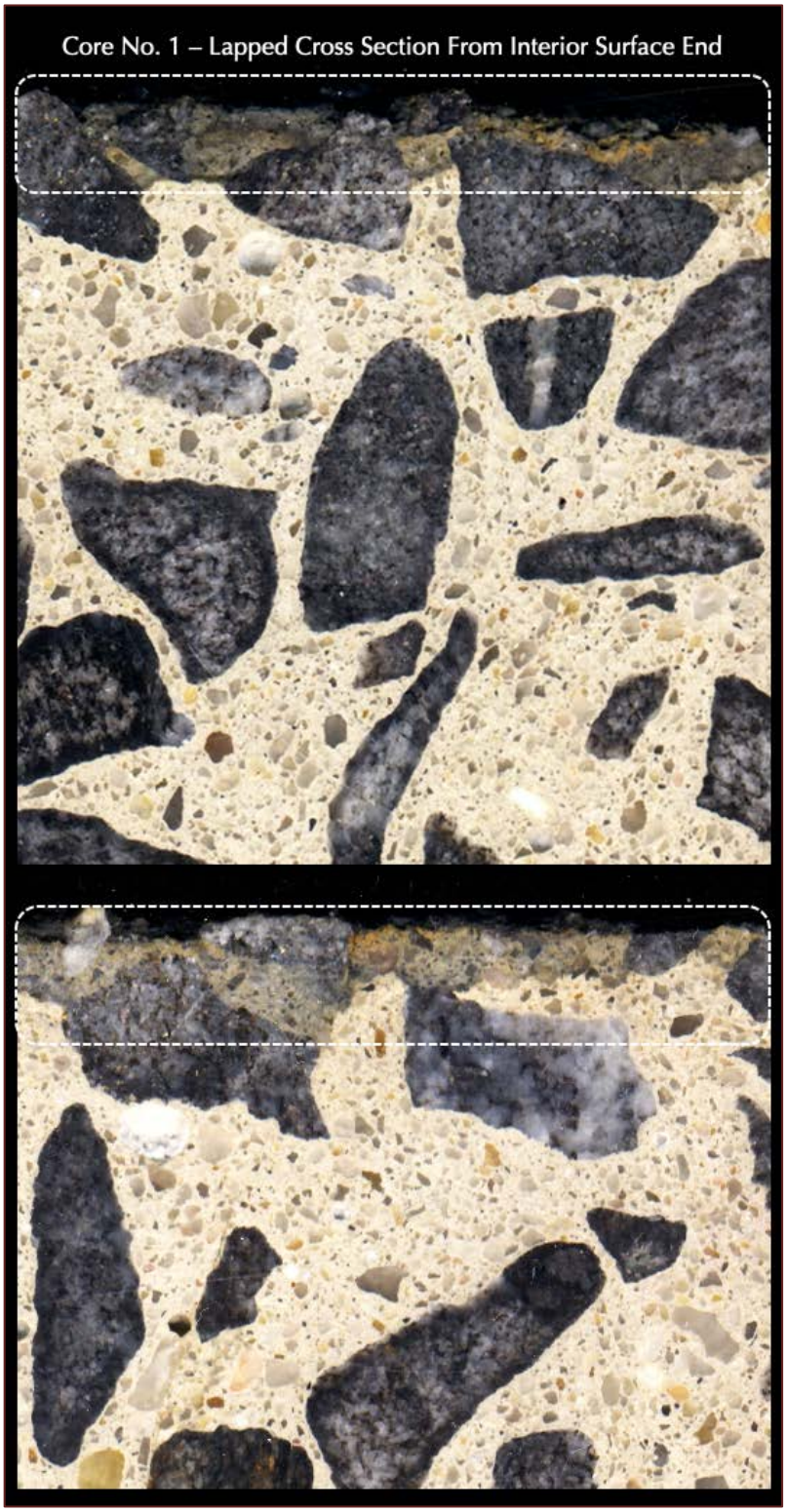

Figure 27: Lapped cross section of Core C1 from the interior surface end showing: (a) layered black and brown discoloration of concrete at the interior surface end due to chemical alterations by interaction with the containment solution of tank to a depth of 5 mm where the altered zone (boxed) is separated from the interior sound unaltered concrete by a sharp boundary; (b) crushed schist and gneiss coarse aggregate particles many with dark rims where particles are angular, dense, hard, medium gray and white, well-graded, and well-distributed; and (c) sound interstitial mortar fraction of concrete made using Portland cement paste and fine siliceous sand.

Figure 28: Lapped cross section of Core C2 from the exterior surface end showing: (a) beige discoloration of concrete at the exterior surface end due to atmospheric carbonation to a depth of 56 mm where the carbonated zone is separated from the interior non-carbonated concrete by the dashed white line; (b) a vertical crack at one edge of the core from the exterior surface end marked with arrows; (c) crushed schist and gneiss coarse aggregate particles many with dark rims where particles are angular, dense, hard, medium gray and white, well-graded, and well-distributed; and (d) sound interstitial mortar fraction of concrete made using Portland cement paste and fine siliceous sand.

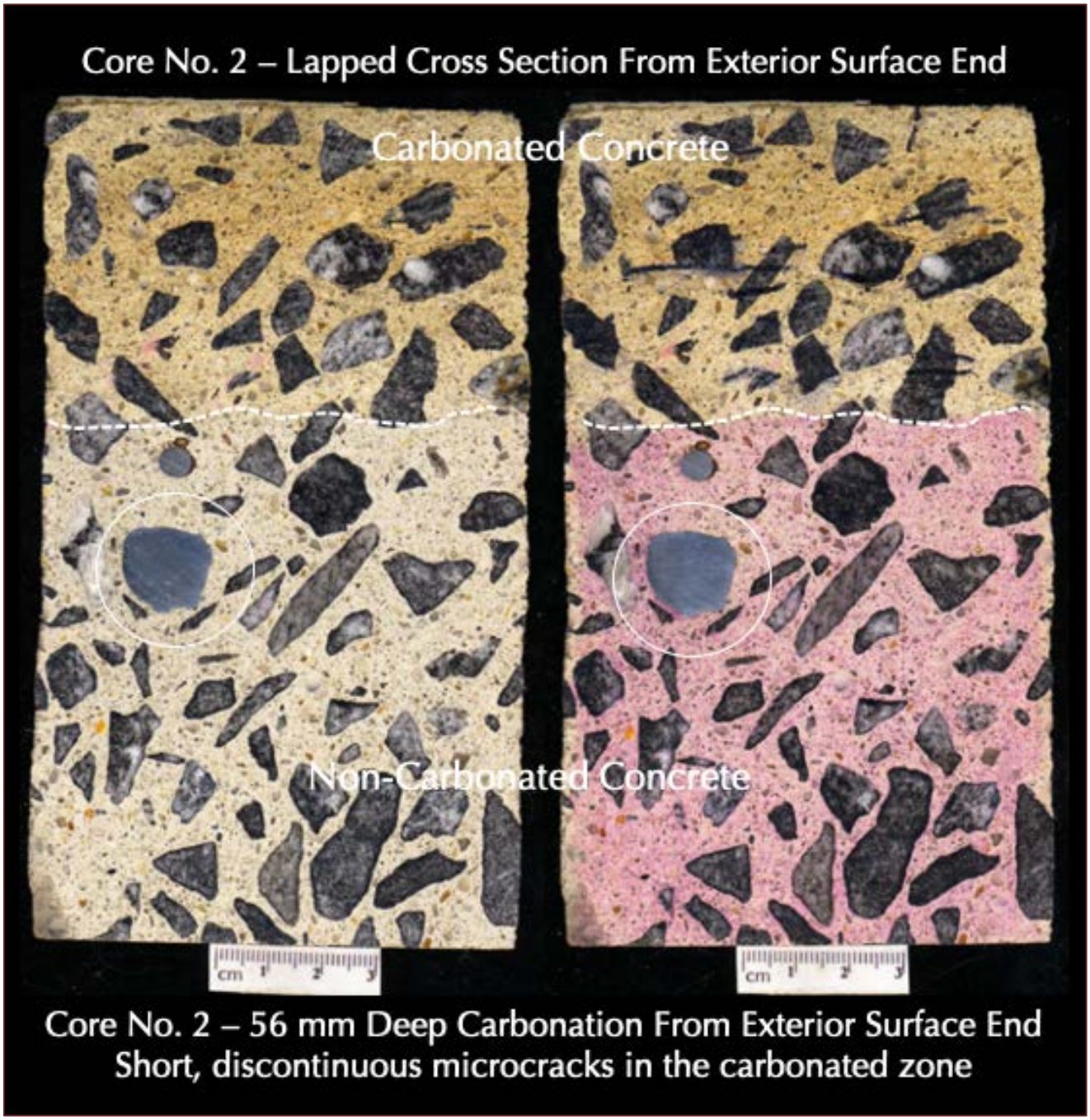

Figure 29: Lapped cross section of Core C2 from the exterior surface end showing before (left) and after (right) treatment with phenolphthalein alcoholic solutions to show carbonated zone at the exterior end where the concrete maintained its original beige discolored zone from interaction with atmospheric carbon dioxide, whereas pink discoloration of paste in the interior non-carbonated concrete. The depth of carbonation is measured to be 56 mm from the exterior end despite having a protective cementitious coating indicating prolonged interaction of the exterior tank wall surface with air prior to the placement of protecive coating.

Figure 30: Lapped cross section of Core C2 from the interior surface end showing: (a) black discoloration of concrete at the interior surface end due to chemical alterations by interaction with the containment solution of tank to a depth of 10 mm where the altered zone (boxed) is separated from the interior sound unaltered concrete by a sharp boundary; (b) crushed schist and gneiss coarse aggregate particles many with dark rims where particles are angular, dense, hard, medium gray and white, well-graded, and well-distributed; and (c) sound interstitial mortar fraction of concrete made using Portland cement paste and fine siliceous sand.

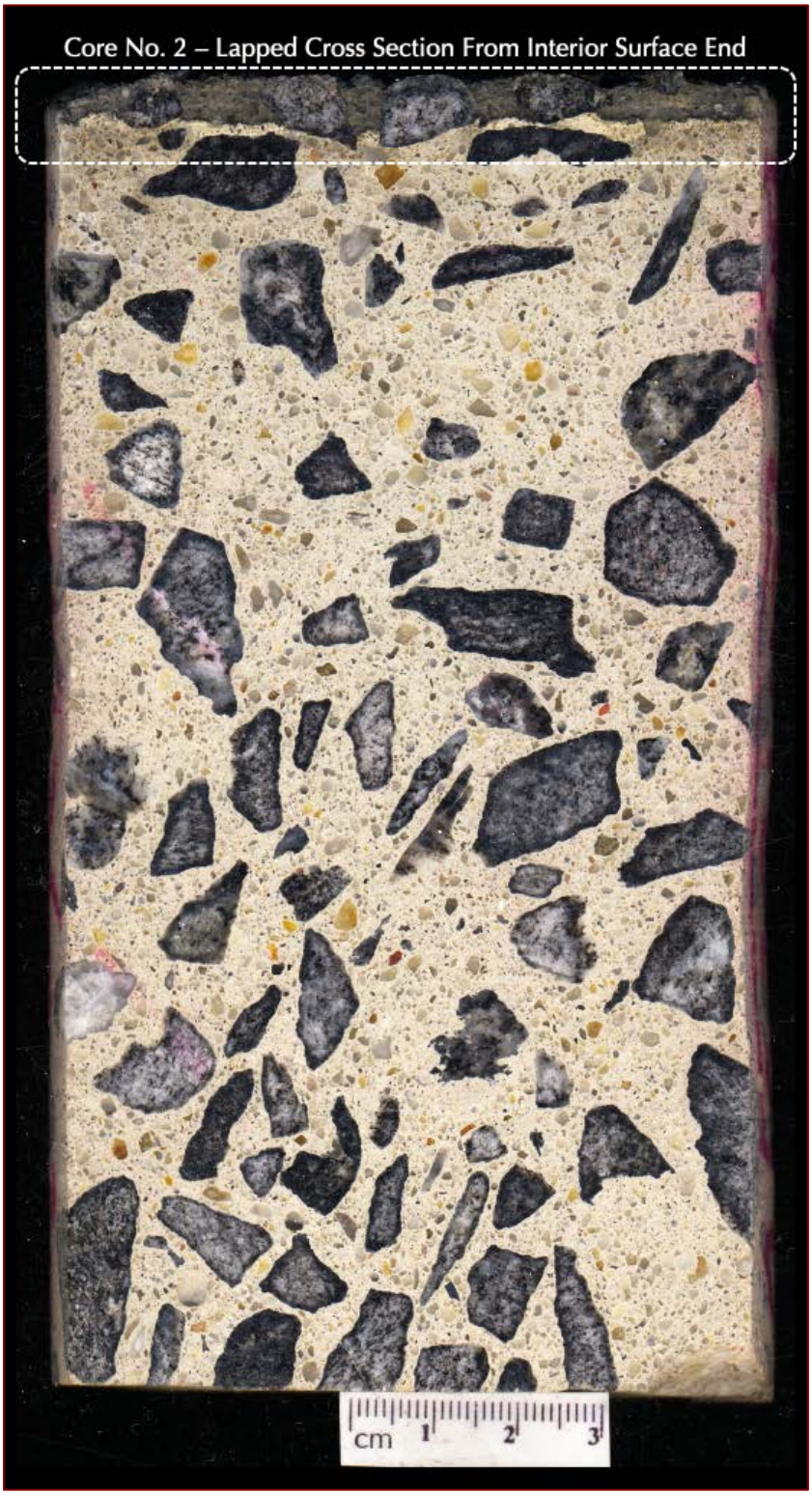

Figure 31: Lapped cross section of Core C2 from the interior surface end showing: (a) black discoloration of concrete at the interior surface end due to chemical alterations by interaction with the containment solution of tank to a depth of 10 mm where the altered zone (boxed) is separated from the interior sound unaltered concrete by a sharp boundary; (b) crushed schist and gneiss coarse aggregate particles many with dark rims where particles are angular, dense, hard, medium gray and white, well-graded, and well-distributed; and (c) sound interstitial mortar fraction of concrete made using Portland cement paste and fine siliceous sand.

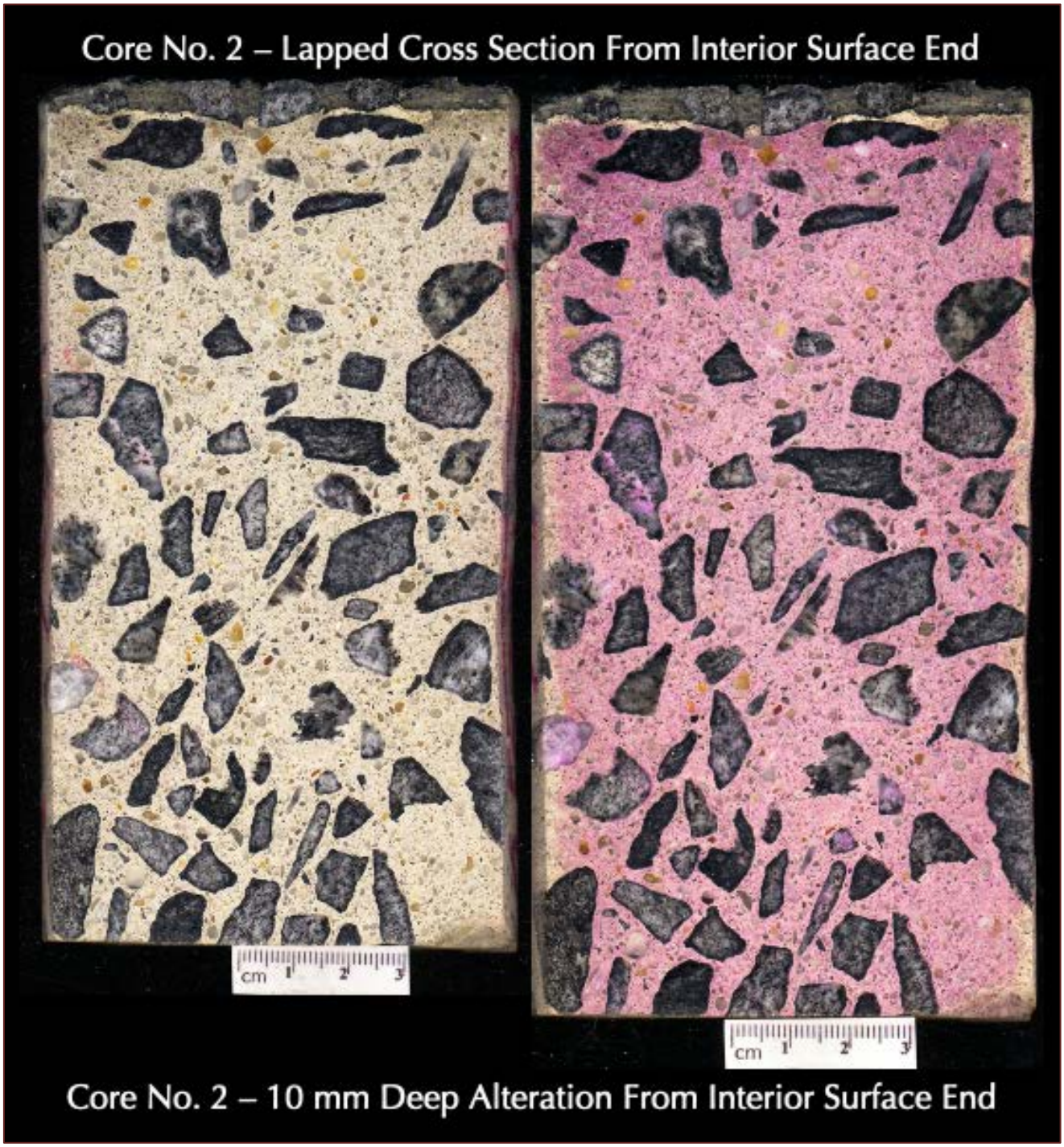

Figure 32: Lapped cross section of Core C2 from the interior surface end showing before (left) and after (right) treatment with phenolphthalein alcoholic solutions to show carbonated zone at the interior end where the concrete maintained its original black discolored zone from interaction with atmospheric carbon dioxide, whereas pink discoloration of paste in the interior non-carbonated concrete. The depth of carbonation is measured to be 10 mm from the interior end, which is noticeably lower than the carbonation depth measured from the exterior end.

Figure 33: Lapped cross section of Core C2 from the interior surface end showing: (a) black discoloration of concrete at the interior surface end due to chemical alterations by interaction with the containment solution of tank to a depth of 10 mm where the altered zone (boxed) is separated from the interior sound unaltered concrete by a sharp boundary; (b) crushed schist and gneiss coarse aggregate particles many with dark rims where particles are angular, dense, hard, medium gray and white, well-graded, and well-distributed; and (c) sound interstitial mortar fraction of concrete made using Portland cement paste and fine siliceous sand.

Figure 34: Lapped cross section of Core C4 from the exterior surface end showing: (a) beige discoloration of concrete at the exterior surface end due to atmospheric carbonation to a depth of 14 mm where the carbonated zone is separated from the interior non-carbonated concrete by the dashed white box; (b) a vertical crack at one edge of the core from the exterior surface end marked with arrows; (c) crushed schist and gneiss coarse aggregate particles many with dark rims where particles are angular, dense, hard, medium gray and white, well-graded, and well-distributed; and (d) sound interstitial mortar fraction of concrete made using Portland cement paste and fine siliceous sand.

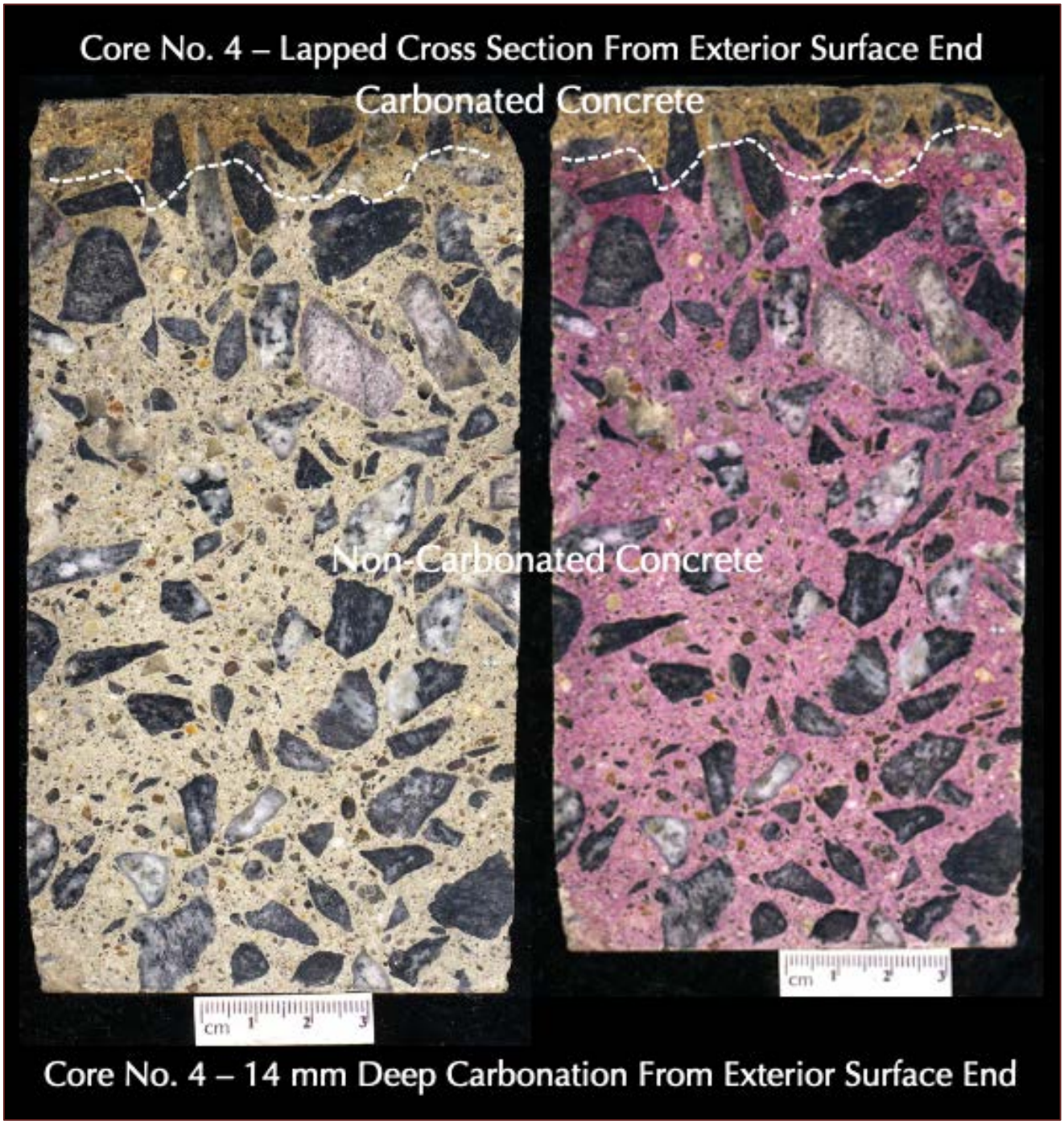

Figure 35: Lapped cross section of Core C4 from the exterior surface end showing before (left) and after (right) treatment with phenolphthalein alcoholic solutions to show carbonated zone at the exterior end where the concrete maintained its original beige discolored zone from interaction with atmospheric carbon dioxide whereas pink discoloration of paste in the interior non-carbonated concrete. The depth of carbonation is measured to be 14 mm from the exterior end despite having a protective cementitious coating indicating prolonged interaction of the exterior tank wall surface with air prior to the placement of protecive coating.

Figure 36: Lapped cross section of Core C4 from the interior surface end showing: (a) brown discoloration of concrete at the interior surface to a depth of 7 mm where the altered zone (boxed) is separated from the interior sound unaltered concrete by a sharp boundary; (b) crushed schist and gneiss coarse aggregate particles many with dark rims where particles are angular, dense, hard, medium gray and white, well-graded, and well-distributed; and (c) sound interstitial mortar fraction of concrete made using Portland cement paste and fine siliceous sand.

Figure 37: Lapped cross section of Core C4 from the interior surface end showing: (a) brown discoloration of concrete at the interior surface end to a depth of 7 mm where the altered zone (boxed) is separated from the interior sound unaltered concrete by a sharp boundary; (b) crushed schist and gneiss coarse aggregate particles many with dark rims where particles are angular, dense, hard, medium gray and white, well-graded, and well-distributed; and (c) sound interstitial mortar fraction of concrete made using Portland cement paste and fine siliceous sand.

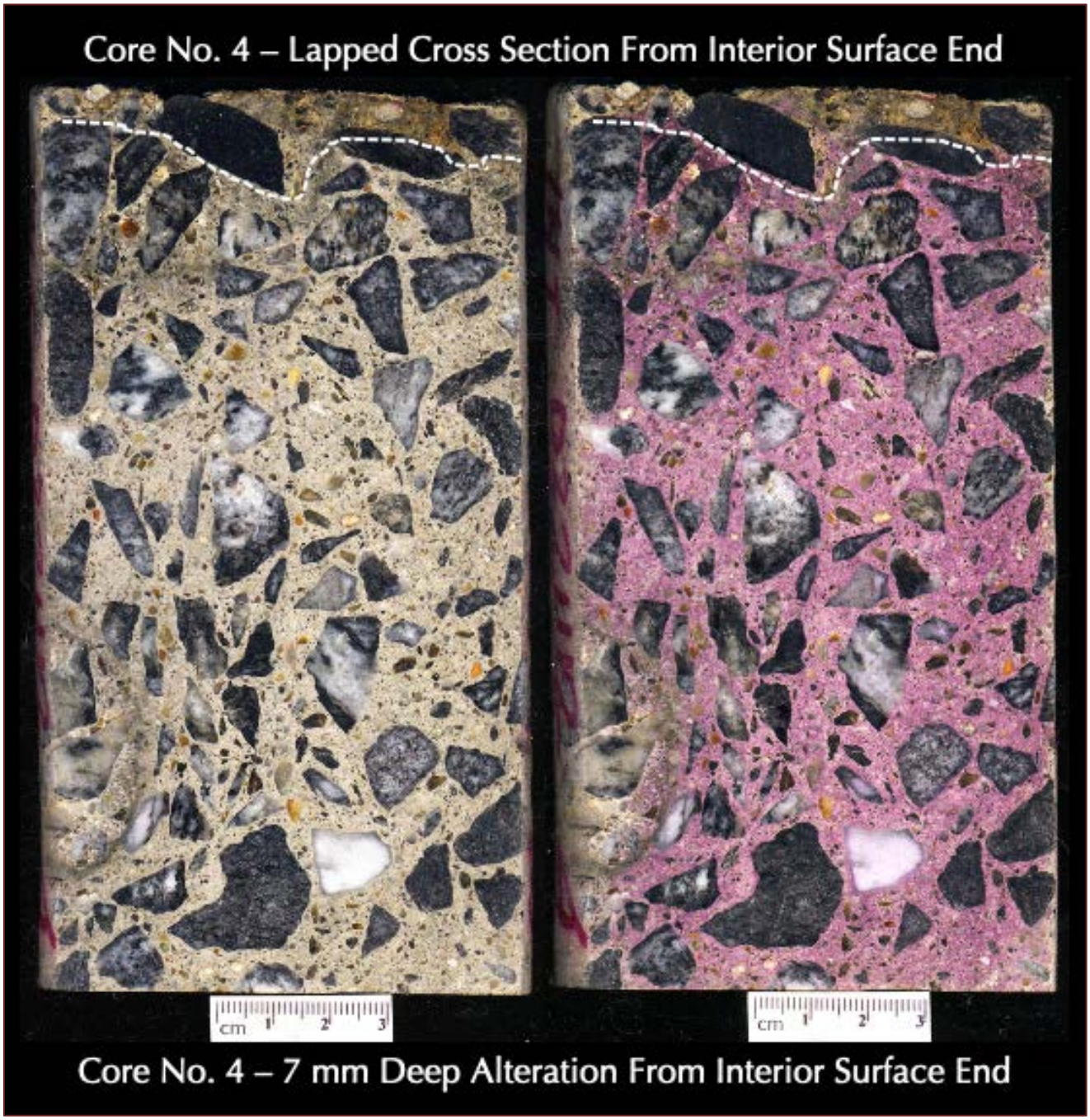

Figure 38: Lapped cross section of Core C4 from the interior surface end showing before (left) and after (right) treatment with phenolphthalein alcoholic solutions to show carbonated zone at the interior end where the concrete maintained its original black discolored zone from interaction with atmospheric carbon dioxide, whereas pink discoloration of paste in the interior non-carbonated concrete. The depth of carbonation is measured to be 7 mm from the interior end, which is noticeably lower than the carbonation depth measured from the exterior end.

Figure 39: Lapped cross section of Core C4 from the interior surface end showing: (a) brown discoloration of concrete at the interior surface end to a depth of 7 mm where the altered zone (boxed) is separated from the interior sound unaltered concrete by a sharp boundary; (b) crushed schist and gneiss coarse aggregate particles many with dark rims where particles are angular, dense, hard, medium gray and white, well-graded, and well-distributed; and (c) sound interstitial mortar fraction of concrete made using Portland cement paste and fine siliceous sand.

Figure 40: Interior discolored and distressed surface of tank wall in four cores at left and their lapped cross sections at right showing: (a) layered black and brown discoloration to a depth of 5 mm in Core C1 due to interaction with containment solution, (b) black discoloration to a depth of 10 mm in Core C2 due to interactions with containment solution, and (c) brown discoloration with exposed aggregate to a depth of 7 mm in Core C4 due to interaction with gases and moisture from the containment solution.

The waterline is reportedly between 5 and 10 ft. from the tank top. Core C1 (15′ from tank top) is from an area that is continuously below the waterline, and Core C4 (3′ from tank top) is from the aerated zone continuously above the waterline; Cores C2 and C3 (7 to 11 ft. from tank top) are from middle transitional zone of intermittent submersions.

Figure 41: Exterior cement gray surface of protective coating on the tank wall in four cores at left and their lapped cross sections at right showing: (a) beige discoloration due to atmospheric carbonation to a depth of 48 mm in Core C1, (b) beige discoloration due to atmospheric carbonation to a depth of 56 mm in Core C2, and (c) beige discoloration due to atmospheric carbonation to a depth of 14 mm in Core C4.

The following conclusions are drawn from the observations done so far:

a. The waterline is reportedly between 5 and 10 ft. from the tank top. Core C1 (15′ from tank top) is from an area that is continuously below the waterline, and Core C4 (3′ from tank top) is from the aerated zone continuously above the waterline. Cores C2 and C3 (7 to 11 ft. from tank top) are from middle transitional zone of intermittent submersions.

b. Concrete in the interior surface of tank was subjected to chemicals from the containment solutions as well as air-born gases from moisture to carbon dioxide to other gases residues of the chemicals from containment solutions, whereas the exterior surface of the tank was primarily exposed to atmospheric carbon dioxide.

c. For the interior wall, concrete at the middle and lower zones were exposed to the intermittent and continuously submerged conditions of the containment solution at and below the waterline, respectively, where the waterline is reportedly between 5 and 10 ft. from the tank top.

d. Exposed coarse aggregate particles in otherwise gray toned surface are seen at the top aerated portion of the interior surface of the tank wall whereas orange to brown discoloration is observed in the middle and lower zones where concrete was in contact with the containment solution. Darkest reddish-brown discoloration of the interior surface occurred in the middle zone of interior surface whereas lighter brown discoloration occurred at the lower zone of interior wall concrete. In fact, there is a distinct color zoning of the interior tank wall surface from cement gray at the very top to orange, dark reddish-brown to lighter brown/orange zones of discolored concretes found at the successively deeper levels with relatively sharp contact between the color zones which are best revealed in Figures 1 and 3. Such color zoning is the result of interaction of concrete with the chemicals in the containment solution of tank along with differential drying of the chemical-soaked concrete in the aerated portions. The very top cement gray zone is probably not contaminated with chemicals to bring the distinct discolorations seen in the lower zones even though concrete in the gray zone showed deterioration as leaching and loss of cement paste around coarse aggregate particles to expose long streaks of coarse aggregate particles similar to the situations where a Portland cement concrete is exposed to an acidic solution.

e. Compared to the concrete-chemical interactions and resultant discolorations, alterations, etc. in the interior wall, the exterior tank surface is relatively sound, with its characteristic cement gray color tone not only from the concrete but also from the thin protective cementitious coating applied, except only a few isolated areas of sheet-like spalling of the protective coats. The exterior surface ends of Cores C1, C3, and C4 showed this protective cementitious coating of less than a millimeter thickness, which are more distinct in the following micrographs of lapped cross sections of cores.

f. Depths of carbonation of concrete are always greater from the exterior surface of the tank than the depths measured from the interior surface. For example, depths of carbonation of cores measured from exterior surface ends varied from 48 mm in Core C1 to 56 mm in Core C2 to only 14 mm in Core C4, whereas

corresponding carbonation depths from the interior surfaces are only 5 mm in Core C1, 10 mm in Core C2, and 7 mm in Core C4 which are associated with the zones of chemical alteration of concrete from the interior surfaces.

g. Cores C1 and C2 taken from the 15 ft. and 11 ft. depths from the tank top, respectively, showed significantly deeper atmospheric carbonation from the exterior surfaces, measured to be 48 mm and 56 mm, respectively, whereas Core C4 from the aerated portion of the tank taken from only 3 ft. depth from the tank top showed only 14 mm deep carbonation from the exterior surface. Therefore, depths of carbonation of concrete at the exterior surface of tank is deeper at the lower and middle zones but noticeably shallower at the top aerated zone.

h. Interior tank surfaces show black discoloration of concrete in Cores C1 and C2 taken from 15′ and 11′ depths from the tank top whereas no such black discoloration except only carbonation in Core C4 taken from the aerated portion of interior wall above the water line.

i. Along with deep carbonation of concrete from the exterior tank wall surface from the middle and lower zones, Core C2 shows some softening, and short, discontinuous cracking of concrete within the top 56 mm of carbonated zone from the exterior surface which is judged to be related not only to atmospheric carbonation but distress due to cyclic freezing and thawing at critically saturated conditions. Core C2 is taken from a portion that has intermittent submersion and exposures to moisture which if permeates through the tank wall to the exterior surface end and freezes can develop such near-exterior-surface cracks from cyclic freezing and thawing.

j. Concrete in all four cores from the top to the bottom of the tank show overall compositional similarities in coarse aggregates consisting of crushed schist and gneiss coarse aggregate particles that are angular, dense, hard, equidimensional to elongated, well-graded, and well-distributed across the thickness of the tank wall (i.e. depth of the cores). Aggregate particles are sound and did not contribute to any distress to be noticed on the lapped cross sections.

MICROGRAPHS OF LAPPED CROSS SECTION

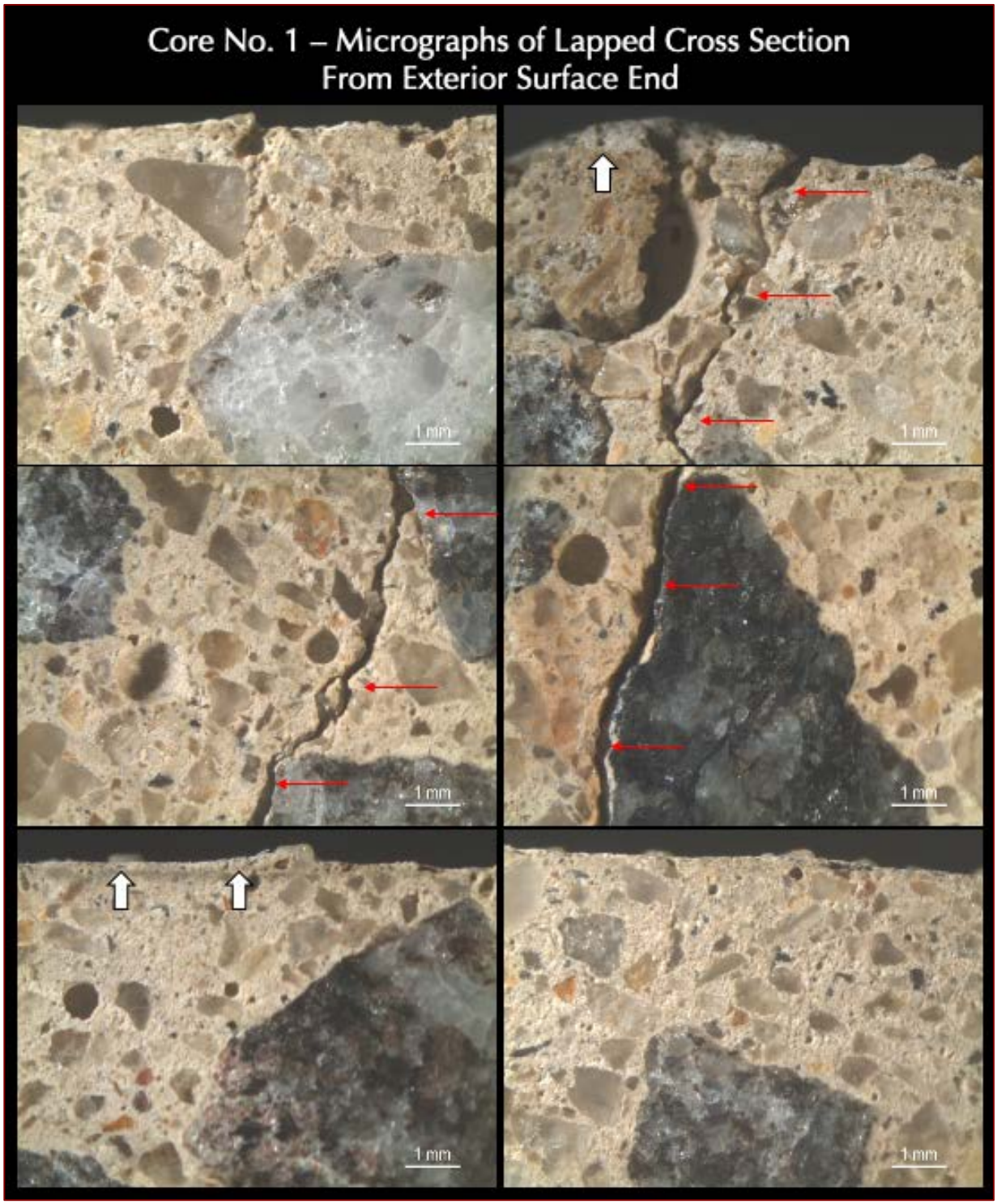

Figure 42: Micrographs of lapped cross section of Core C1 from the exterior end showing: (a) the protective cementitious coating of less than 1 mm thickness that is adhered to the main concrete body (top right); (b) beige discoloration of carbonated concrete at the exterior end immediately beneath the protective coat; (c) non-air-entrained nature of concrete without any intentionally introduced spherical <1 mm size entrained air (all photos); (d) visible cracks within the carbonated zone that has transected and circumscribed the aggregate particles (marked in red arrows).

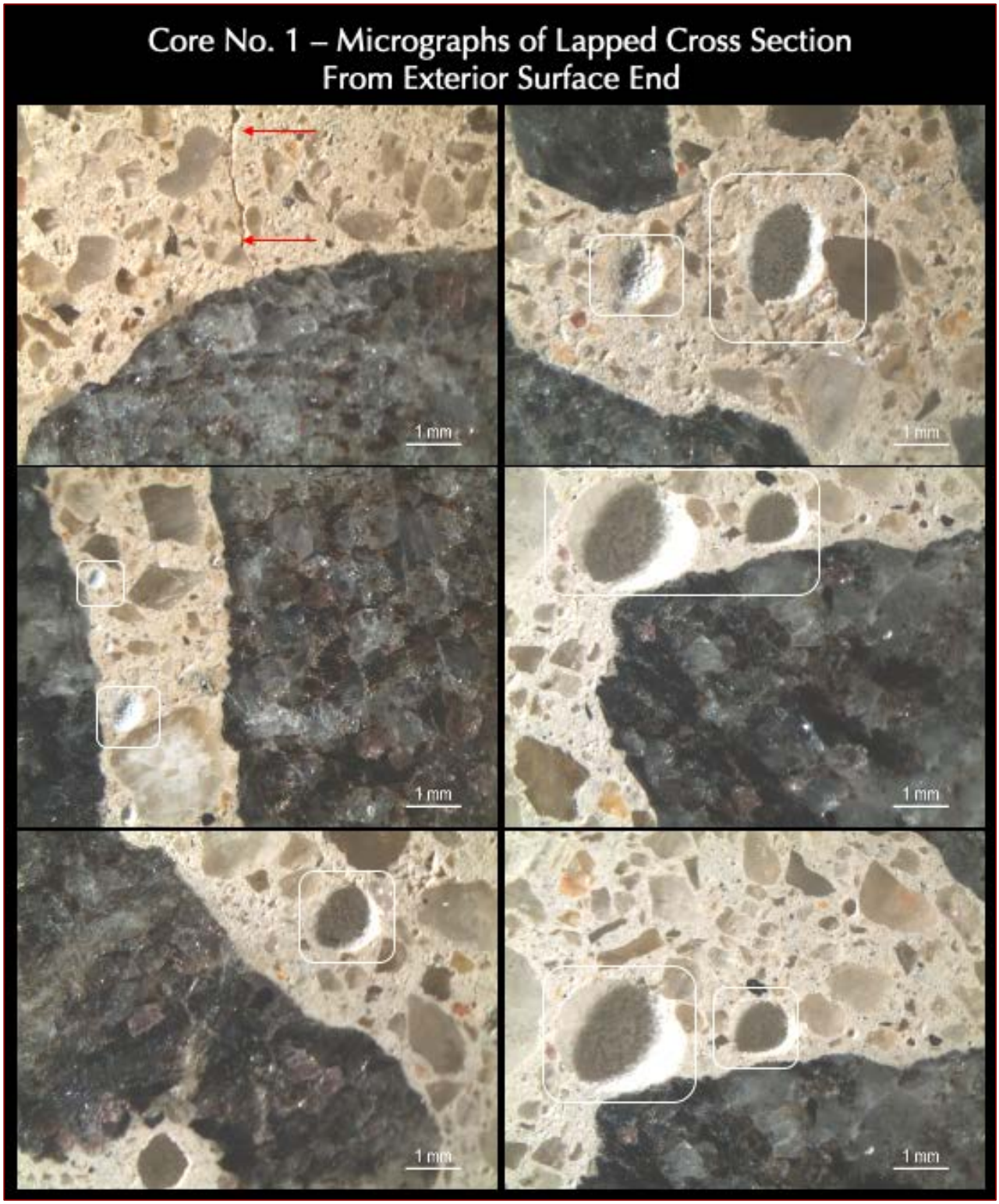

Figure 43: Micrographs of lapped cross section of Core C1 from the exterior end showing: (a) non-air-entrained nature of concrete without any intentionally introduced spherical <1 mm size entrained air (all photos); (b) secondary ettringite deposits lining the walls of air voids (boxed) indicating prolonged presence of moisture in concrete during service; and (c) a vertical crack (marked in red arrows).

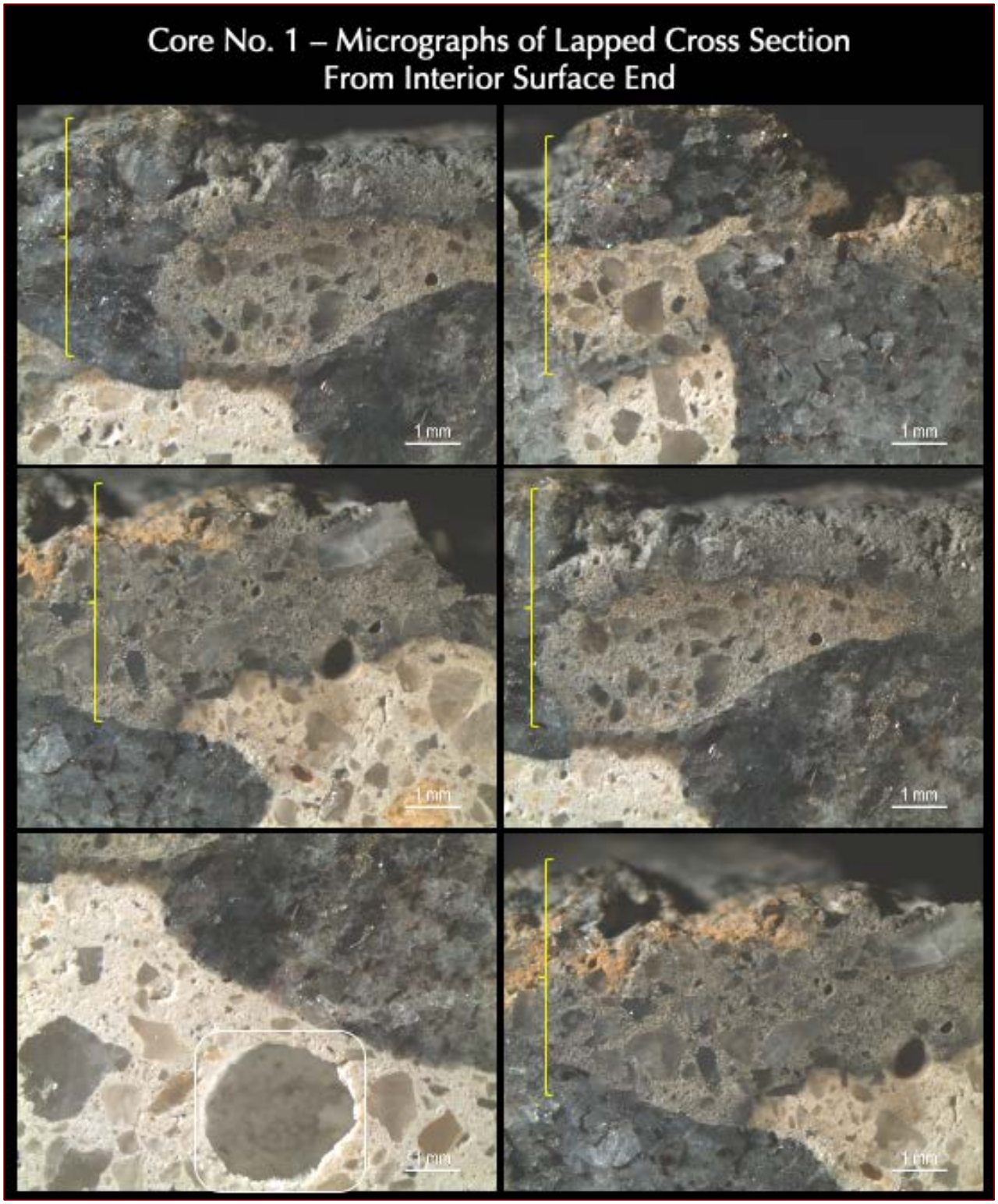

Figure 44: Micrographs of lapped cross section of Core C1 from the interior end showing: (a) layered black, gray, and brown altered zones at the top 5 mm due to interaction of concrete with containment solution in the tank; (b) sharp boundary between the top 5 mm altered zone and interior unaltered concrete; (c) secondary ettringite deposits lining the walls of air voids (boxed) indicating prolonged presence of moisture in concrete during service; and (d) non-air-entrained nature of concrete without any intentionally introduced spherical <1 mm size entrained air (all photos).

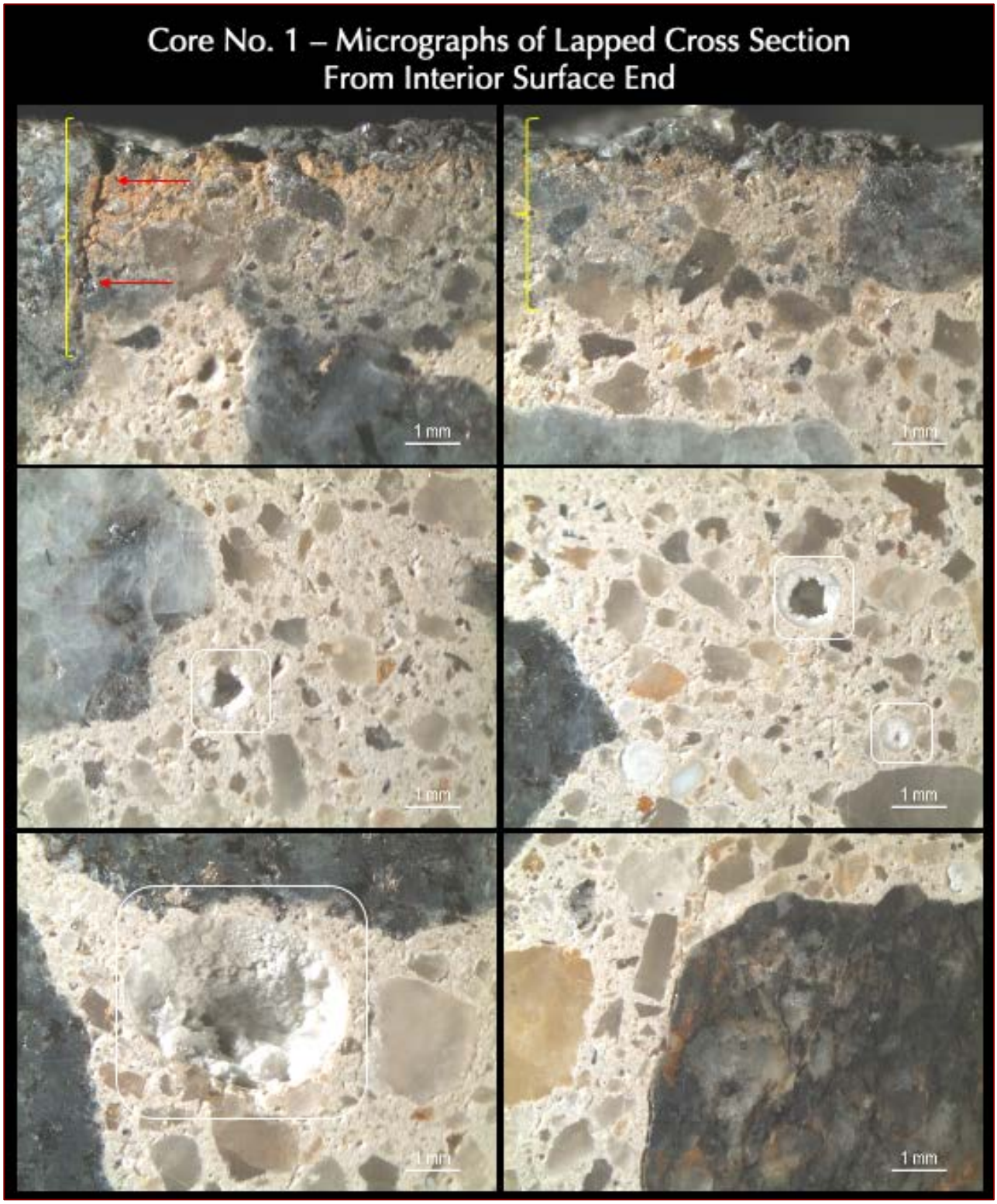

Figure 45: Micrographs of lapped cross section of Core C1 from the interior end showing: (a) layered zones consisting of a thin black top, a middle gray layer, and a brown layer within the surface altered zones at the top 5 mm of the interior wall due to interaction of concrete with containment solutions in the tank; (b) a sharp boundary between the top 5 mm altered zone and the interior unaltered concrete; (c) secondary ettringite deposits lining the walls of air voids (boxed) indicating prolonged presence of moisture in concrete during service; and (d) non-air-entrained nature of concrete without any intentionally introduced spherical <1 mm size entrained air (all photos).

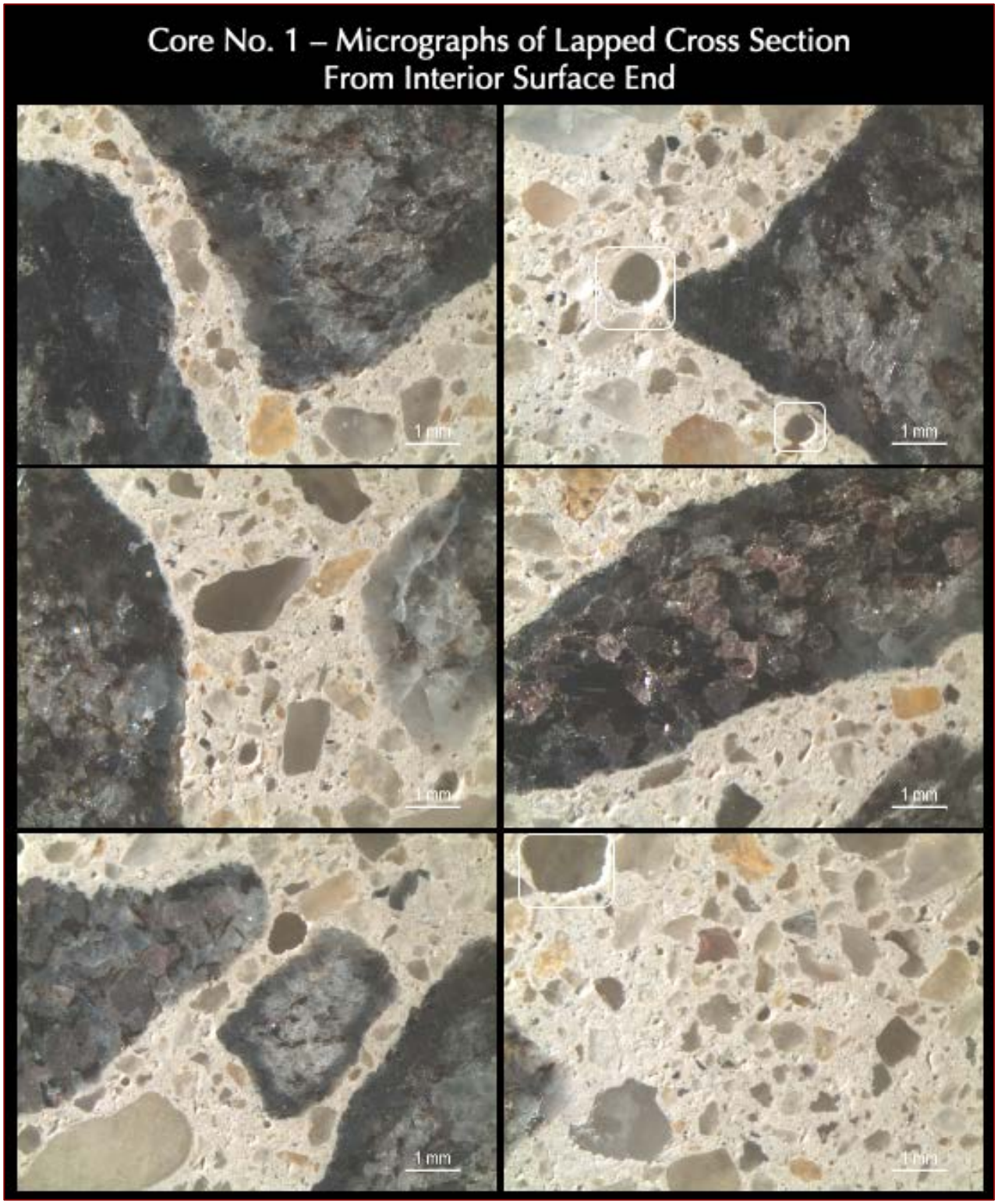

Figure 46: Micrographs of lapped cross section of Core C1 from the interior end showing: (a) secondary ettringite deposits lining the walls of air voids (boxed) indicating prolonged presence of moisture in concrete during service; and (b) non-air-entrained nature of concrete without any intentionally introduced spherical <1 mm size entrained air (all photos).

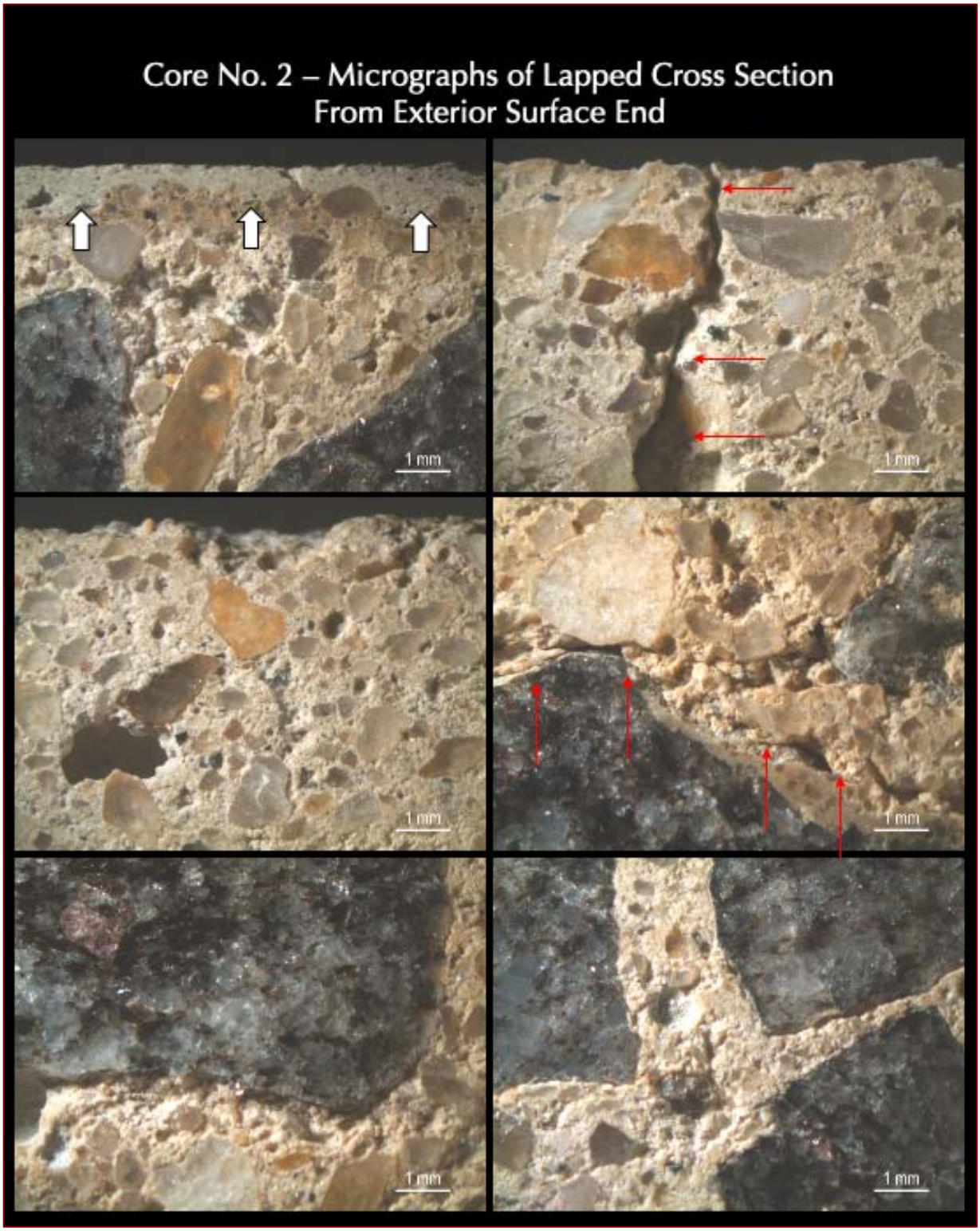

Figure 47: Micrographs of lapped cross section of Core C2 from the exterior end showing: (a) the protective cementitious coating of less than 1 mm thickness that is adhered to the main concrete body (top left); (b) beige discoloration of carbonated concrete at the exterior end immediately beneath the protective coat due to atmopsheric carbonation; (c) non-air-entrained nature of concrete without any intentionally introduced spherical <1 mm size entrained air (all photos); and (d) visible cracks within the carbonated zone that has transected and circumscribed the aggregate particles (marked in red arrows).

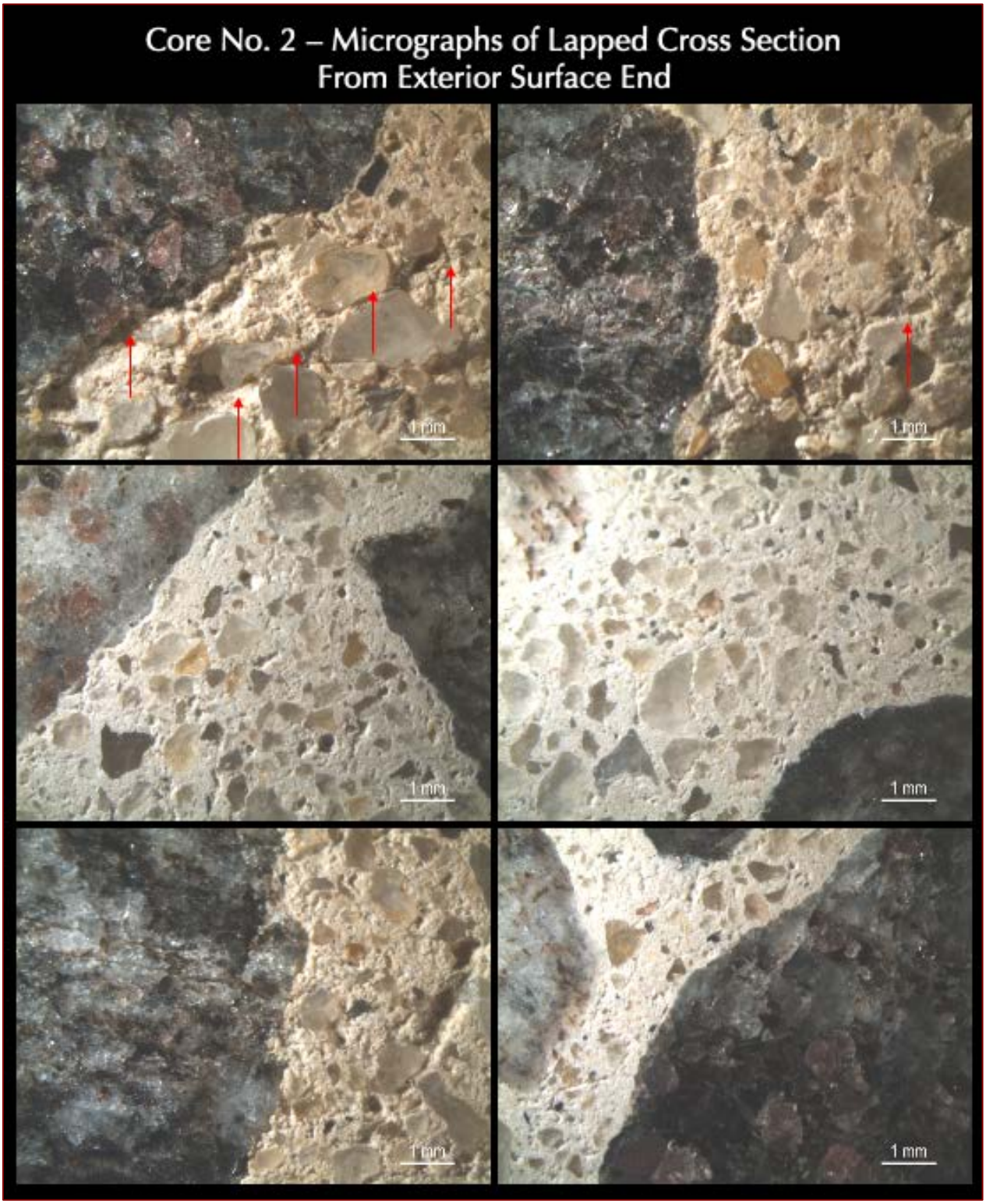

Figure 48: Micrographs of lapped cross section of Core C2 from the exterior end showing: (a) beige discoloration of carbonated concete at the exterior end due to interaction with atmopshere; (b) non-air-entrained nature of concrete without any intentionally introduced spherical <1 mm size entrained air (all photos); and (c) visible crack within the carbonated zone that has transected and circumscribed the aggregate particles (marked in red arrows).

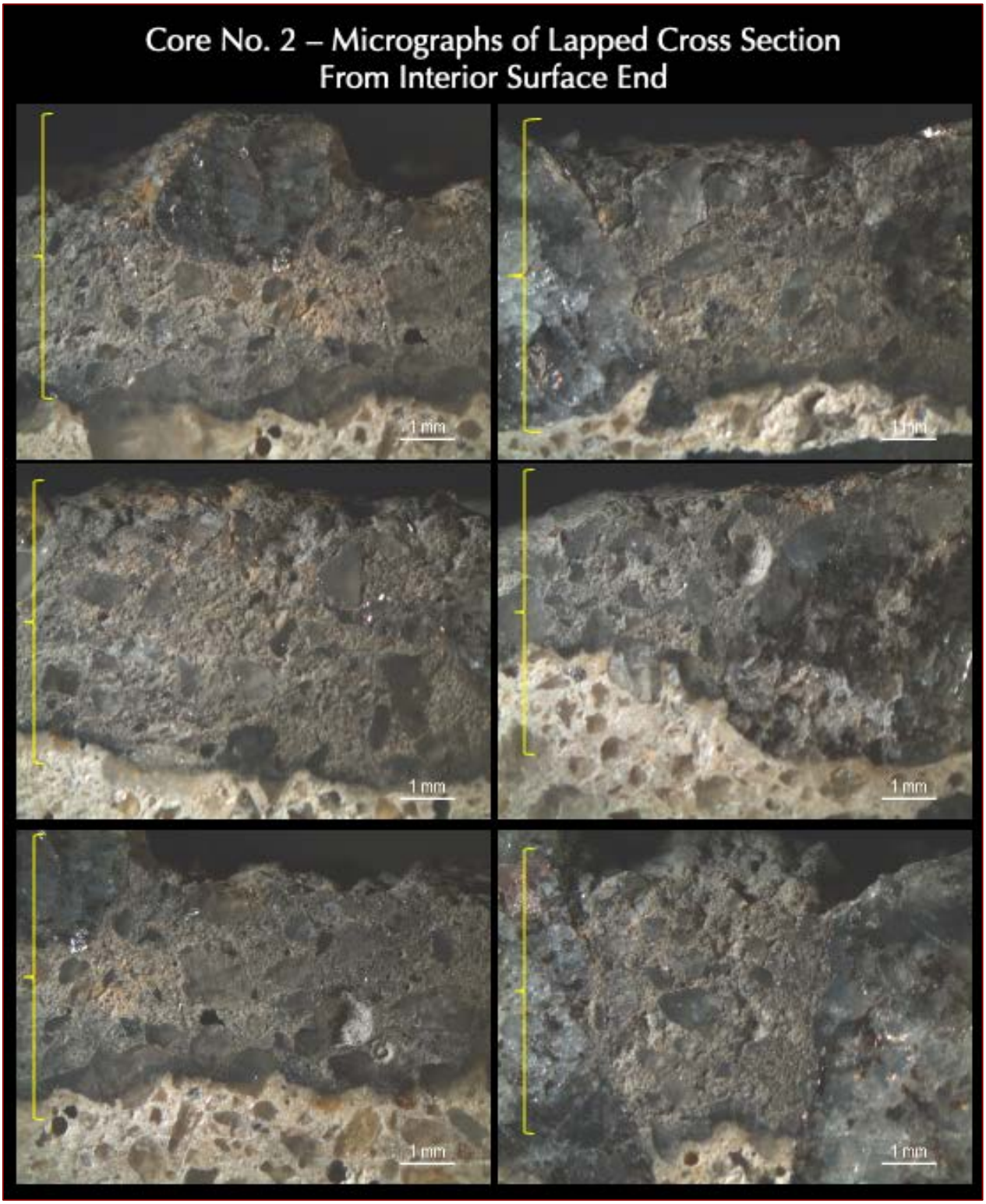

Figure 49: Micrographs of lapped cross section of Core C2 from the interior end showing: (a) black and gray discolored altered zone at the top 10 mm due to interaction of concrete with containment solution in the tank; (b) sharp boundary between the top 10 mm altered zone and interior unaltered concrete; and (c) non-air-entrained nature of concrete without any intentionally introduced spherical <1 mm size entrained air (all photos).

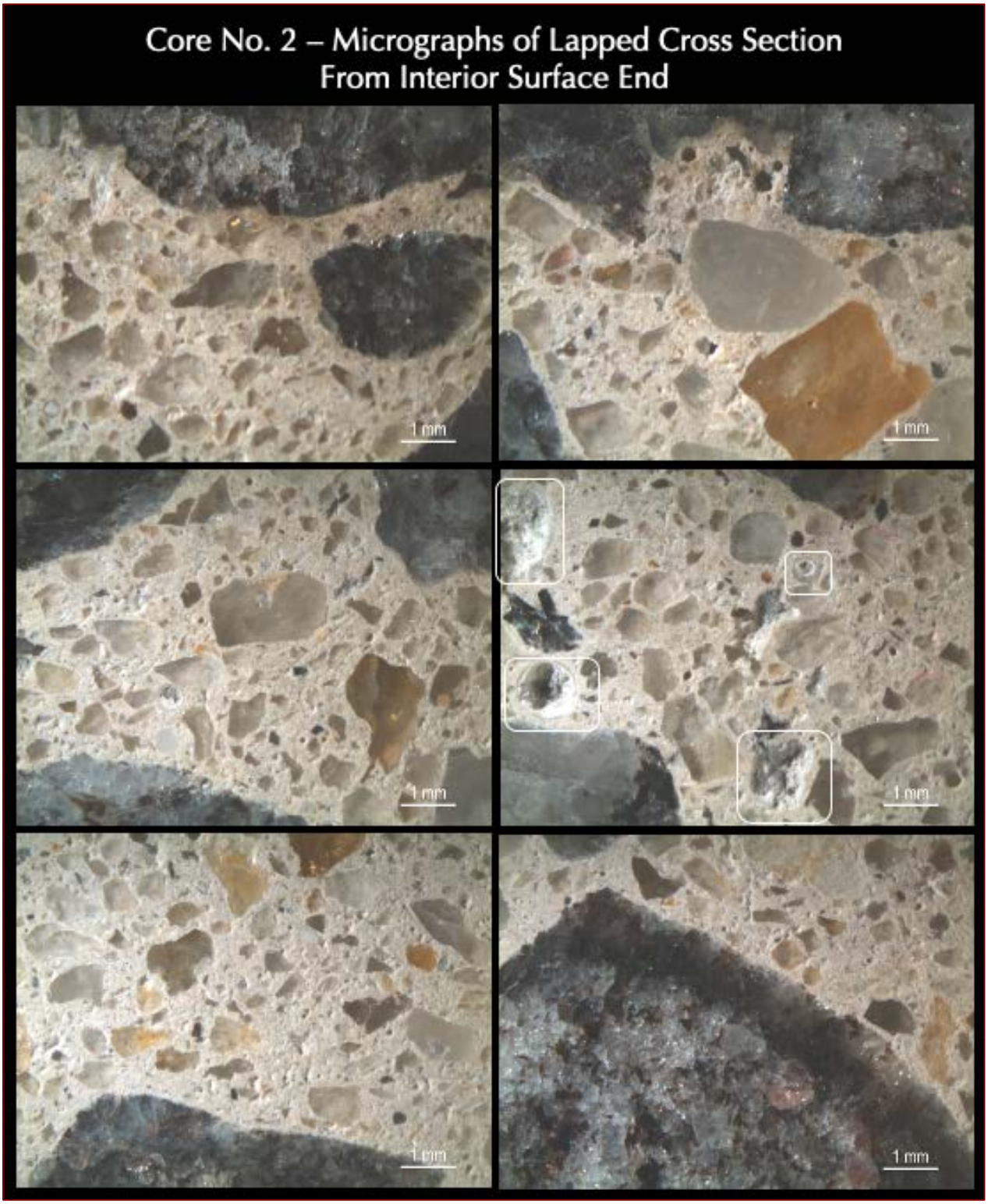

Figure 50: Micrographs of lapped cross section of Core C2 from the interior end showing: (a) non-air-entrained nature of concrete without any intentionally introduced spherical <1 mm size entrained air (all photos); and (b) secondary ettringite deposits lining the walls of air voids (boxed) indicating prolonged presence of moisture in concrete during service. Notice dark weathering rims in many crushed schist and gneiss coarse aggregate particles.

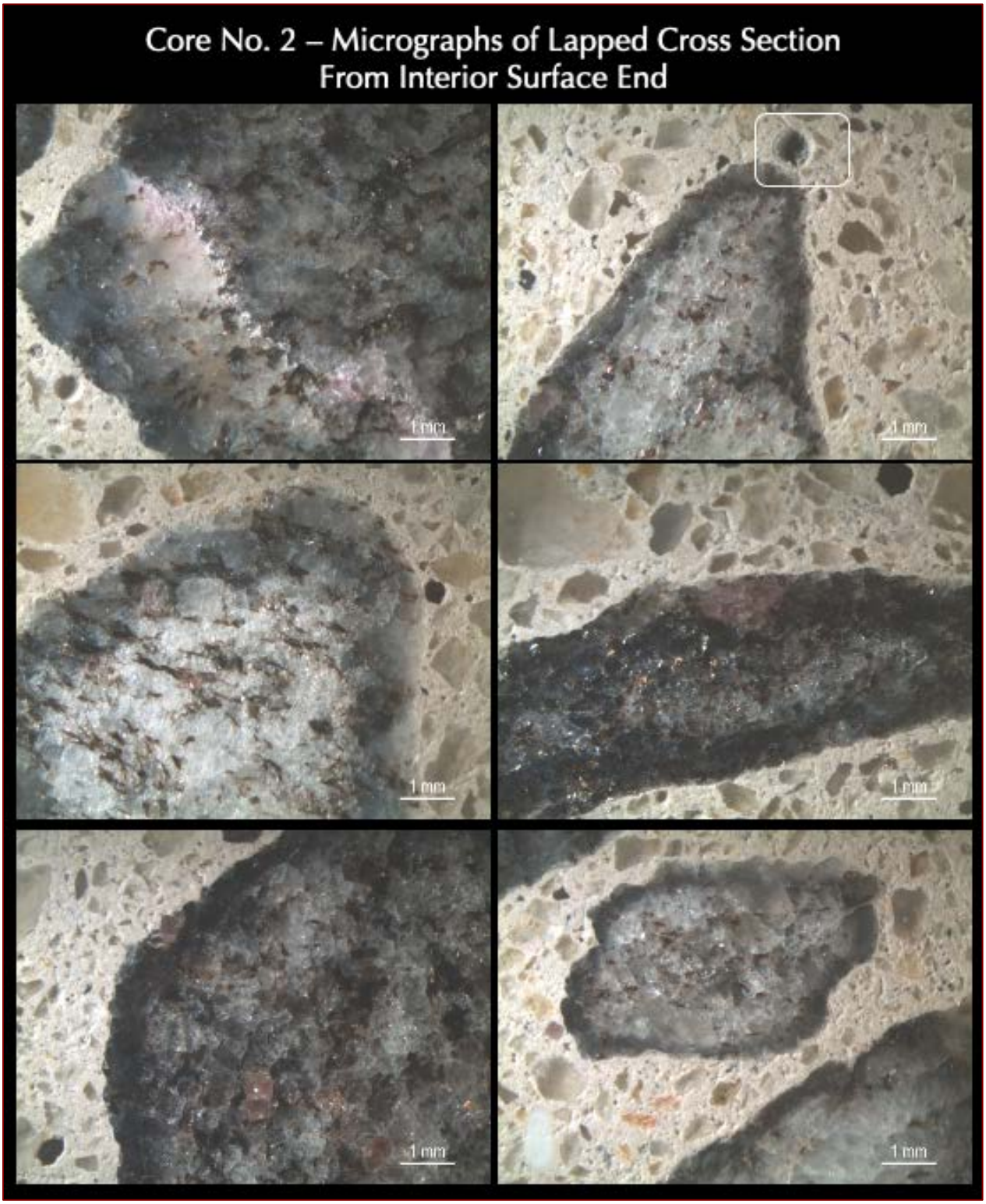

Figure 51: Micrographs of lapped cross section of Core C2 from the interior end showing: (a) non-air-entrained nature of concrete without any intentionally introduced spherical <1 mm size entrained air (all photos); and (b) secondary ettringite deposits lining the walls of air voids (boxed) indicating prolonged presence of moisture in concrete during service. Notice dark weathering rims in many crushed schist and gneiss coarse aggregate particles.

Figure 52: Micrographs of lapped cross section of Core C2 from the interior end showing: (a) black and gray discolored altered zone at the top 10 mm due to interaction of concrete with containment solution in the tank; (b) sharp boundary between the top 10 mm altered zone and interior unaltered concrete; and (c) non-air-entrained nature of concrete without any intentionally introduced spherical <1 mm size entrained air (all photos).

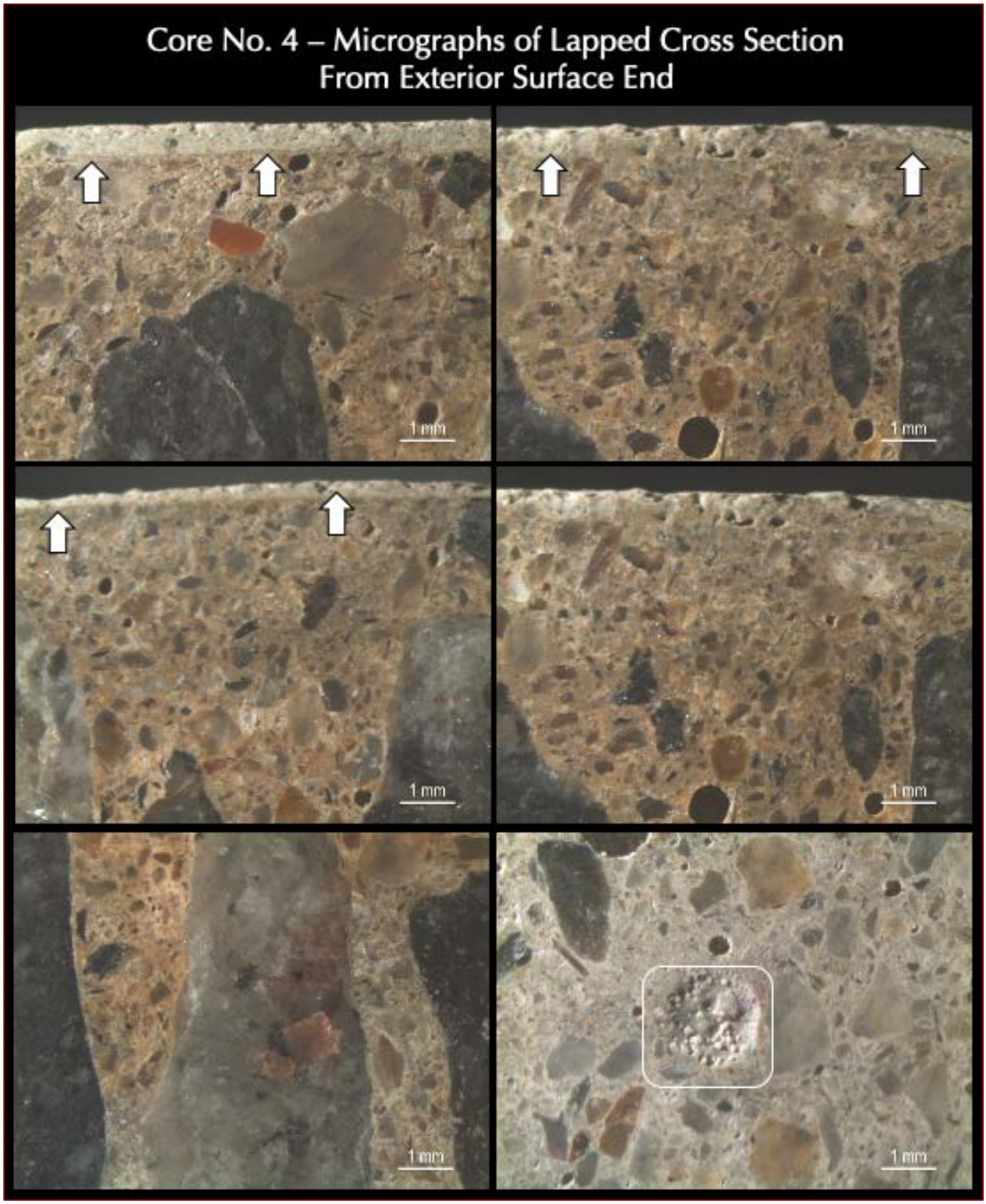

Figure 53: Micrographs of lapped cross section of Core C4 from the exterior end showing: (a) the protective cementitious coating of less than 1 mm thickness that is adhered to the main concrete body (top and middle rows); (b) beige discoloration of carbonated concete at the exterior end immediately beneath the protective coat; (c) non-air-entrained nature of concrete without any intentionally introduced spherical <1 mm size entrained air (all photos); (d) secondary ettringite deposits lining the walls of air voids indicating prolonged presence of moisture in concrete.

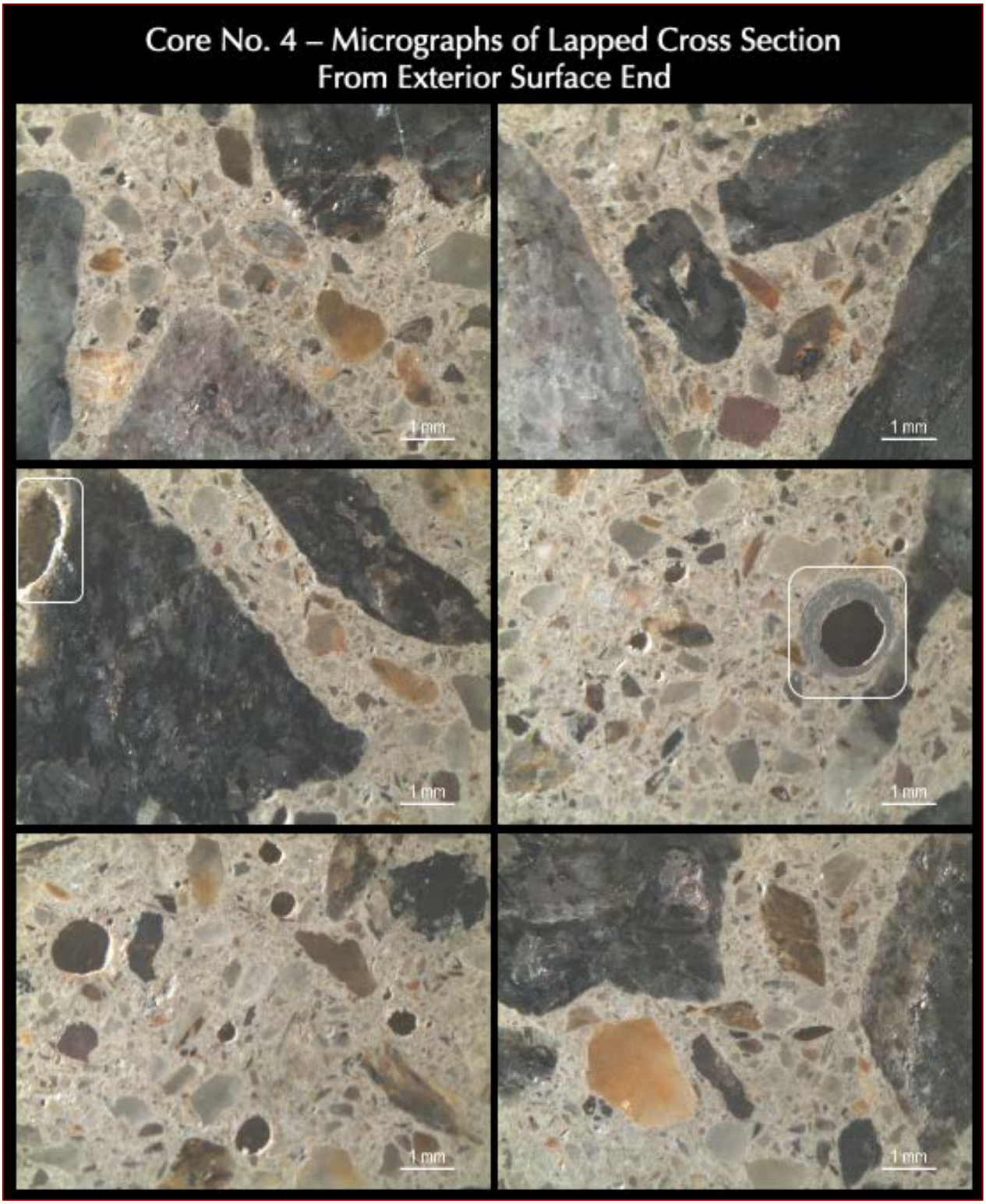

Figure 54: Micrographs of lapped cross section of Core C4 from the exterior end showing: (a) non-air-entrained nature of concrete without any intentionally introduced spherical <1 mm size entrained air (all photos); and (b) secondary ettringite deposits lining the walls of air voids indicating prolonged presence of moisture in concrete (boxed).

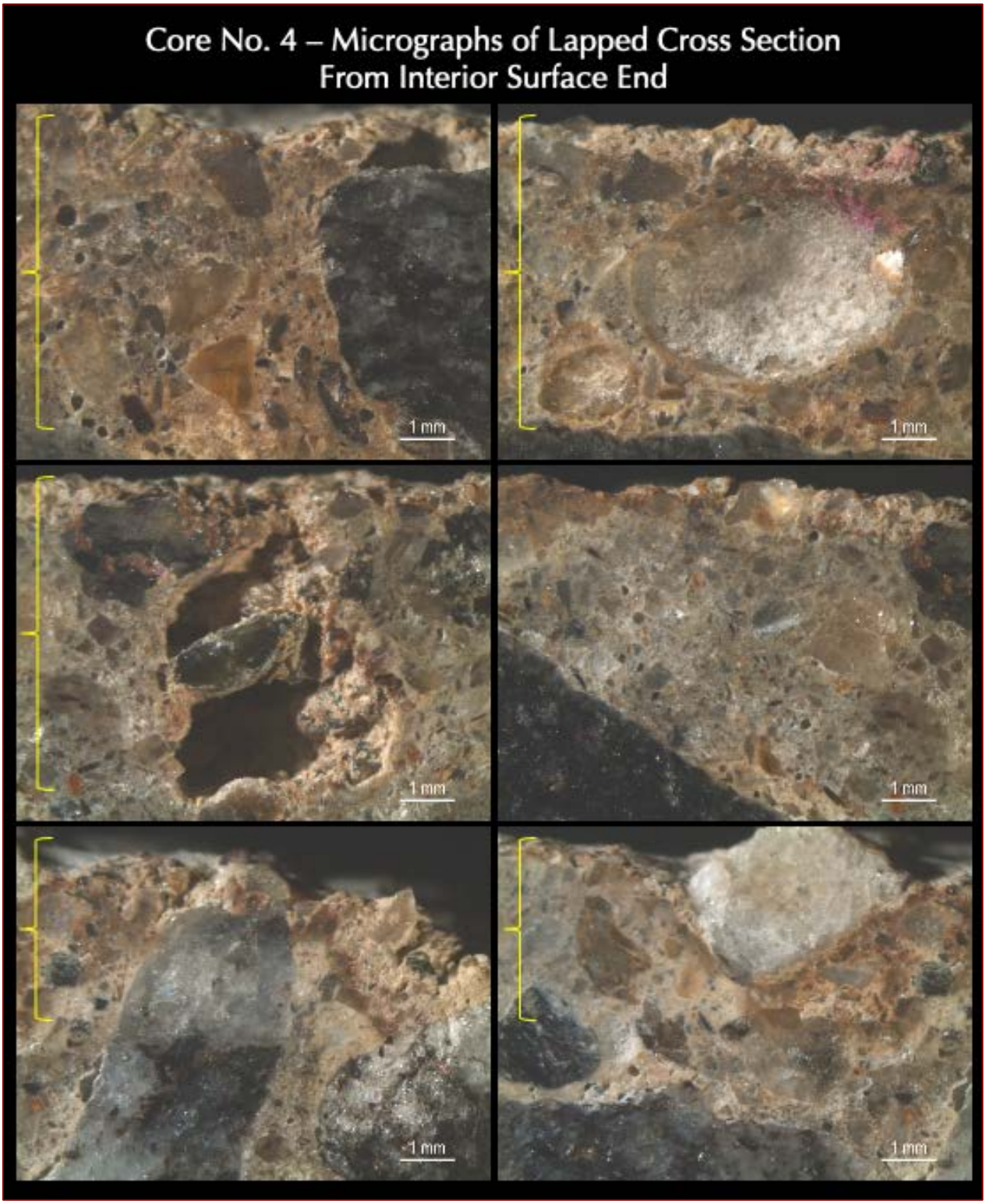

Figure 55: Micrographs of lapped cross section of Core C4 from the interior end showing: (a) beige discolored altered zone at the top 7 mm due to interaction of concrete with the gases, air, and moisture emitted from the containment solution in the tank; (b) secondary ettringite deposits lining the walls of air voids; and (c) non-air-entrained nature of concrete without any intentionally introduced spherical <1 mm size entrained air (all photos).

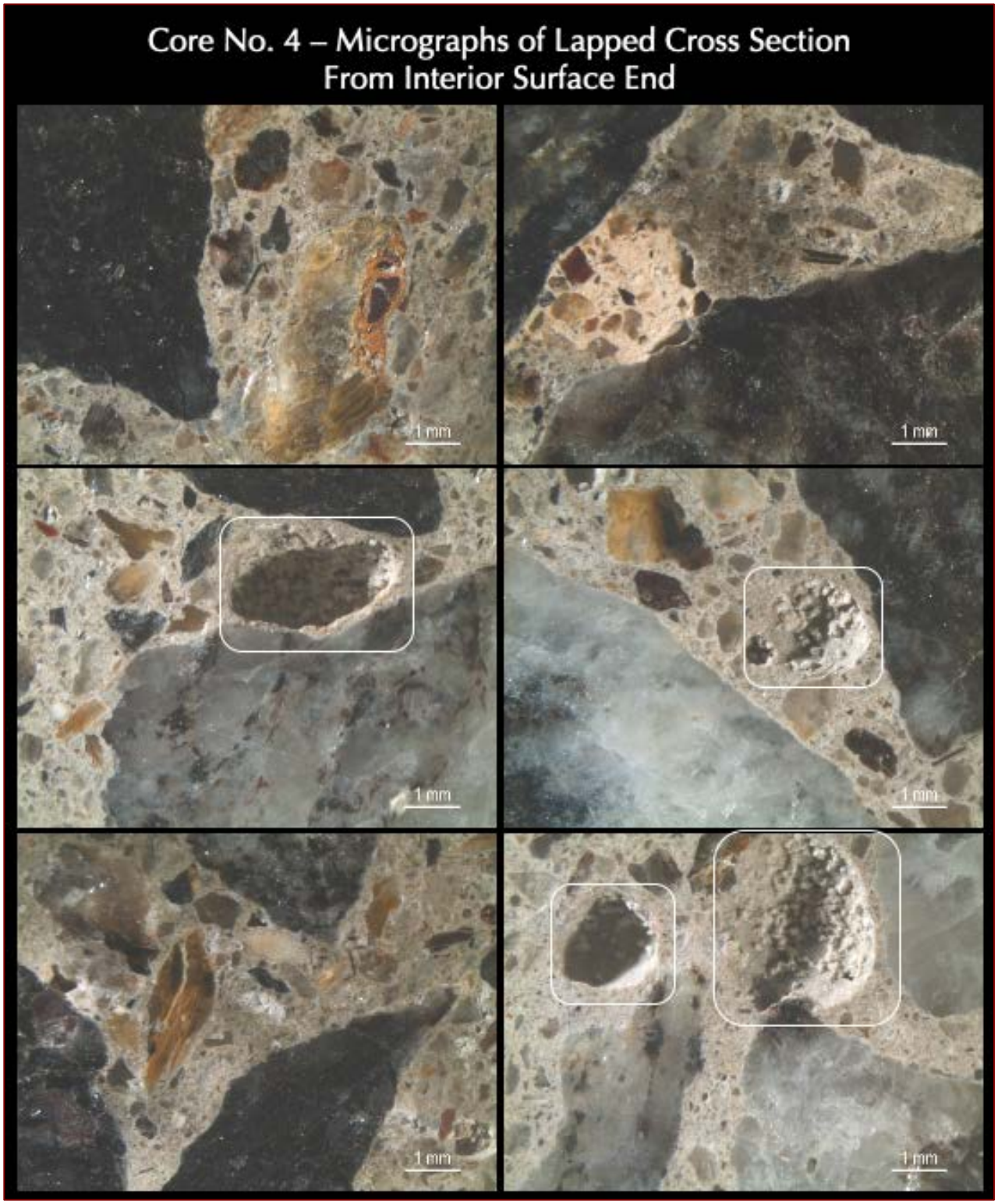

Figure 56: Micrographs of lapped cross section of Core C4 from the interior end showing: (a) beige discolored altered zone at the top 7 mm due to interaction of concrete with the gases, air, and moisture emitted from the containment solution in the tank; (b) secondary ettringite deposits lining the walls of air voids (boxed) indicating prolonged presence of moisture in concrete; and (c) non-air-entrained nature of concrete without any intentionally introduced spherical <1 mm size entrained air (all photos).

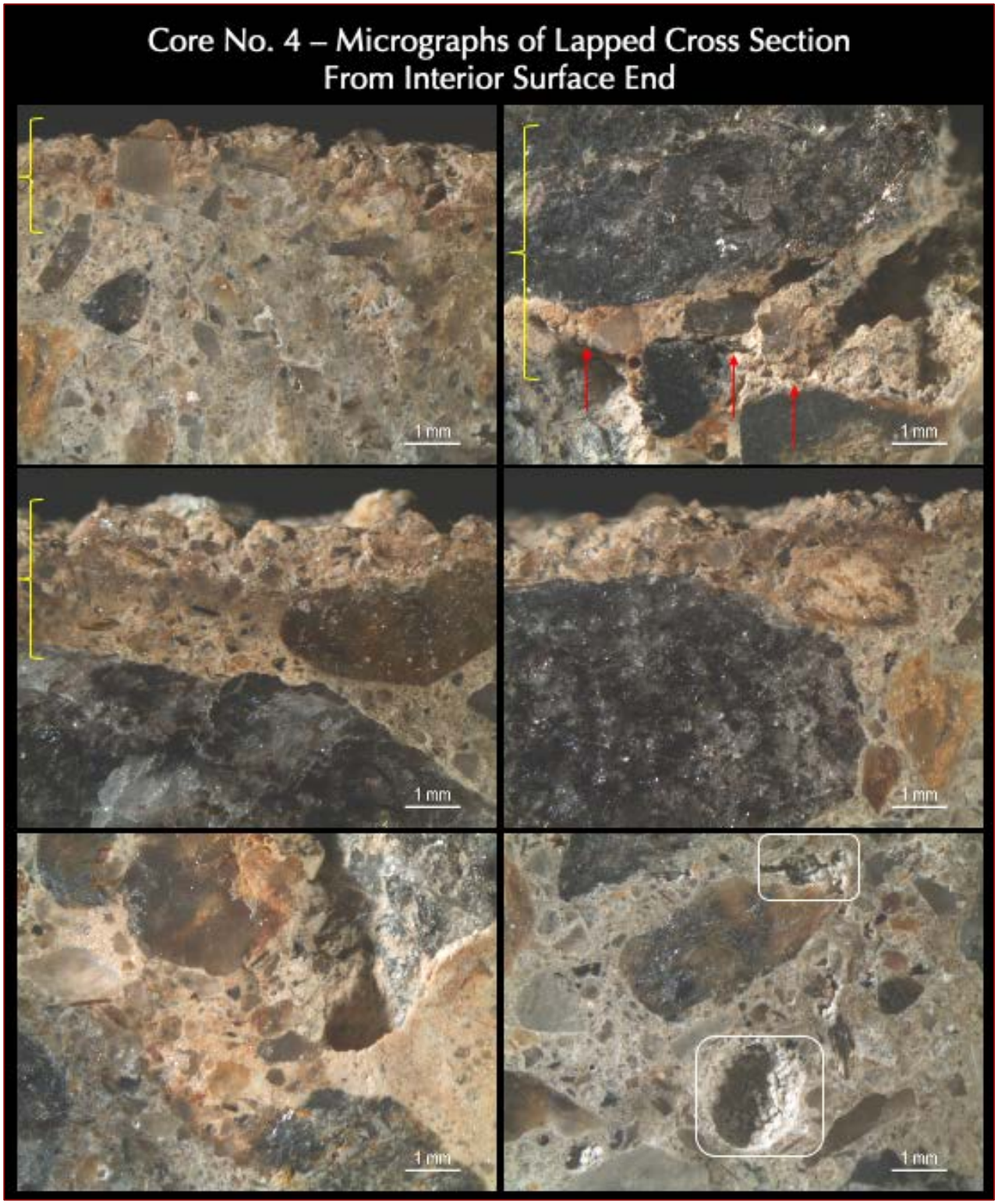

Figure 57: Micrographs of lapped cross section of Core C4 from the interior end showing: (a) beige discolored altered zone at the top 7 mm due to interaction of concrete with the gases, air, and moisture emitted from the containment solution in the tank; (b) secondary ettringite deposits lining the walls of air voids (boxed) indicating prolonged presence of moisture in concrete; and (c) non-air-entrained nature of concrete without any intentionally introduced spherical <1 mm size entrained air (all photos).

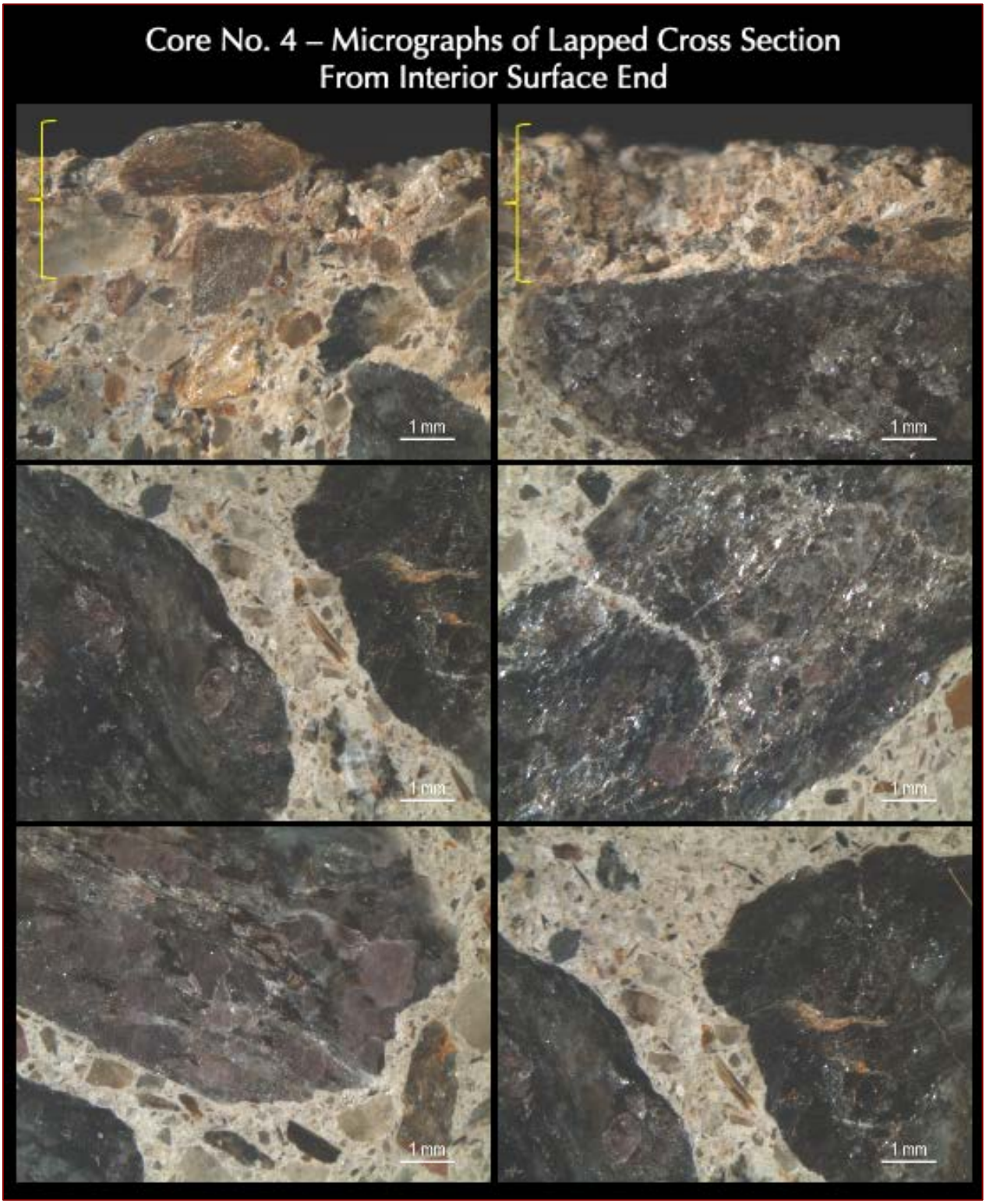

Figure 58: Micrographs of lapped cross section of Core C4 from the interior end showing: (a) beige discolored altered zone at the top 7 mm due to interaction of concrete with the gases, air, and moisture emitted from the containment solution in the tank; and (b) non-air-entrained nature of concrete without any intentionally introduced spherical <1 mm size entrained air (all photos). Notice parallel alignment of micaceous and quarto-feldspathic minerals in crushed schist and gneiss coarse aggregate particles defining the schistose and banded (gneissose) textures.

THIN SECTIONS

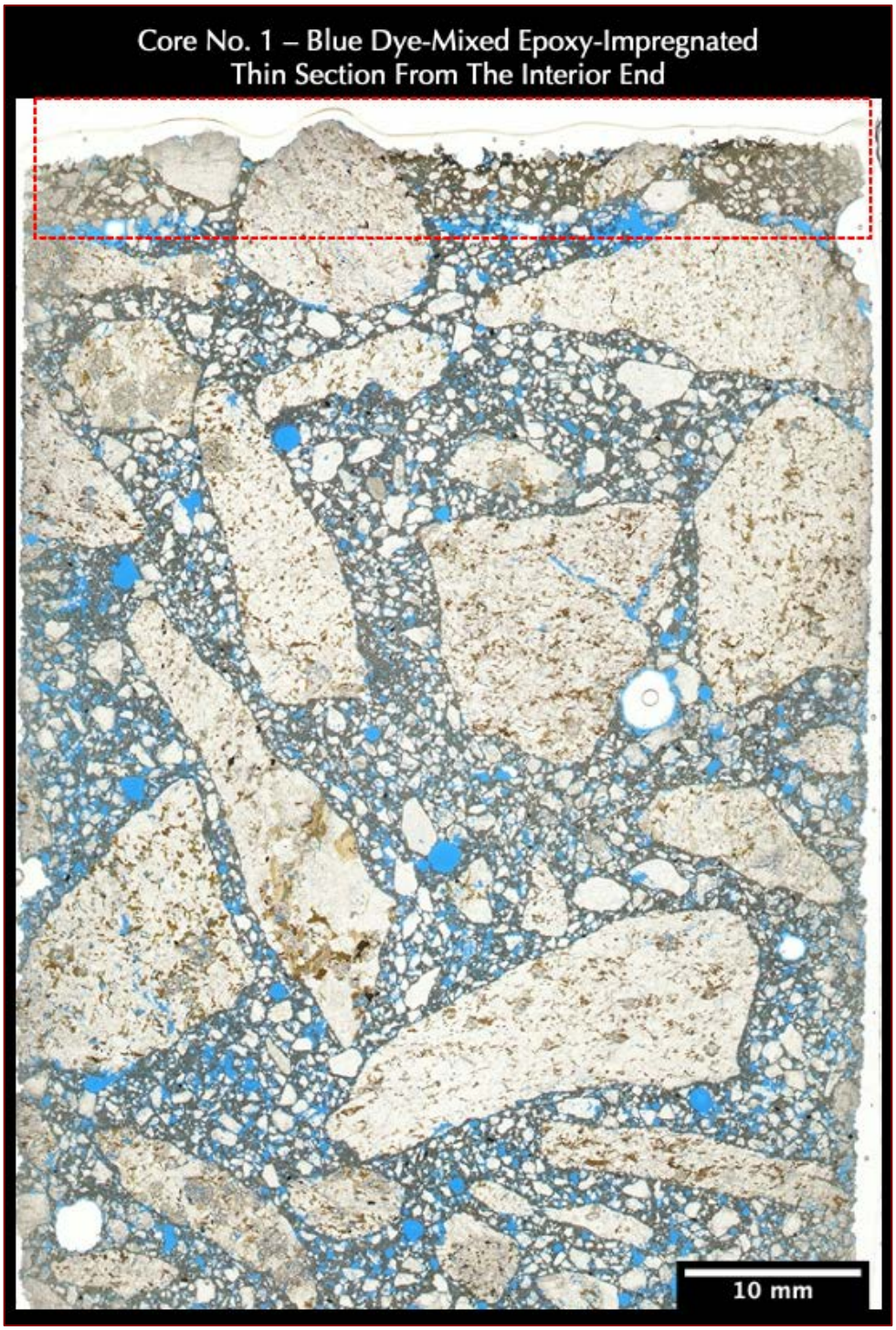

Figure 59: Blue dye-mixed epoxy-impregnated thin section of Core C1 in plane polarized light (PPL) showing: (a) the chemically altered zone at the top 5 mm of interior surface end (boxed); (b) crushed schist and gneiss coarse aggregate and natural siliceous sand fine aggregate; and (c) interstitial paste where air voids and pore spaces are highlighted by blue epoxy.

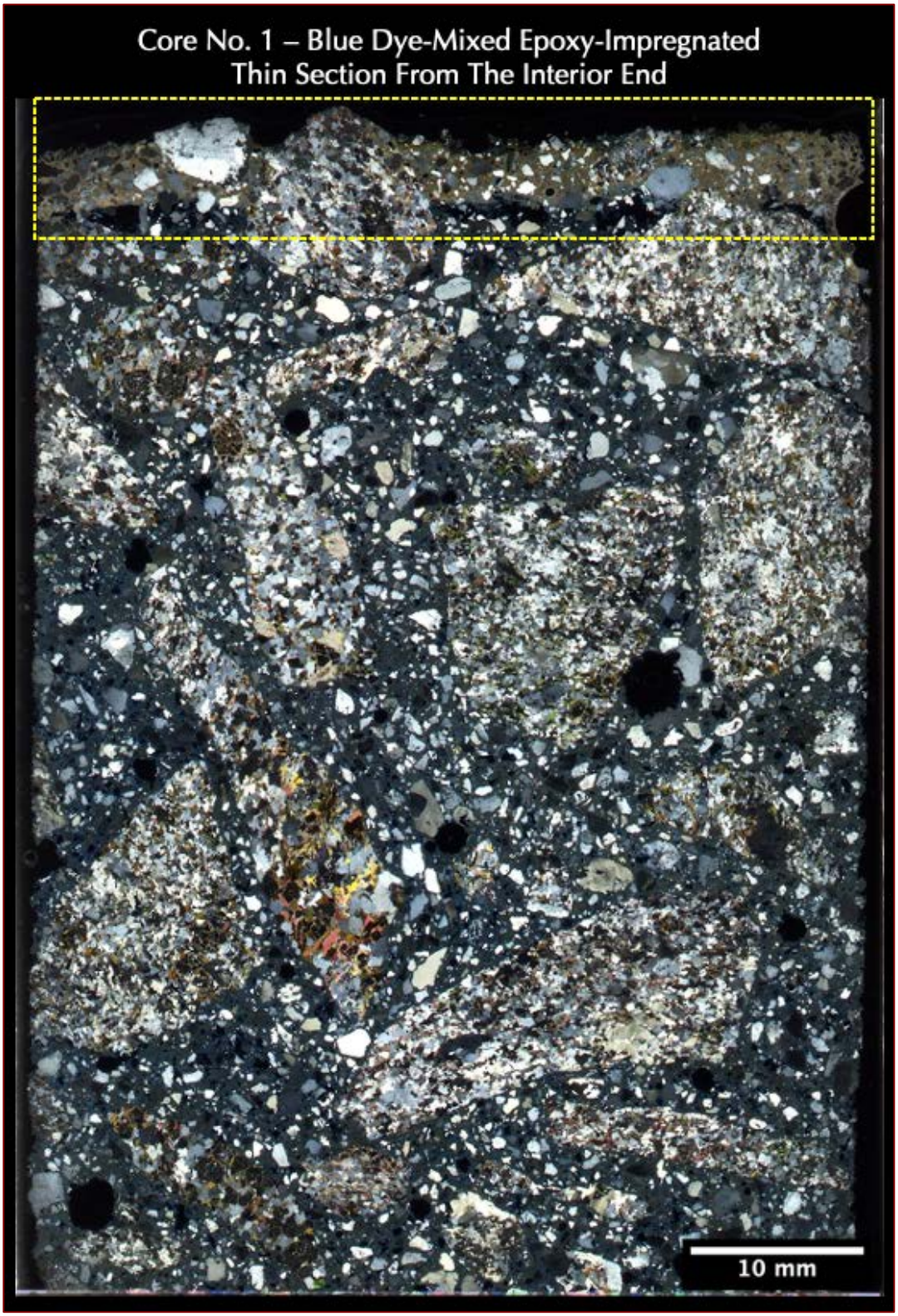

Figure 60: Blue dye-mixed epoxy-impregnated thin section of Core C1 in crossed polarized light (XPL) showing: (a) the chemically altered zone at the top 5 mm of interior surface end (boxed) where paste is carbonated as opposed to non-carbonated interior concrete; and (b) crushed schist and gneiss coarse aggregate and natural siliceous sand fine aggregate.

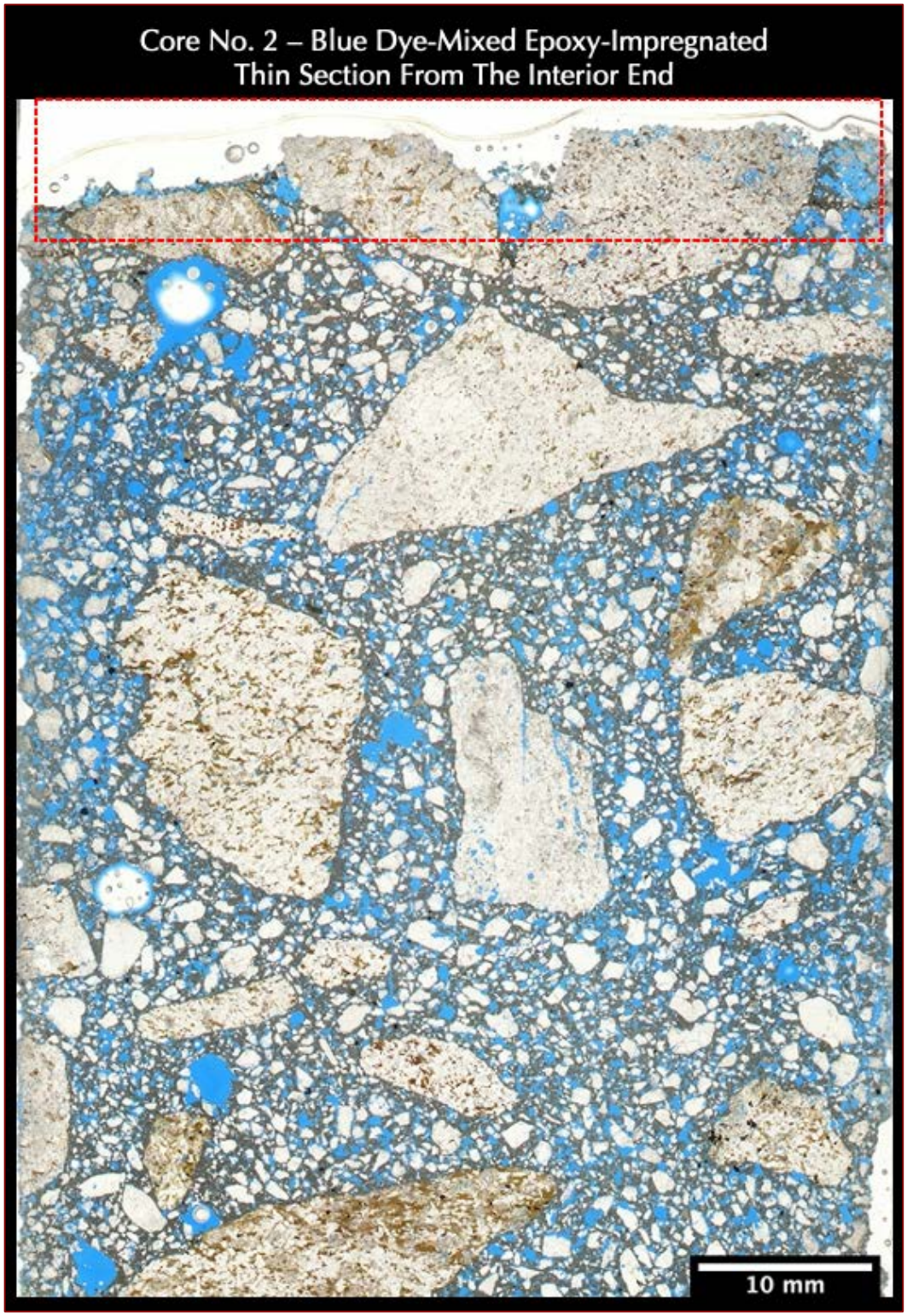

Figure 61: Blue dye-mixed epoxy-impregnated thin section of Core C2 in plane polarized light (PPL) showing: (a) the chemically altered zone at the top 10 mm of interior surface end (boxed); (b) crushed schist and gneiss coarse aggregate and natural siliceous sand fine aggregate; and (c) interstitial paste where air voids and pore spaces are highlighted by blue epoxy.

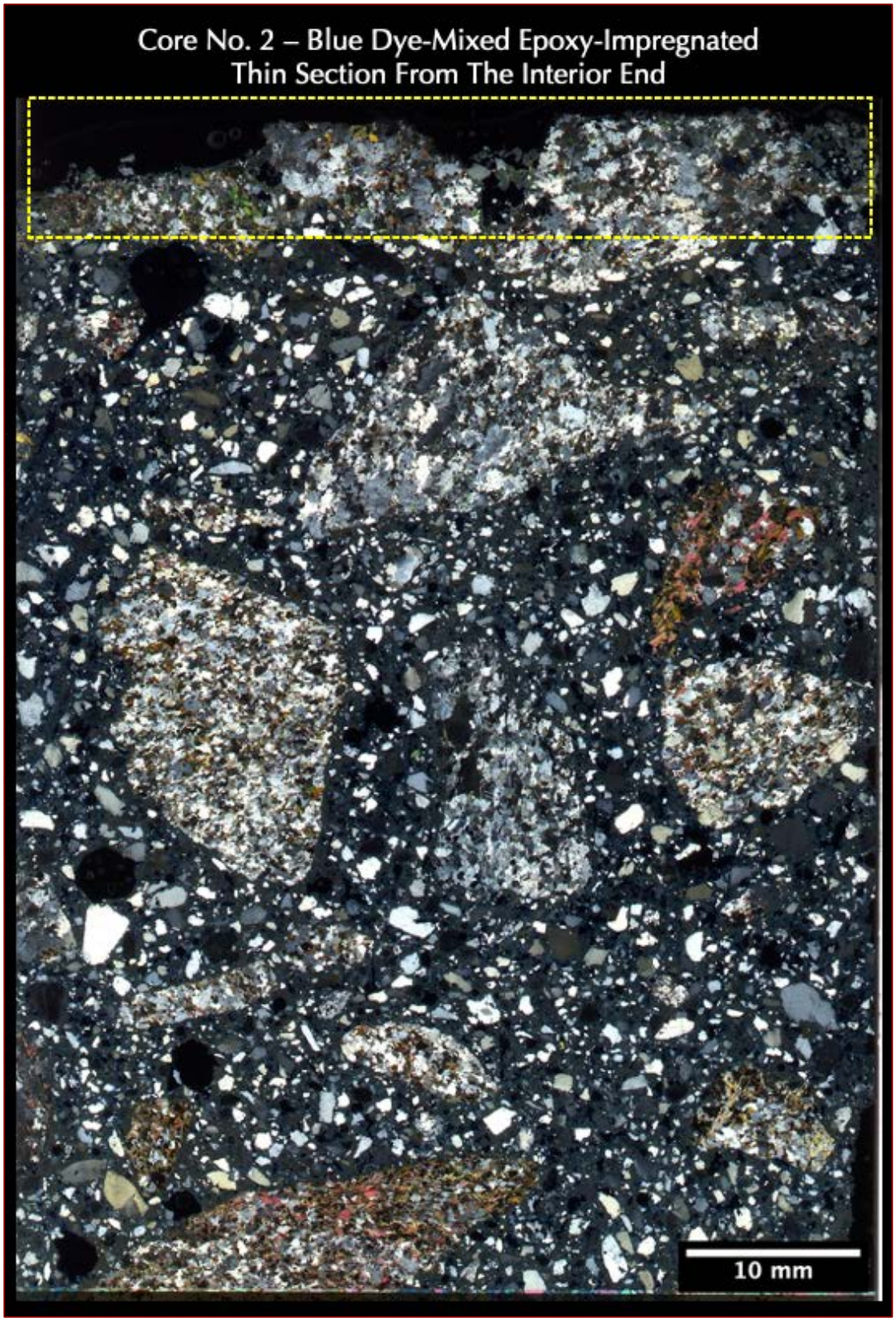

Figure 62: Blue dye-mixed epoxy-impregnated thin section of Core C2 in crossed polarized light (XPL) showing: (a) the chemically altered zone at the top 5 mm of interior surface end (boxed) where paste is carbonated as opposed to non-carbonated interior concrete; and (b) crushed schist and gneiss coarse aggregate and natural siliceous sand fine aggregate.

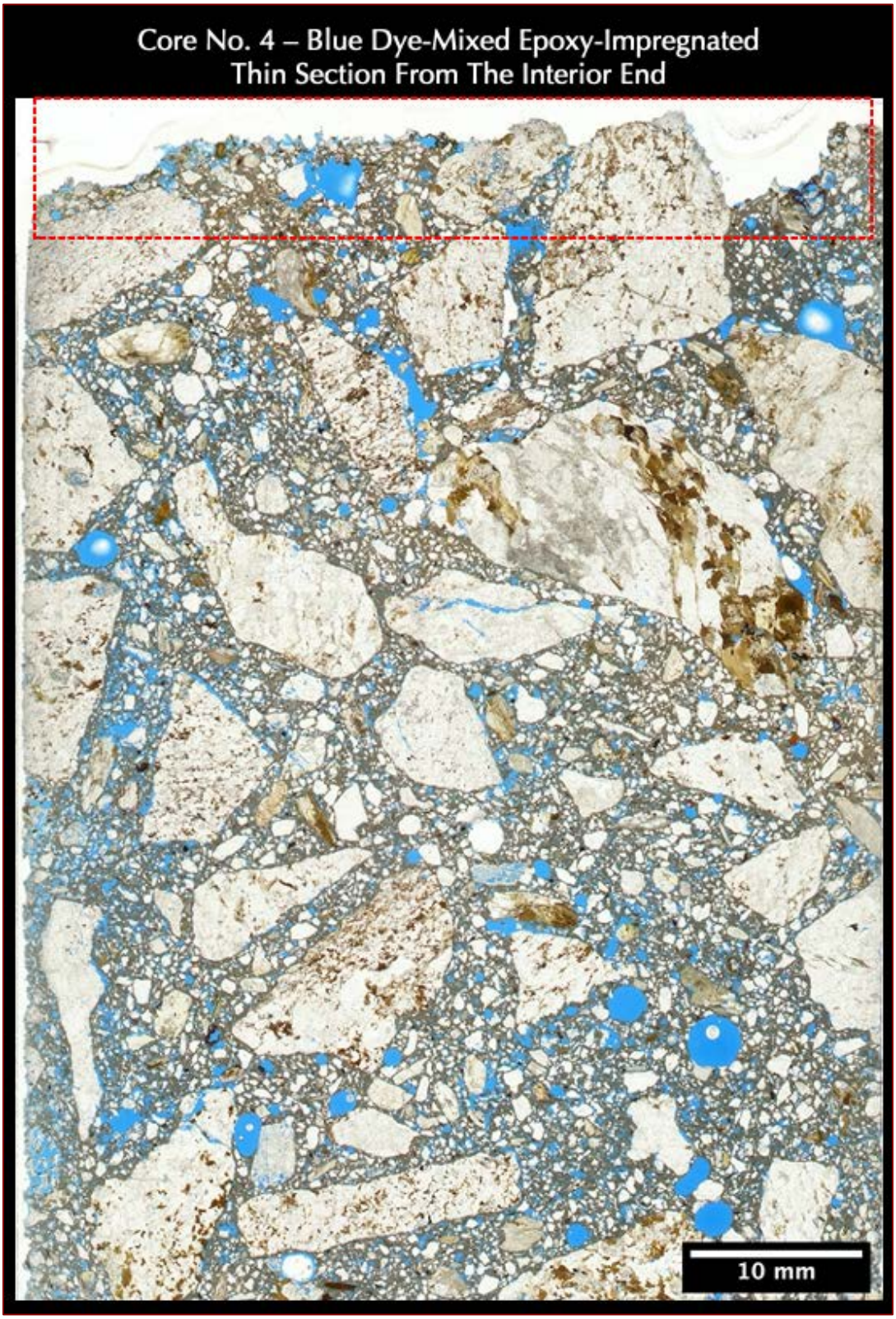

Figure 63: Blue dye-mixed epoxy-impregnated thin section of Core C4 in plane polarized light (PPL) showing: (a) the altered zone at the top 7 mm of interior surface end (boxed); (b) crushed schist and gneiss coarse aggregate and natural siliceous sand fine aggregate; and (c) interstitial paste where air voids and pore spaces are highlighted by blue epoxy.

Figure 64: Blue dye-mixed epoxy-impregnated thin section of Core C4 in crossed polarized light (XPL) showing: (a) the altered zone at the top 7 mm of interior surface end (boxed) where paste is carbonated as opposed to non-carbonated interior concrete; and (b) crushed schist and gneiss coarse aggregate and natural siliceous sand fine aggregate.

MICROGRAPHS OF THIN SECTIONS

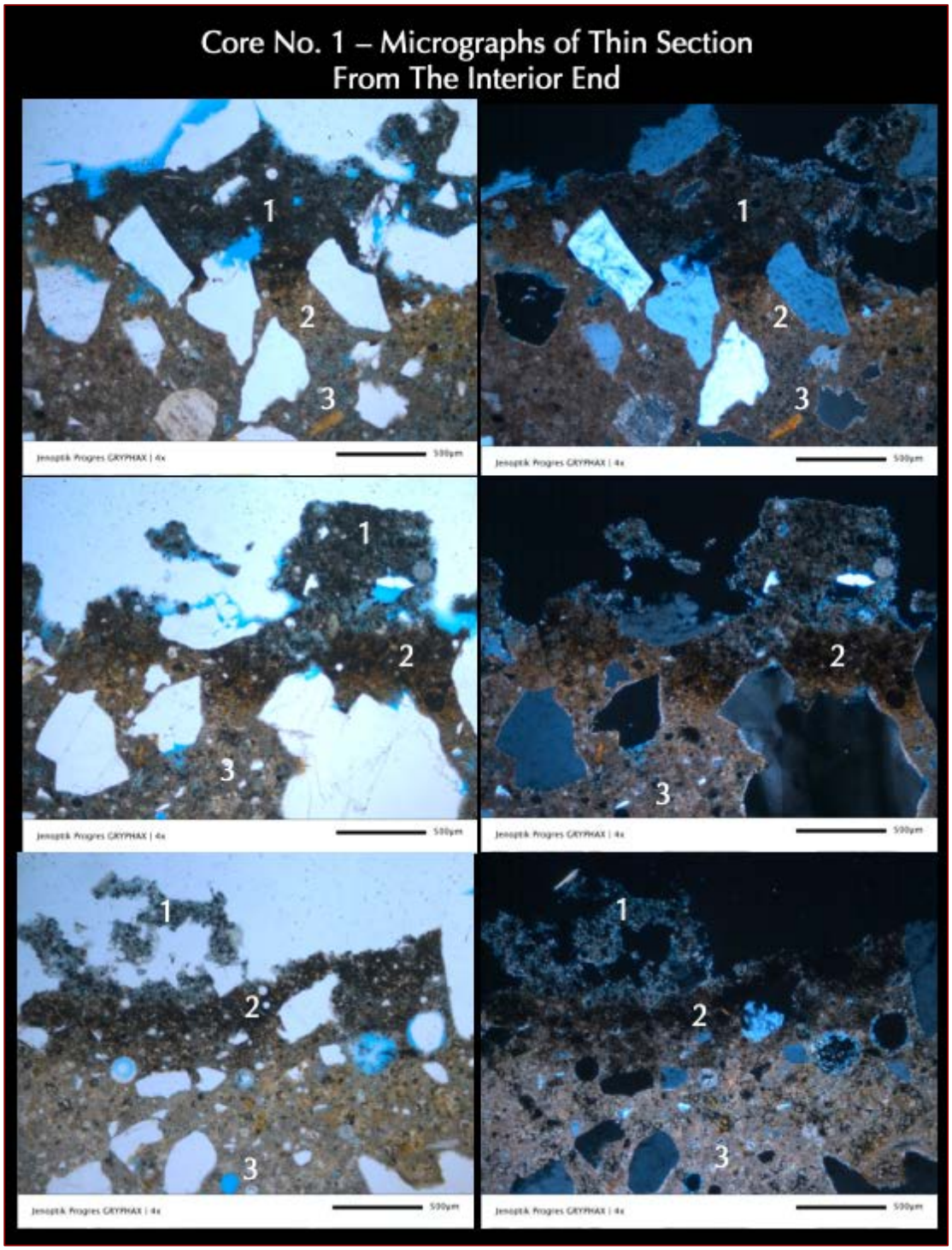

Figure 65: Micrographs of thin section of Core C1 from interior end showing layered zones of alteration of concrete due to interactions with the containment solutions, which are marked as 1, 2, 3, where the dark outermost zone 1 is followed by a reddish-brown mixed oxidized (stained) and carbonated zone 2, then a yellowish-orange carbonated paste zone 3. Scale bars are 0.5 mm in length.

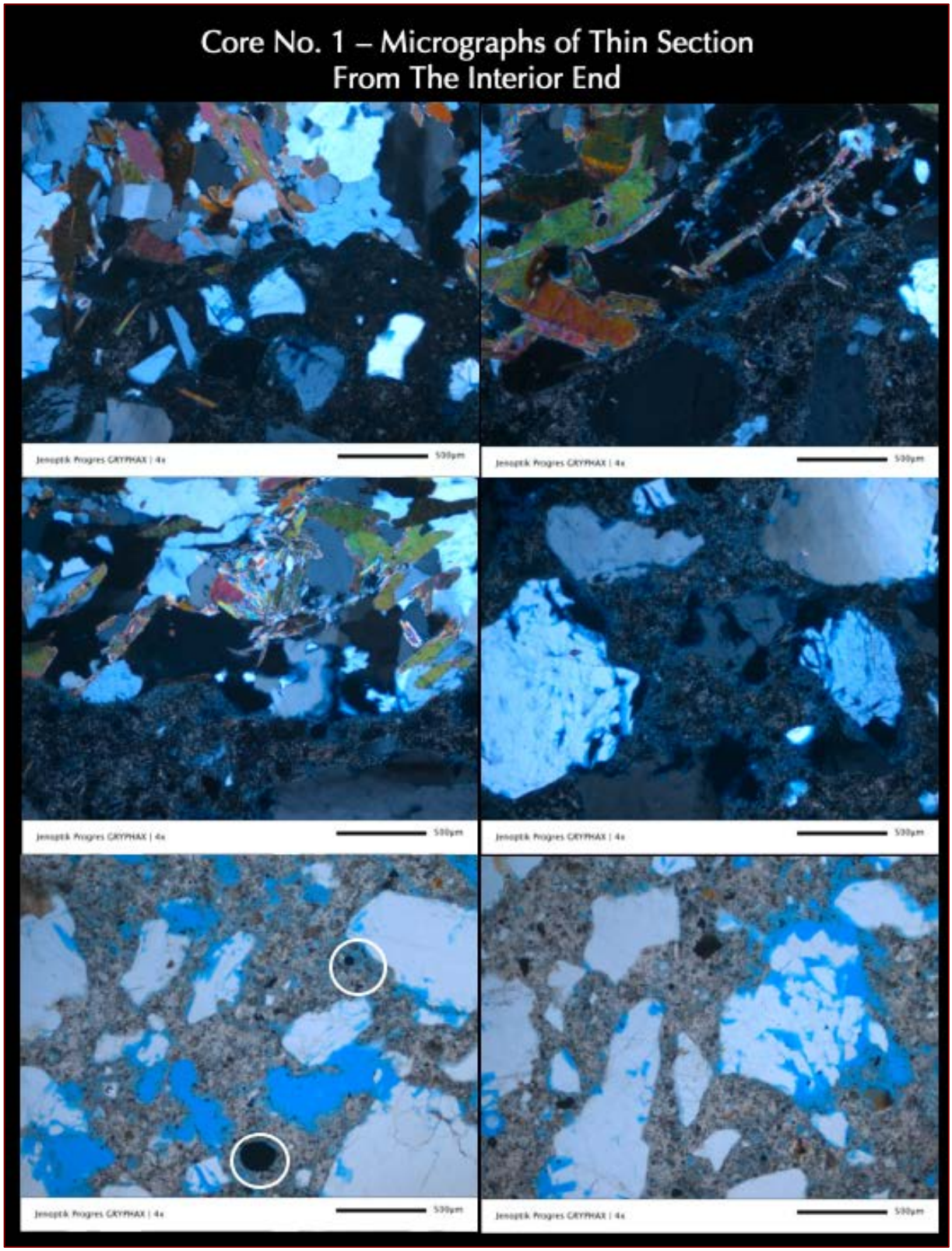

Figure 66: Micrographs of thin section of Core C1 from interior end showing: (a) crushed schist and gneiss coarse aggregate containing quartz, feldspar, micaceous minerals, and disseminated iron sulfide grains, (b) natural siliceous (quartz, quartzite, feldspar) sand fine aggregate, and (c) a hardened paste of major amount of Portland cement and subordinate amount of fly ash where a few spherical residual fly ash particles are circled. Scale bars are 0.5 mm in length.

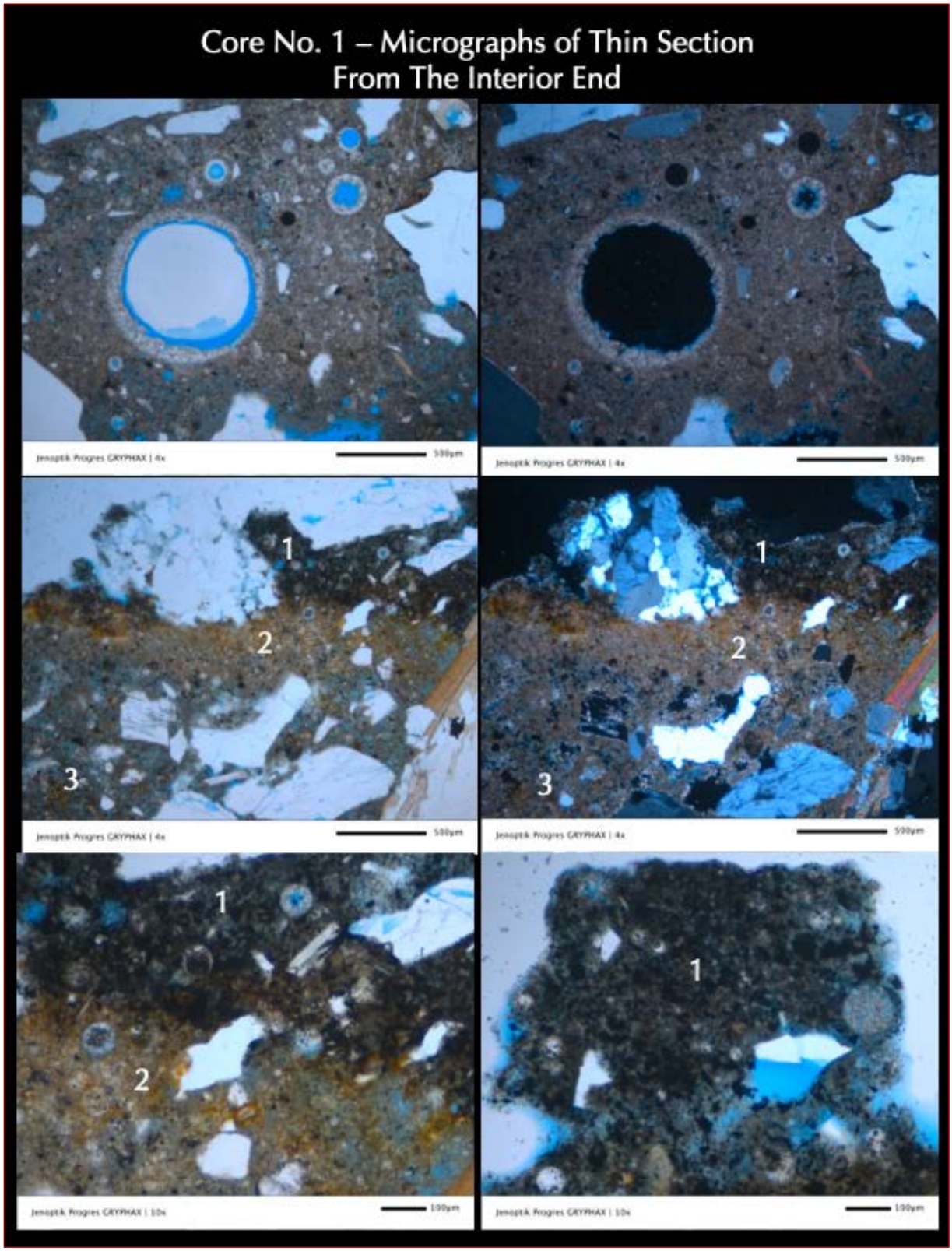

Figure 67: Micrographs of thin section of Core C1 from interior end showing layered zones of alteration of concrete after interaction with the containment solution, which are marked as 1, 2, 3, where the dark outermost zone 1 is followed by a reddish-brown zone 2, then a yellowish-orange carbonated paste zone 3. Scale bars are 0.1 to 0.5 mm in length. The top row photos show secondary calcite precipitation in an air void in the carbonated zone.

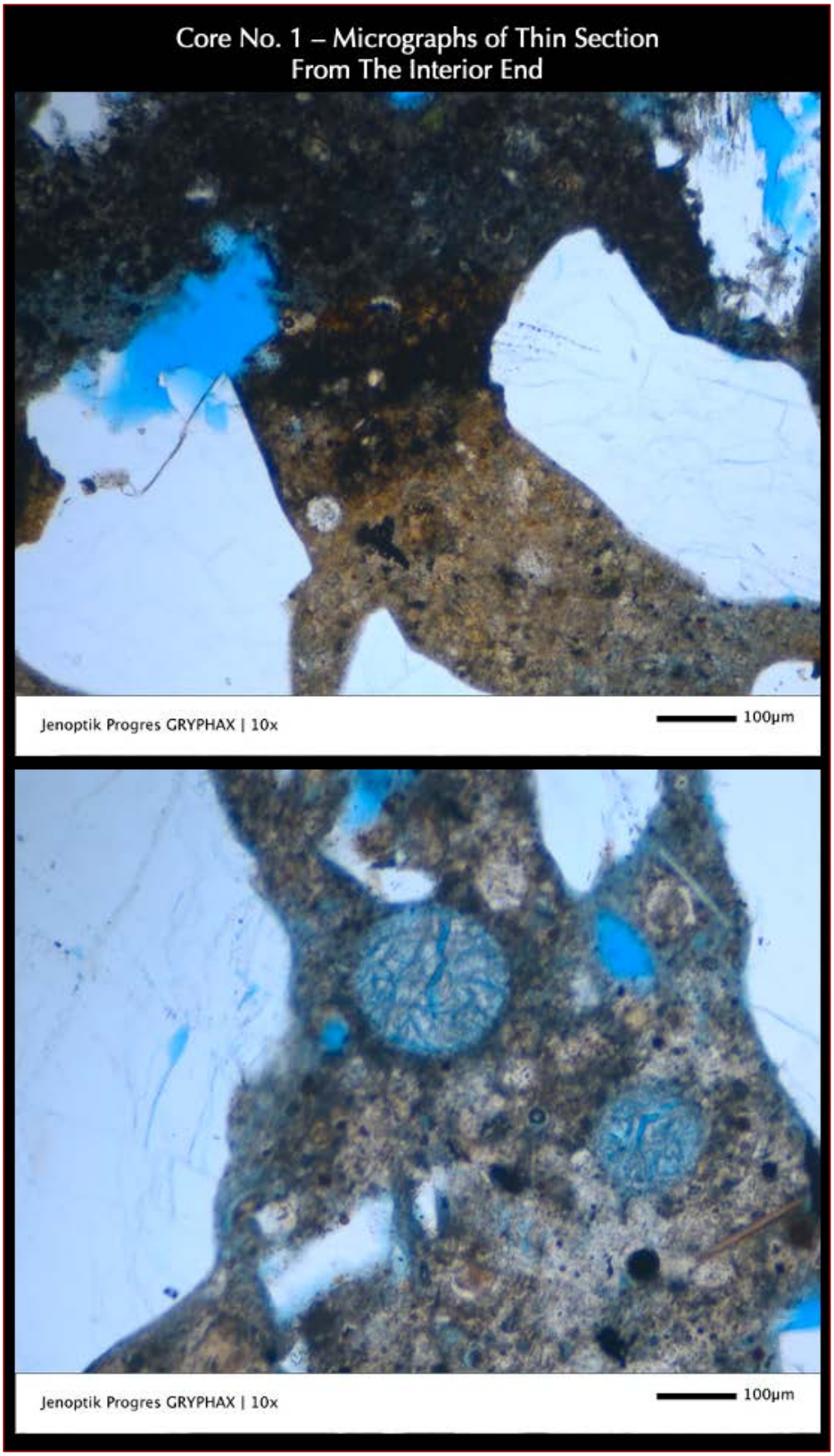

Figure 68: Micrographs of thin section of Core C1 from interior end showing layered zones of alteration of concrete after interaction with the containment solutions at the top photo and secondary ettringite deposits in air voids within the altered zone at the bottom photo. Scale bars are 0.1 mm in length.

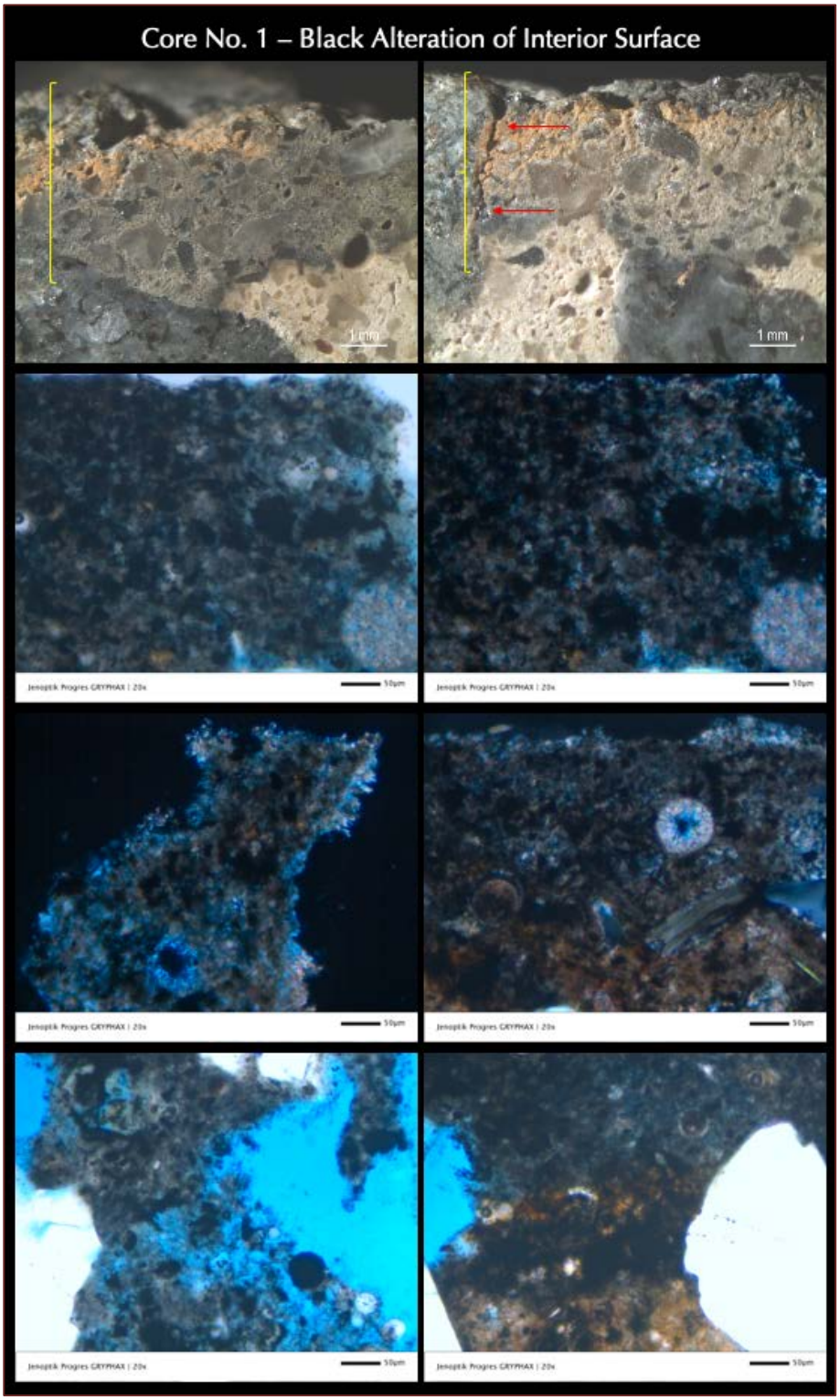

Figure 69: Micrographs of thin section of Core C1 from interior end showing the black, gray, and brown altered zones in lapped cross section at the top row photos and in thin section in the rest of the photos where the black (possibly mixed with some organic materials) altered zone shows carbonation of paste mixed with black deposits of alteration products.

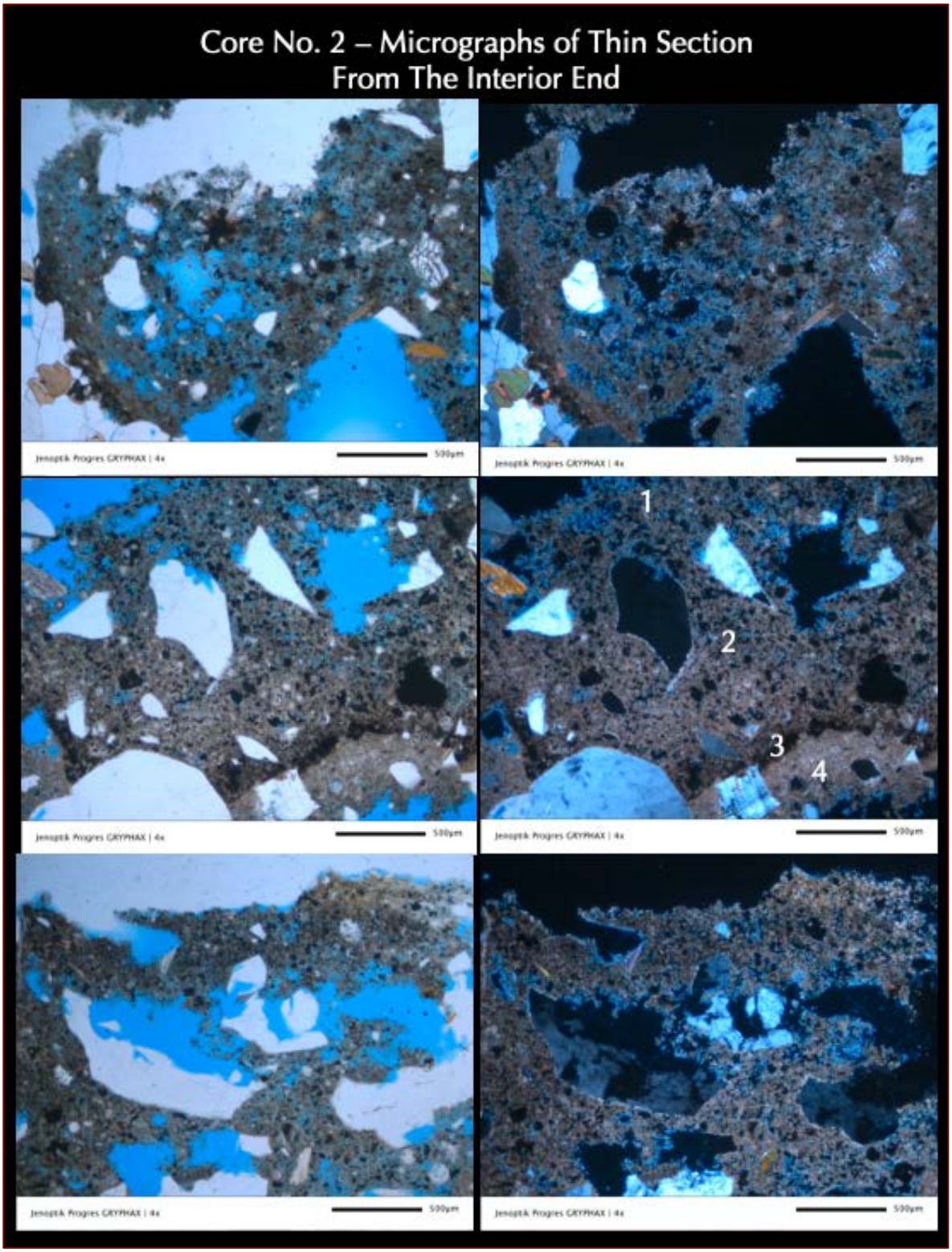

Figure 70: Micrographs of thin section of Core C2 from interior end showing layered zones of alteration of concrete after interaction with the containment solution, which are marked as 1, 2, 3, where the dark outermost zone 1 is followed by a mixed oxidized (stained) and carbonated reddish-brown zone 2, then a yellowish-orange carbonated paste zone 3. Scale bars are 0.5 mm in length.

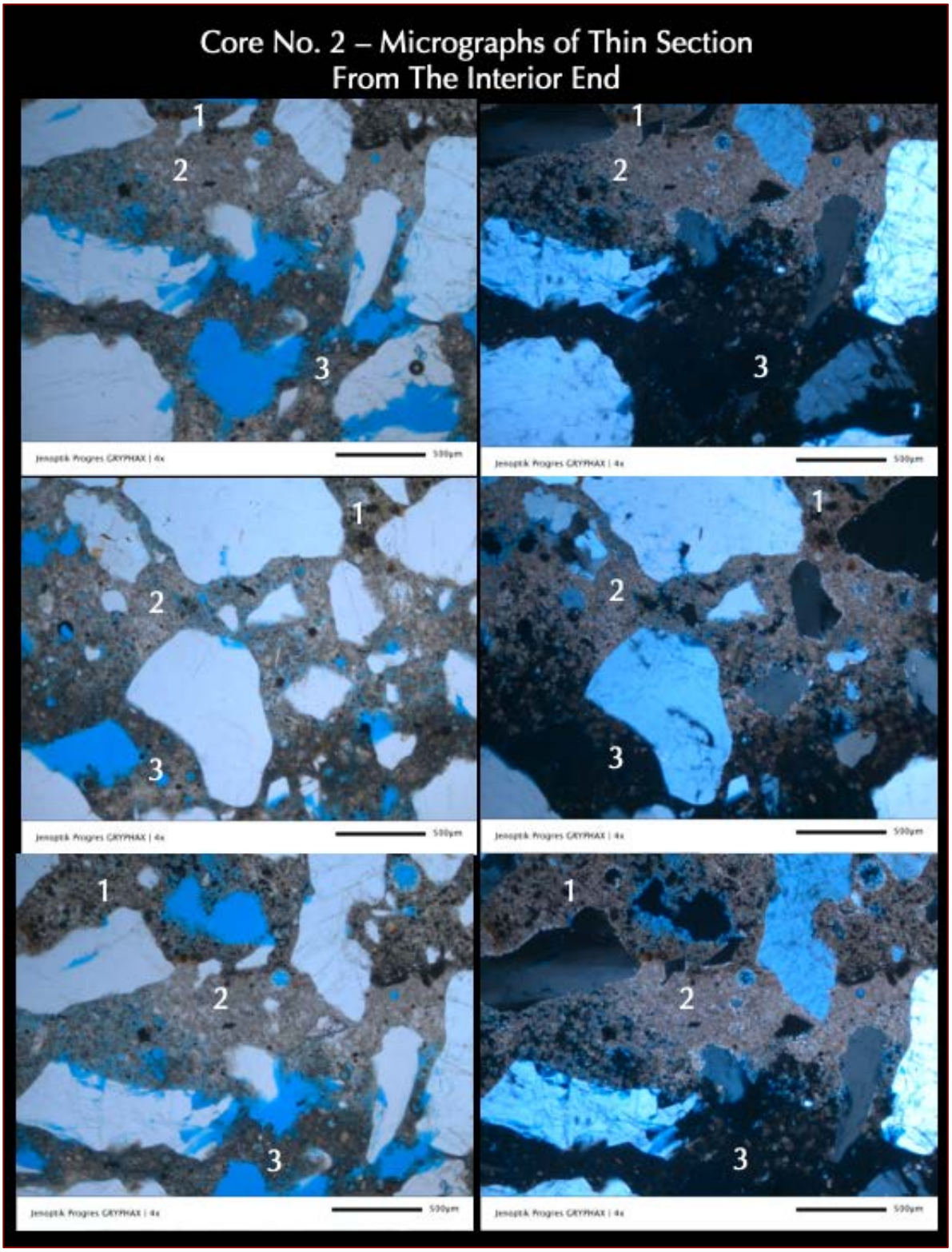

Figure 71: Micrographs of thin section of Core C2 from interior end showing layered zones of alteration of concrete after interaction with the containment solution, which are marked as 1, 2, 3, where the altered zone 1 is followed by a carbonated paste zone 2, and eventually the interior non-carbonated sound concrete in 3. Scale bars are 0.5 mm in length.

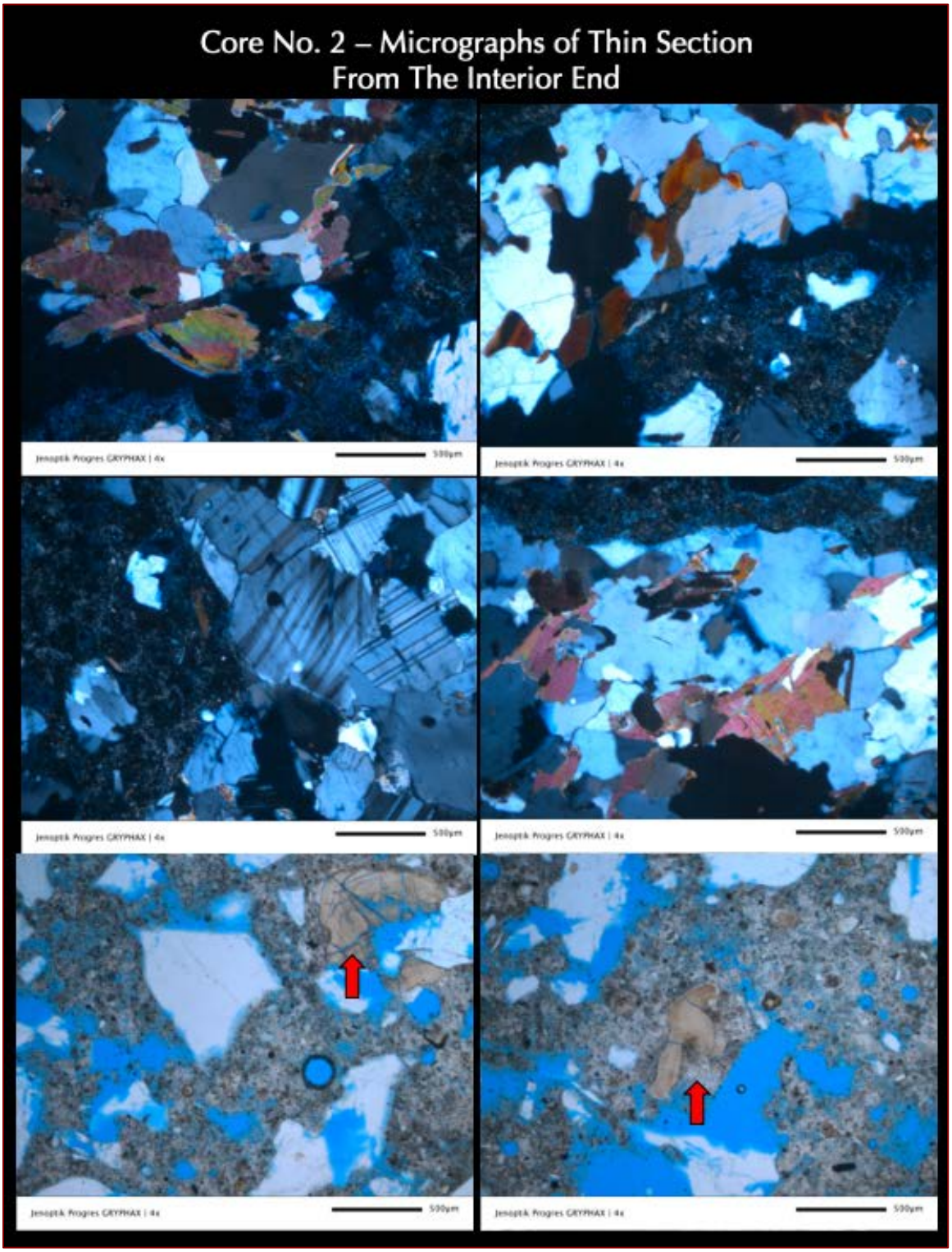

Figure 72: Micrographs of thin section of Core C2 from interior end showing: (a) crushed schist and granite gneiss (middle row) coarse aggregate containing quartz, feldspar, micaceous minerals, and disseminated iron sulfide grains, (b) natural siliceous (quartz, quartzite, feldspar) sand fine aggregate, and (c) a hardened paste of major amount of Portland cement and subordinate amount of fly ash. A few opaline chert particles in fine aggregate that have caused localize alkali-silica reaction and internal cracking are marked with arrows in the bottom row. Scale bars are 0.5 mm in length.

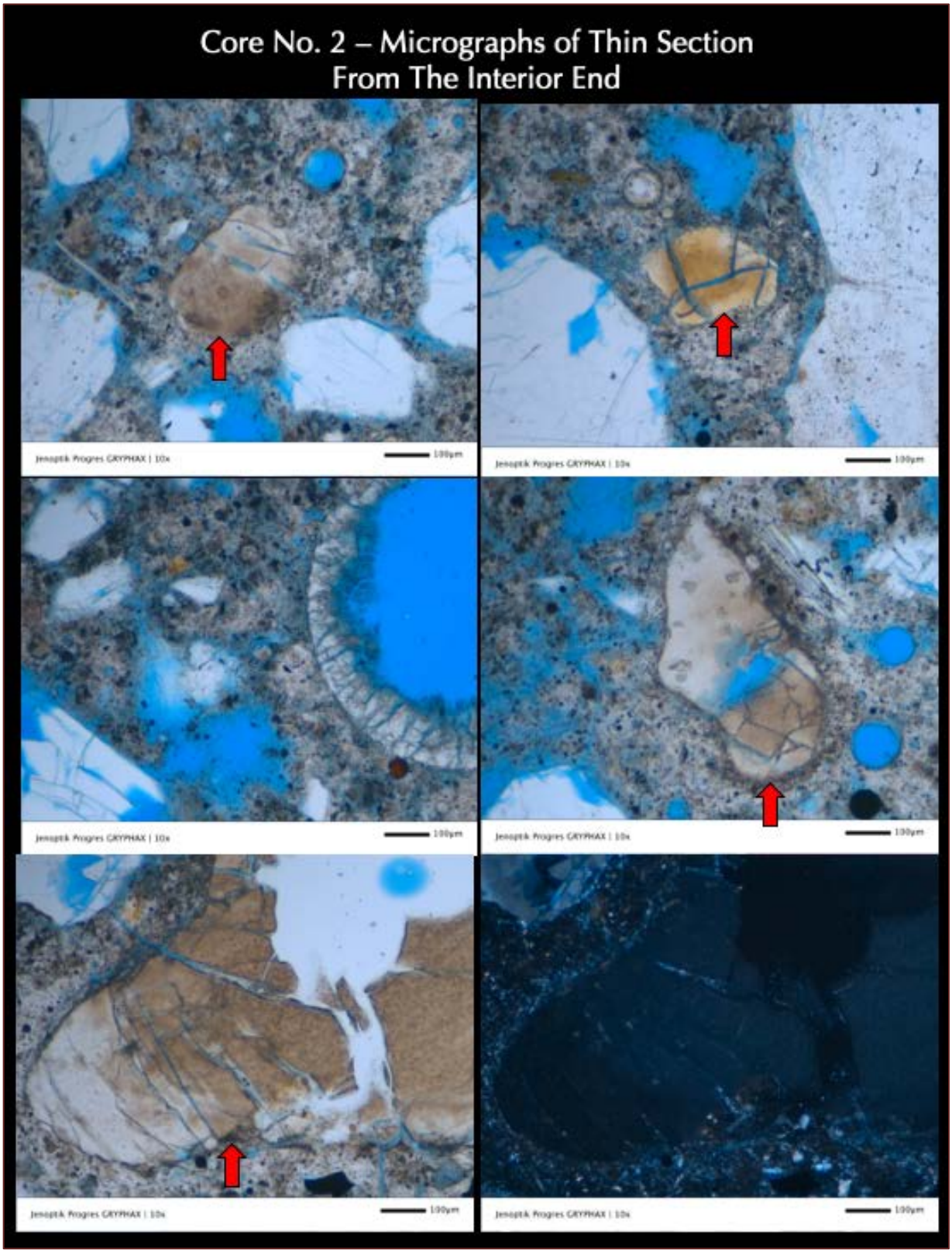

Figure 73: Micrographs of thin section of Core C2 from interior end showing a few opaline chert particles in fine aggregate (arrows) that have caused localize alkali-silica reaction and internal cracking. Scale bars are 0.1 mm in length.

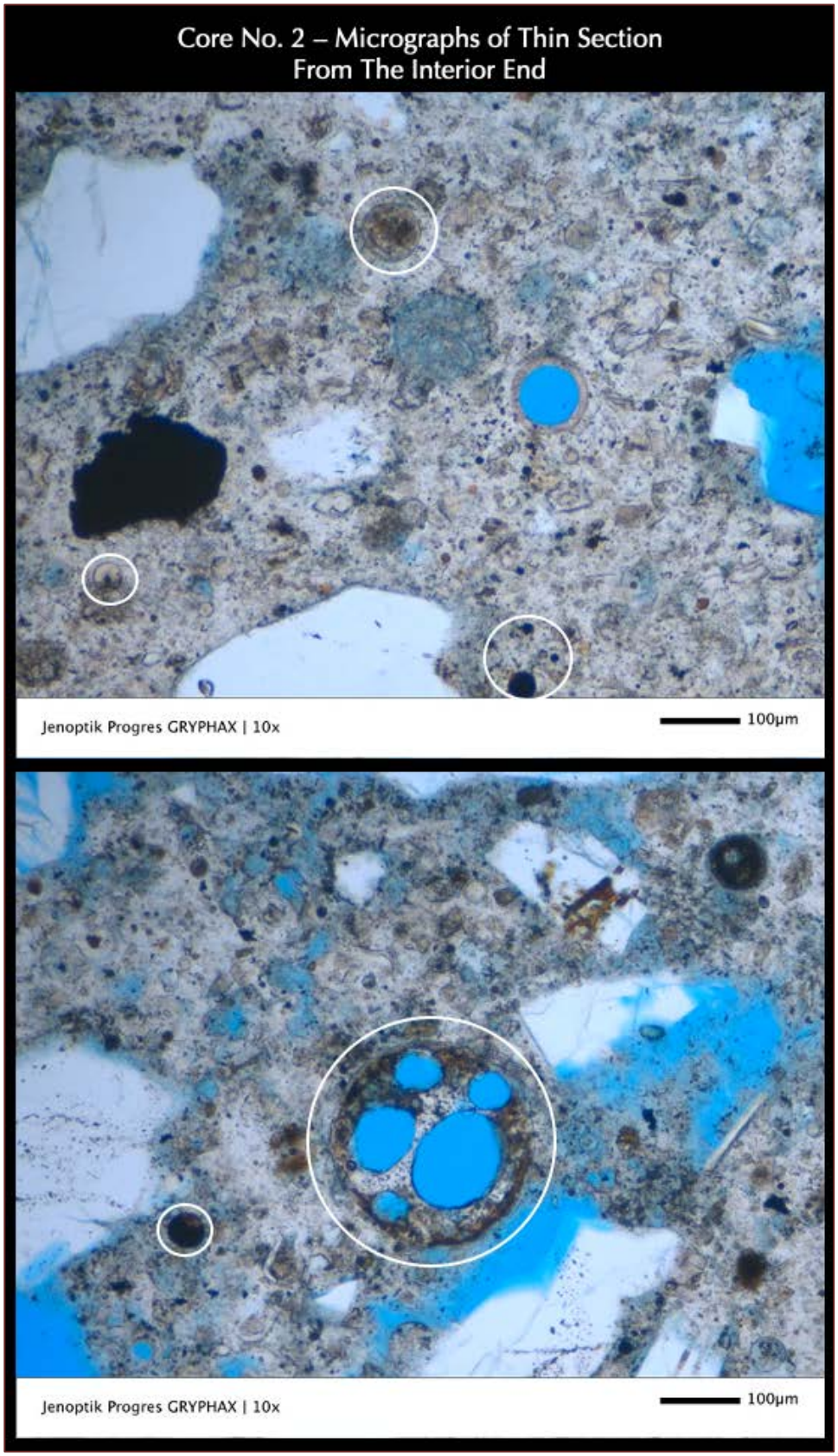

Figure 74: Micrographs of thin section of Core C2 showing a few spherical fly ash particles (circled) scattered over the hardened cement paste.

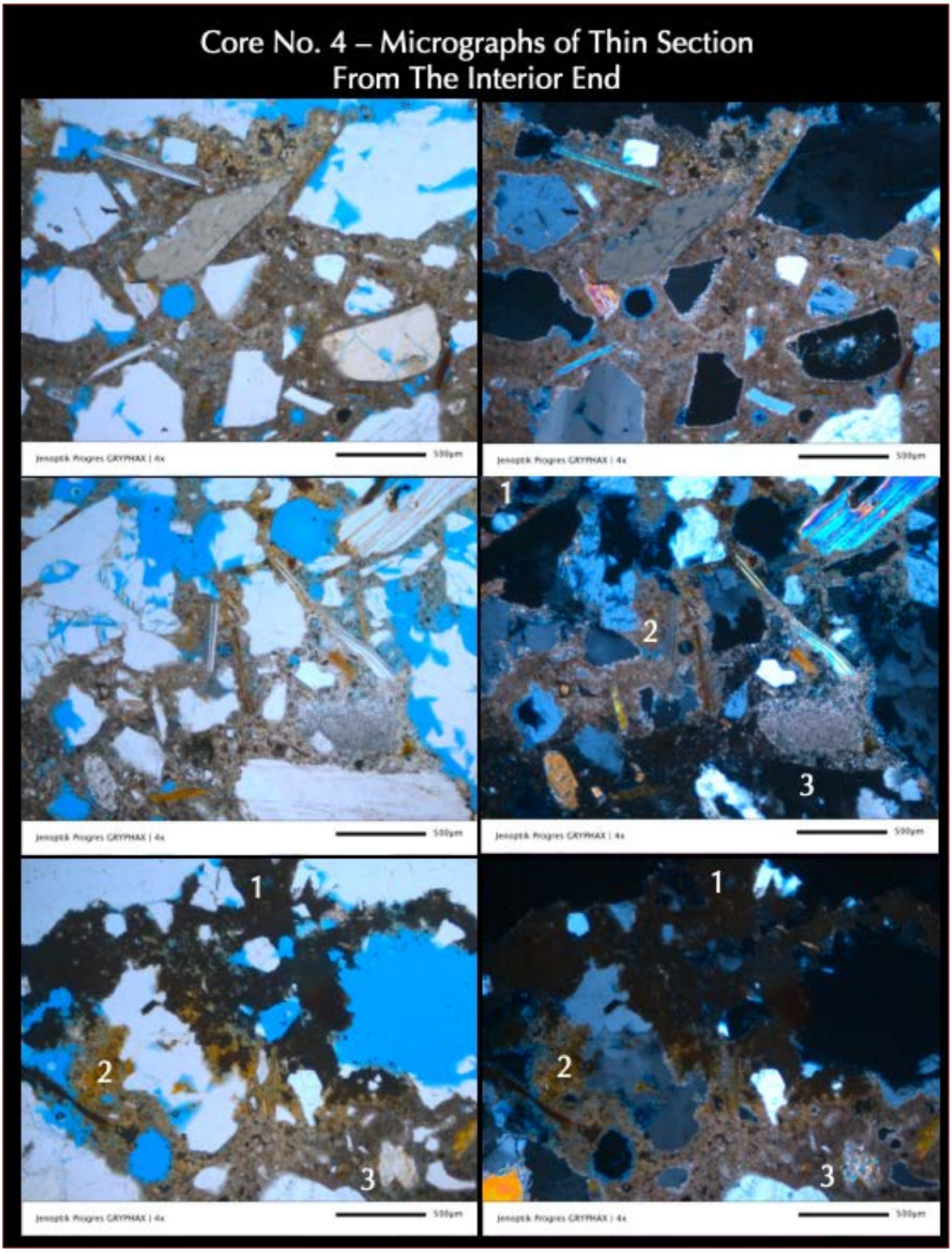

Figure 75: Micrographs of thin section of Core C4 from interior end showing layered zones of alteration of concrete after interaction with the containment solutions, which are marked as 1, 2, 3, where the dark outermost zone 1 is followed by an intermediate mixed oxidized (stained) and carbonated reddish-brown zone 2, then a yellowish-orange carbonated paste zone 3. Scale bars are 0.5 mm in length.

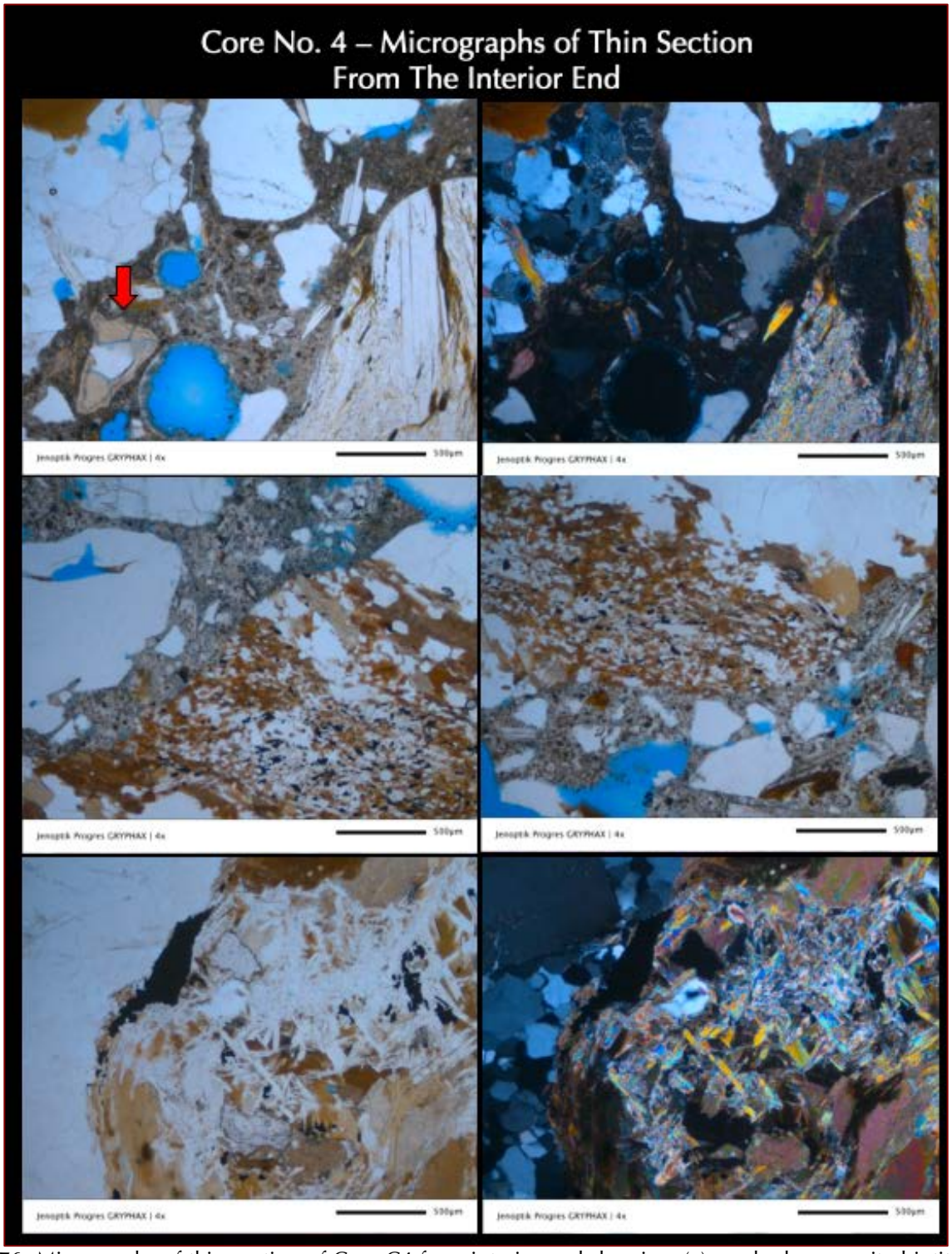

Figure 76: Micrographs of thin section of Core C4 from interior end showing: (a) crushed muscovite-biotite schist coarse aggregate containing quartz, feldspar, micaceous minerals, and disseminated iron sulfide grains, (b) natural siliceous (quartz, quartzite, feldspar) sand fine aggregate, and (c) a hardened paste of major amount of Portland cement and subordinate amount of fly ash. A few opaline chert particles in fine aggregate that have caused localize alkali-silica reaction and internal cracking are marked with arrows in the top left photo. Scale bars are 0.5 mm in length.

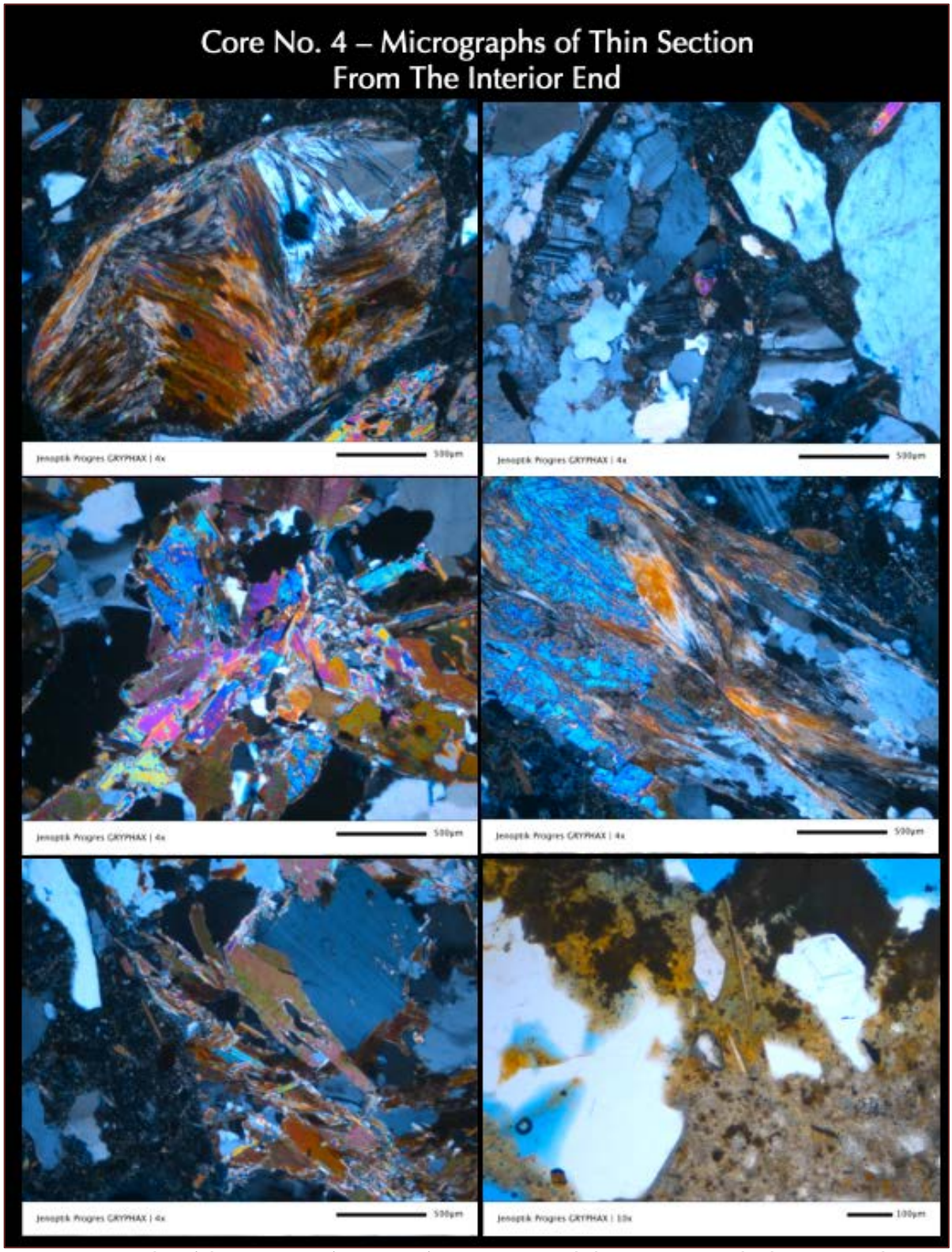

Figure 77: Micrographs of thin section of Core C4 from interior end showing: (a) crushed muscovite-biotite schist coarse aggregate containing quartz, feldspar, micaceous minerals, and disseminated iron sulfide grains, (b) natural siliceous (quartz, quartzite, feldspar) sand fine aggregate, and (c) a hardened paste of major amount of Portland cement and subordinate amount of fly ash. Scale bars are 0.1 to 0.5 mm in length.

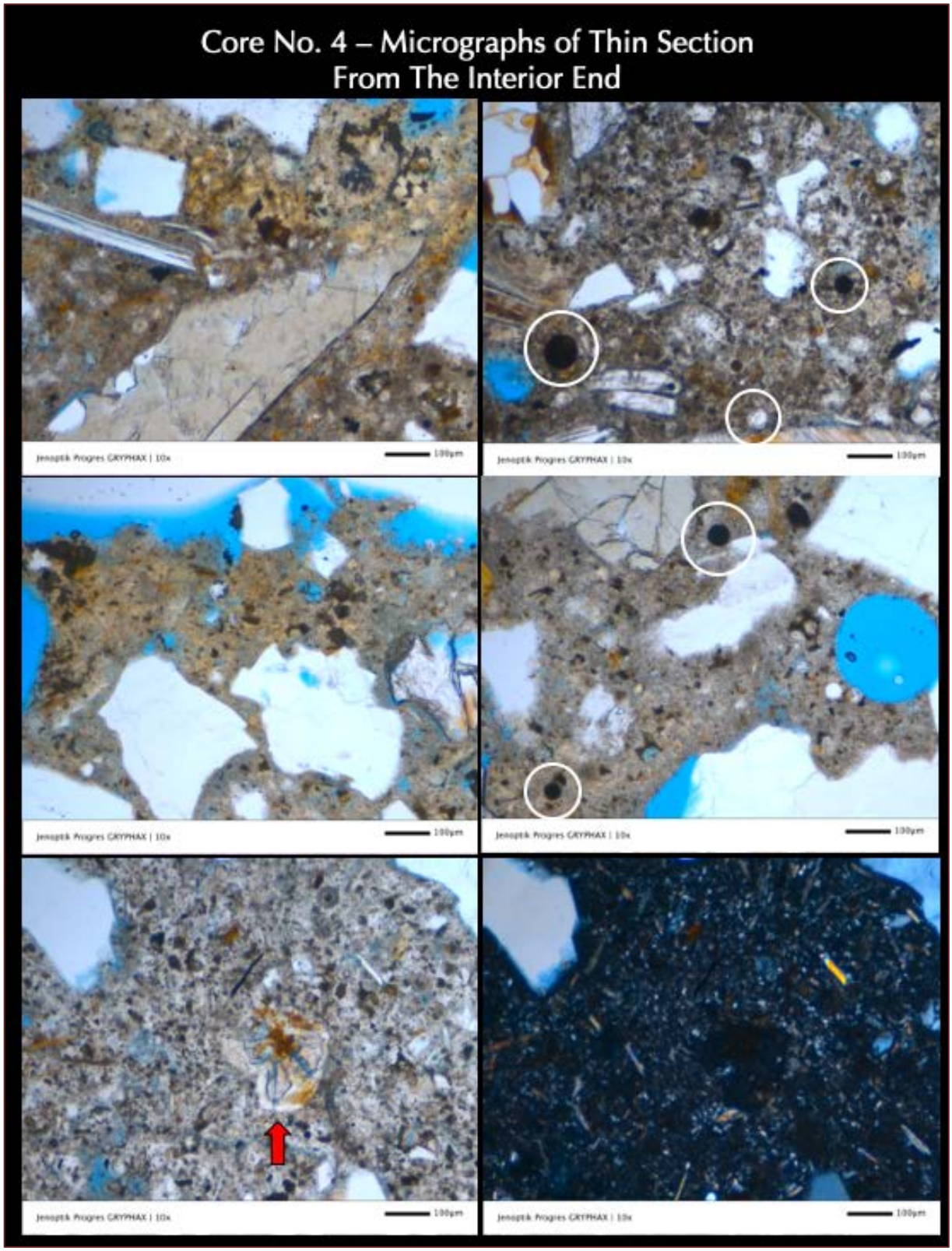

Figure 78: Micrographs of thin section of Core C4 showing a few spherical fly ash particles (circled) scattered over the hardened cement paste. The bottom row shows an opaline chert in fine aggregate (arrow).

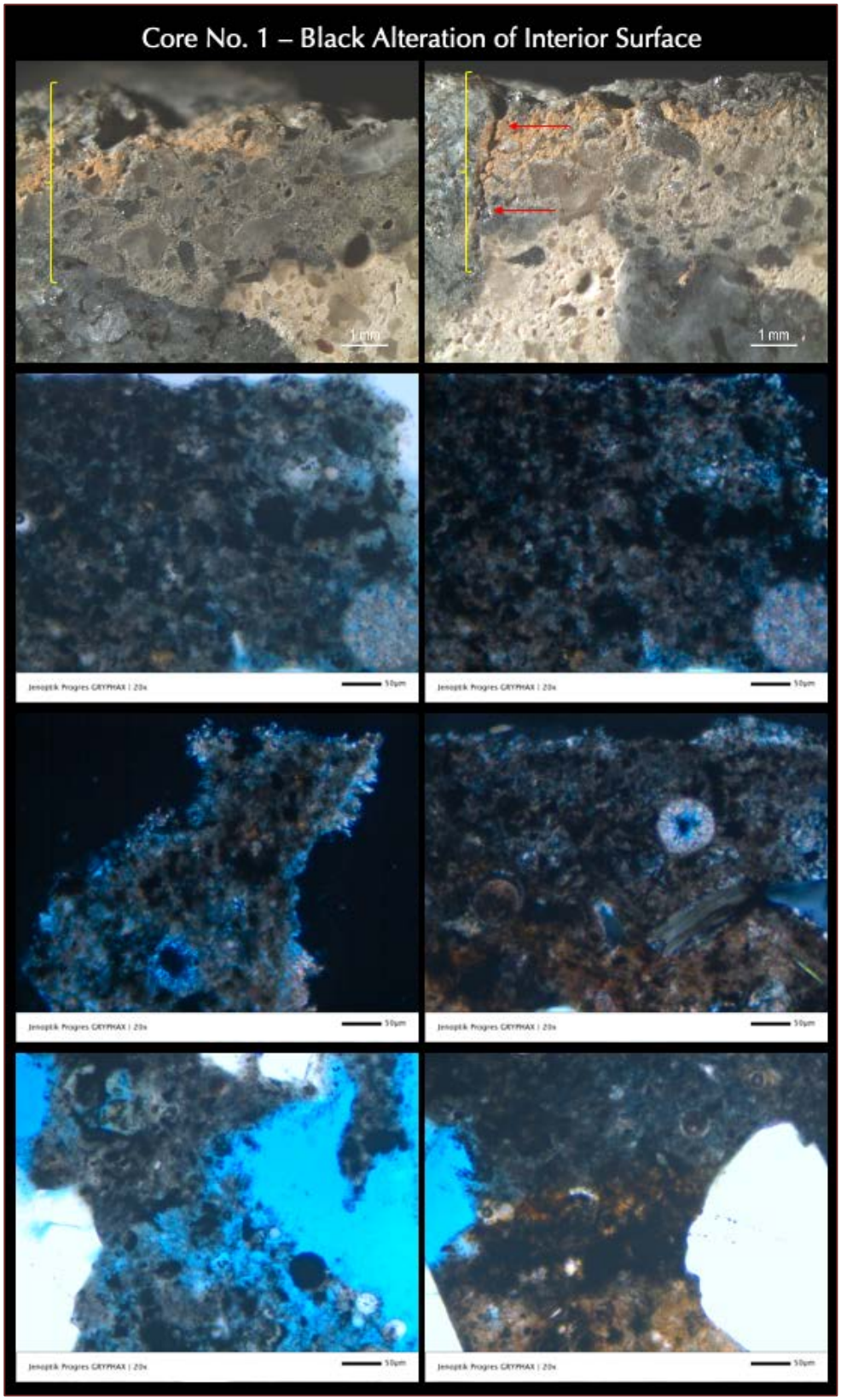

Figure 79: Micrographs of thin section of Core C1 showing various superposed alteration of the interior surface end of tank wall from atmospheric carbonation to precipitation of deposits from the tank's containment solutions.

SEM-EDS ANALYSES OF ALTERED ZONE IN CORE 1

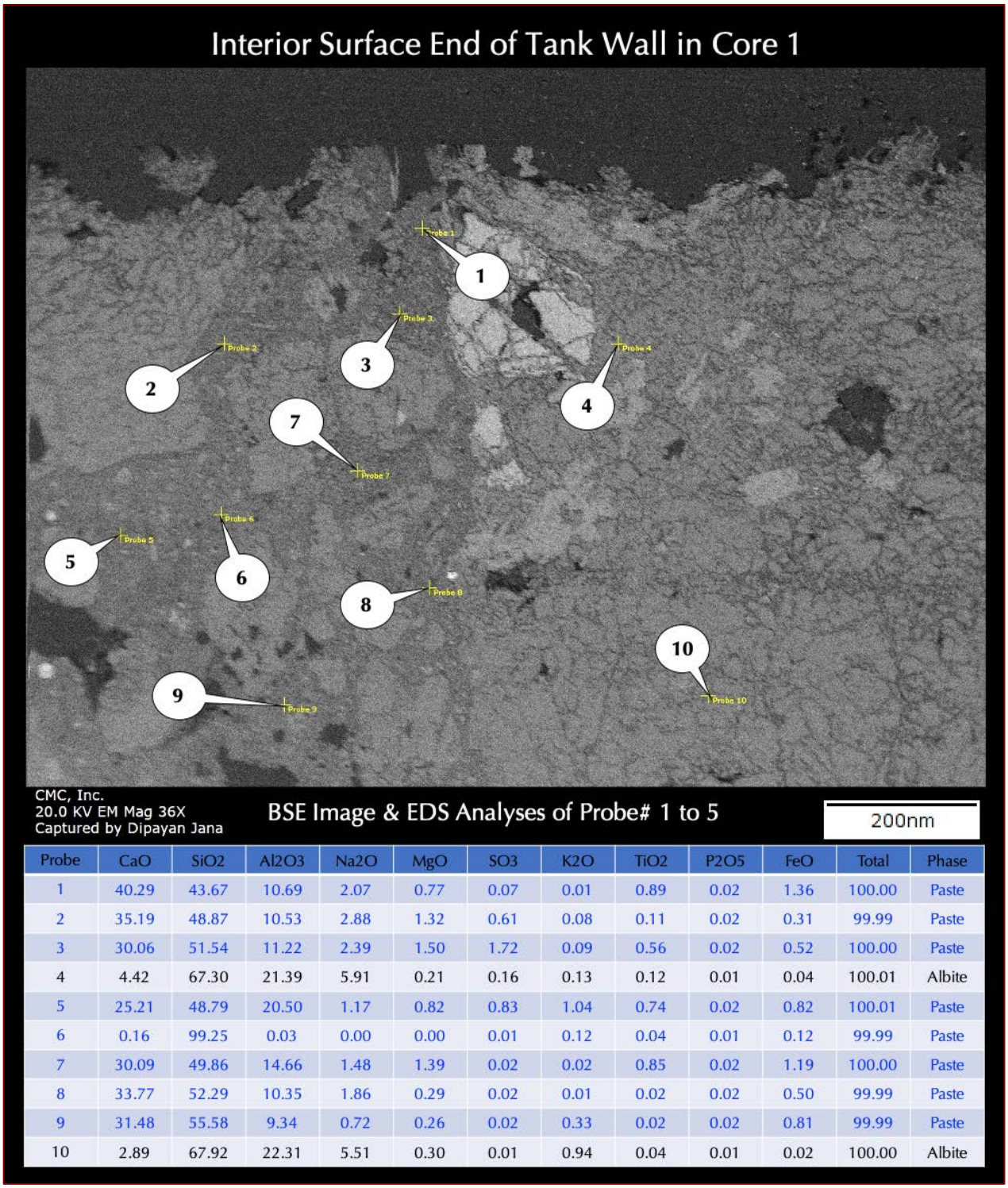

Probe	CaO	SiO2	Al2O3	Na2O	MgO	SO3	K2O	TiO2	P2O5	FeO	Total	Phase
1	40.29	43.67	10.69	2.07	0.77	0.07	0.01	0.89	0.02	1.36	100.00	Paste
2	35.19	48.87	10.53	2.88	1.32	0.61	0.08	0.11	0.02	0.31	99.99	Paste
3	30.06	51.54	11.22	2.39	1.50	1.72	0.09	0.56	0.02	0.52	100.00	Paste
4	4.42	67.30	21.39	5.91	0.21	0.16	0.13	0.12	0.01	0.04	100.01	Albite
5	25.21	48.79	20.50	1.17	0.82	0.83	1.04	0.74	0.02	0.82	100.01	Paste
6	0.16	99.25	0.03	0.00	0.00	0.01	0.12	0.04	0.01	0.12	99.99	Paste
7	30.09	49.86	14.66	1.48	1.39	0.02	0.02	0.85	0.02	1.19	100.00	Paste
8	33.77	52.29	10.35	1.86	0.29	0.02	0.01	0.02	0.02	0.50	99.99	Paste
9	31.48	55.58	9.34	0.72	0.26	0.02	0.33	0.02	0.02	0.81	99.99	Paste
10	2.89	67.92	22.31	5.51	0.30	0.01	0.94	0.04	0.01	0.02	100.00	Albite

Figure 80: Backscatter electron image (top) and X-ray elemental analyses (as oxide weight percentages) of various locations (at the tips of callouts) at the altered interior surface end of Core C1. Paste compositions are given in the Table.

COARSE AGGREGATES

Coarse aggregate particles in all four cores are compositionally similar crushed schist and gneiss having nominal maximum sizes of 3/4 in. (19 mm). Particles are dense, hard, angular, equidimensional to elongated, well-graded-, and well-distributed across the thickness of the tank wall (i.e., the depths of the cores).

A few crushed stone particles show dark weathering rims that are not indicative of any deleterious reactions in the particles but rather innocuous interactions during storage in the aggregate stockpile.

Particles show characteristic parallel alignment of quartzo-feldspathic and micaceous minerals defining the schistose and banded (gneissose) textures.

There is no evidence of any deleterious reactions of coarse aggregate particles found in the cores even in the interior ends of the tank wall where chemical alterations of paste have occurred to the point of exposing the near-surface aggregate particles.

FINE AGGREGATES

Fine aggregates are compositionally similar natural siliceous sands of nominal maximum sizes 3/8 in. (9.5 mm) consisting of major amount of quartz and quartzite and subordinate amounts of granite, feldspar, and other siliceous rocks.

Fine aggregate particles are angular (due to some light crushing) to subangular to subrounded, dense, hard, equidimensional to elongated, unaltered, uncoated, and uncracked.

There is no evidence of alkali-aggregate reactions or any other potentially deleterious reactions except a few brown opaline chert particles that have shown internal microcracking (Figures 72, 73, and 78).

Properties and Compositions of Aggregates	Cores C1 through C4
Coarse Aggregate	
Types	Crushed schist and gneiss
Nominal maximum size (in.)	3/4 in. (19 mm)
Rock Types	Quartzo-feldspathic and micaceous (muscovite, biotite) minerals defining the schistose and banded (gneissose) textures
Angularity, Density, Hardness, Color, Texture, Sphericity	Angular, equidimensional to elongated, well-graded, and well-distributed. A few crushed stone particles show dark weathering rims.
Cracking, Alteration, Coating	Unaltered, Uncoated, and Uncracked
Grading & Distribution	Well-graded, well-distributed
Soundness	Sound
Alkali-Aggregate Reactivity	None

Properties and Compositions of Aggregates	Cores C1 through C4
Fine Aggregates	
Types	Natural siliceous sands
Nominal maximum size (in.)	3/8 in. (9.5 mm)
Rock Types	Major amount of quartz and quartzite and subordinate amounts of granite, feldspar, and other siliceous rocks
Cracking, Alteration, Coating	Clear to gray, subangular to rounded, dense, hard, equant to elongated
Grading & Distribution	Well-graded and Well-distributed
Soundness	Sound, except a few opaline chert particles that have shown internal microcracking
Alkali-Aggregate Reactivity	None except perhaps in some opaline chert particles (Figures 72, 73, and 78)

Table 2: Properties of coarse and fine aggregates of concretes in Cores 1 through 4.

PASTE

Properties and composition of hardened cement pastes in four cores are summarized in Table 3.

Paste is compositionally similar moderately dense, and moderately hard in the interior bodies except visible discoloration and alteration at the interior surface ends to depths of less than 5 mm to 10 mm consisting of a black altered zone at the exposed interior wall surface followed by a mixed oxidized (stained) and carbonated brown discolored zone and a gray discolored zone followed by a carbonated zone.

Paste at the exterior surface ends of the cores show deep carbonation due to interaction with atmospheric carbon dioxide, which are measured to be 48 mm in Core 1 to 56 mm in Core 2 to only 14 mm in Core 4, whereas corresponding carbonation depths from the interior surfaces are only 5 mm in Core 1, 10 mm in Core 2, and 7 mm in Core 4. Freshly fractured surfaces have subvitreous lusters and subconchoidal textures.

Residual and relict Portland cement particles are present and estimated to constitute 10 to 12 percent of the paste volumes in the interior bodies.

Distributed throughout the paste are a few fine, spherical, clear, dark brown to black glassy particles of fly ash having the fineness of Portland cement. Hydration of Portland cement is normal.

Lining the walls of some entrapped air voids especially towards the interior surface ends are secondary ettringite deposits that are indicative of the prolonged presence of moisture in the concrete during service due to penetration of containment solutions from the interior tank wall.

The textural and compositional features of pastes are indicative of cementitious materials contents estimated to be equivalent to 6 to 6 1/2 bags of Portland cement per cubic yard of which 10 to 15 percent is estimated to be fly ash and water-cementitious materials ratios similar in all four cores and estimated to be 0.45 to 0.50.

Properties and Compositions of Paste	Cores C1 through C4
Color, Hardness, Porosity, Luster	Compositionally similar moderately dense, and moderately hard in the interior bodies except visible discoloration and alteration at the interior surface ends to depths of less than 5 mm to 10 mm consisting of a black altered zone at the exposed interior wall surface followed by a mixed oxidized (stained) and carbonated brown discolored zone and a gray discolored zone followed by a carbonated zone. Freshly fractured surfaces have subvitreous lusters and subconchoidal textures
Residual Portland Cement Particles	Normal, 6 to 8 percent by paste volume
Calcium hydroxide from cement hydration	Normal, 10 to 14 percent by paste volume
Pozzolans, Slag, etc.	Fly ash having the fineness of Portland cement
Water-cementitious materials ratio (*w/cm*), estimated	0.45 to 0.50 in the interior bodies (similar in all four cores)
Cementitious materials content (bags per cubic yard)	6 to $6^{1}/_{2}$ bags per cubic yard, of which 10 to 15 percent is estimated to be fly ash
Secondary Deposits	Secondary ettringite deposits on air voids due to prolonged presence of moisture during service
Depth of Carbonation, mm	Paste at the exterior surface ends of the cores show deep carbonation due to interaction with atmospheric carbon dioxide, which are measured to be 48 mm in Core 1 to 56 mm in Core 2 to only 14 mm in Core 4, whereas corresponding carbonation depths from the interior surfaces are only 5 mm in Core 1, 10 mm in Core 2, and 7 mm in Core 4
Microcracking	Except fine shrinkage microcracks at the interior and exterior surface ends, interior bodies of the cores are free from any microcracking due to any deleterious reactions
Aggregate-paste Bond	Tight
Bleeding, Tempering	None
Chemical deterioration	None

Table 3: Proportions and composition of hardened cement paste in four cores.

AIR

Concrete in all four cores are non-air-entrained having air contents estimated to be 1 to 2 percent. Figures 42 to 58 show micrographs of lapped cross sections of cores where lack of any intentionally introduced entrained air except a few accidentally formed entrapped air are found.

X-RAY DIFFRACTION STUDIES OF ALTERED AND UNALTERED ZONES

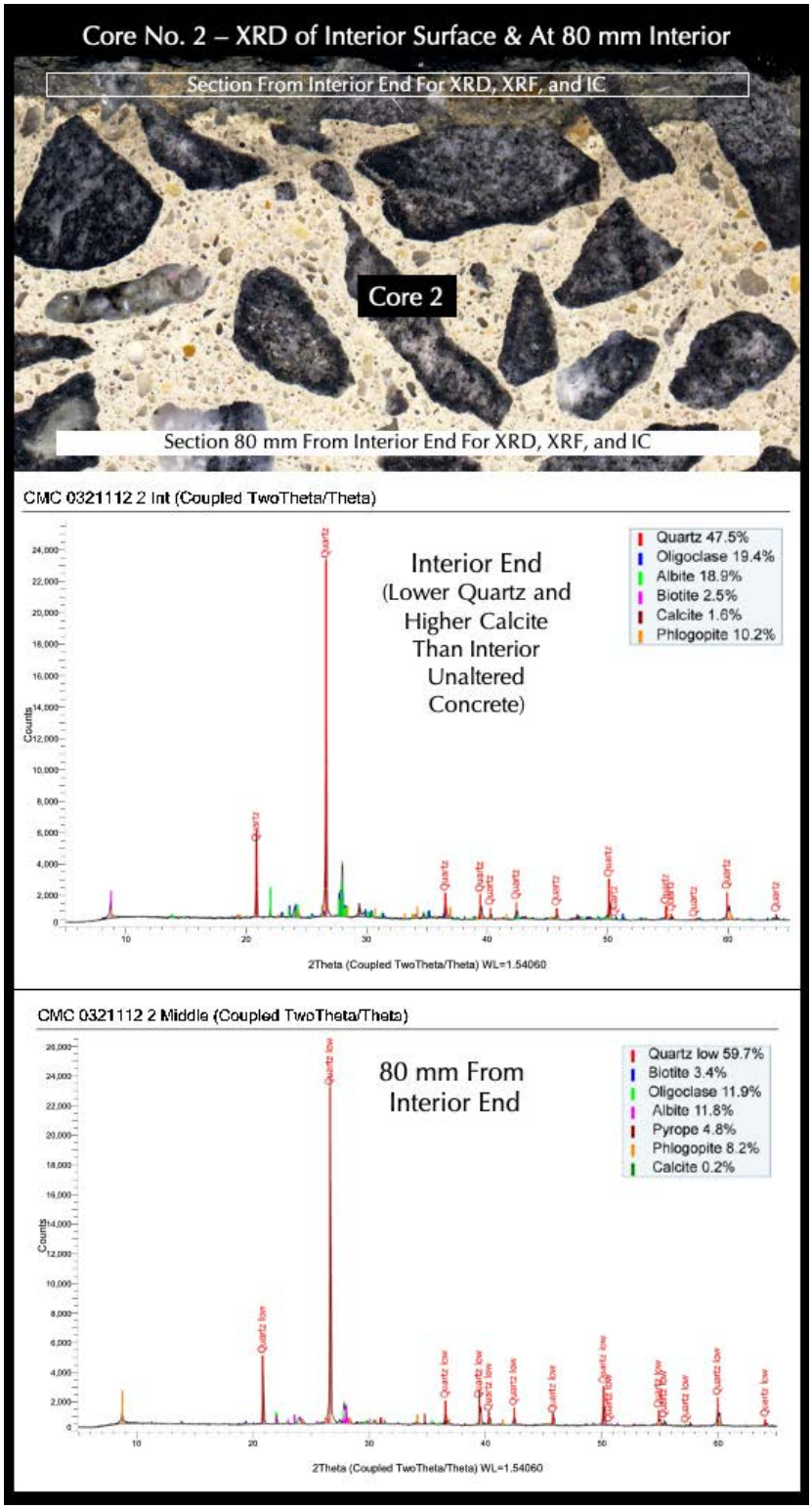

Figure 81: X-ray diffraction patterns of the altered interior surface end (top) and 80 mm inside from the interior end (bottom) of Core C2 showing relatively lower quartz and higher calcite at the altered end than the unaltered interior concrete.

X-RAY FLUORESCENCE STUDIES OF ALTERED AND UNALTERED ZONES

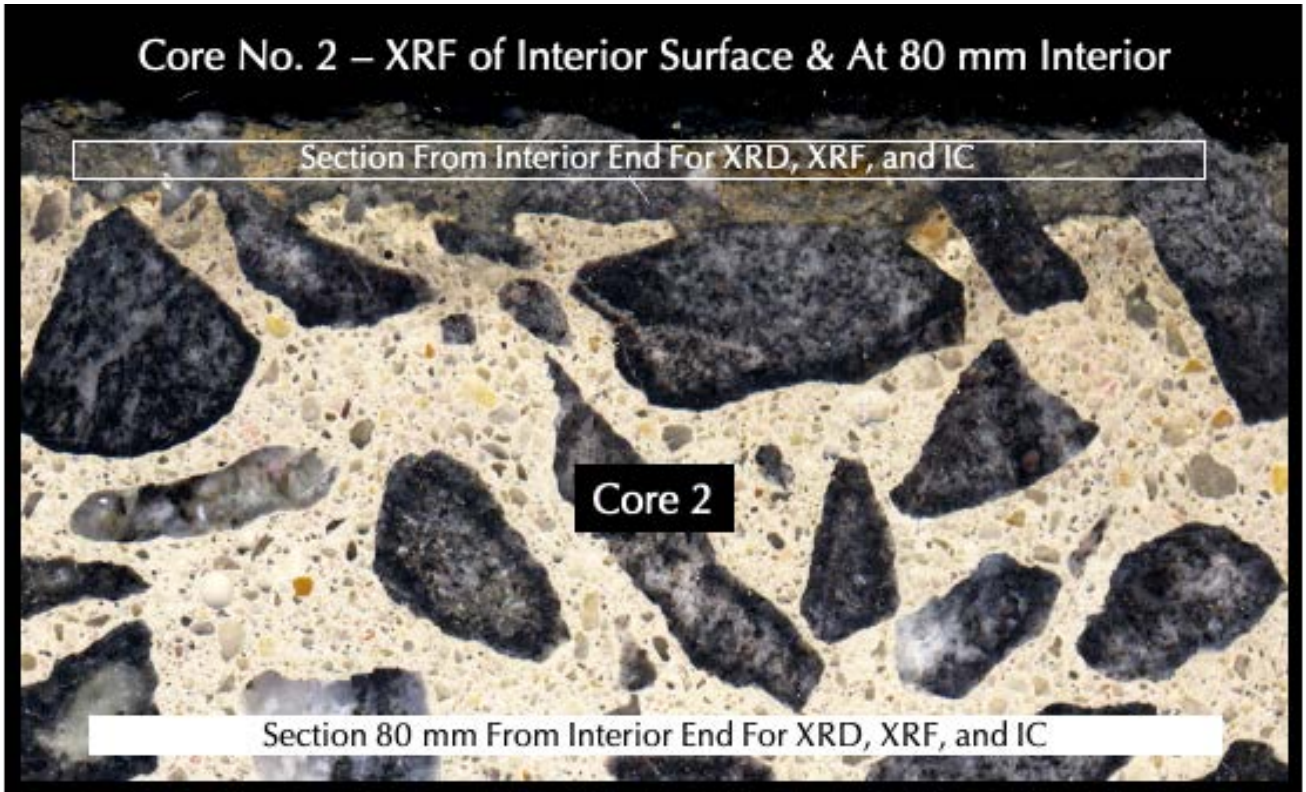

	SiO2	Al2O3	CaO	MgO	Na2O	K2O	Fe2O3	TiO2	P2O5	SO3	Balance	Total
Interior End	59.8	8.36	6.8	2.4	2.42	1.1	4.66	1.16	0.26	1.93	11.1	100
80 mm from Interior End	69.1	6.64	8.1	1.75	1.32	1.1	3.39	0.65	0.13	0.24	7.54	100

Lower Silica (and corresponding enrichment of oxides of Al, Ca, Mg, Na, Fe, and Ti) and higher LOI in the Interior End is consistent with XRD Determination of Lower Quartz and Higher Calcite; High sulfate (as SO_3) in the Interior End Did Not Detect Any Specific Sulfate Phase in XRD

Figure 82: Results of XRF studies of the altered interior surface end and 80 mm inside from the interior end of Core C2 showing lower silica and mainly noticecably higher sulate at the altered zone than the unaltered interior. High sulfate at the altered zone is also reflected in subsequent studies of ion chromatography of water-soluble filtrates indicating a sulfate exposure from the tank containment solutions.

WATER-SOLUBLE ANION CONTENTS

Water-soluble chloride, sulfate and other anion contents from the altered interior end and mid-depth location about 80 mm from the interior end of Cores C1 and C2 are given below. Both cores showed higher sulfate contents at the altered interior ends due to exposures to tank's containment solutions.

Core	Depth (mm)	Chloride Content from Ion Chromatography (% Chloride by mass of concrete)	Sulfate Content from Ion Chromatography (% Sulfate by mass of concrete)
C1	Interior End	0.053	0.385
	80 mm From Interior End	0.025	0.262
C2	Interior End	0.020	0.434
	80 mm From Interior End	0.025	0.334

Table 4: Results of water soluble chloride and sulfate contents in the altered zones and in unaltered interiors of Cores C1 and C2 determined by ion chromatography.

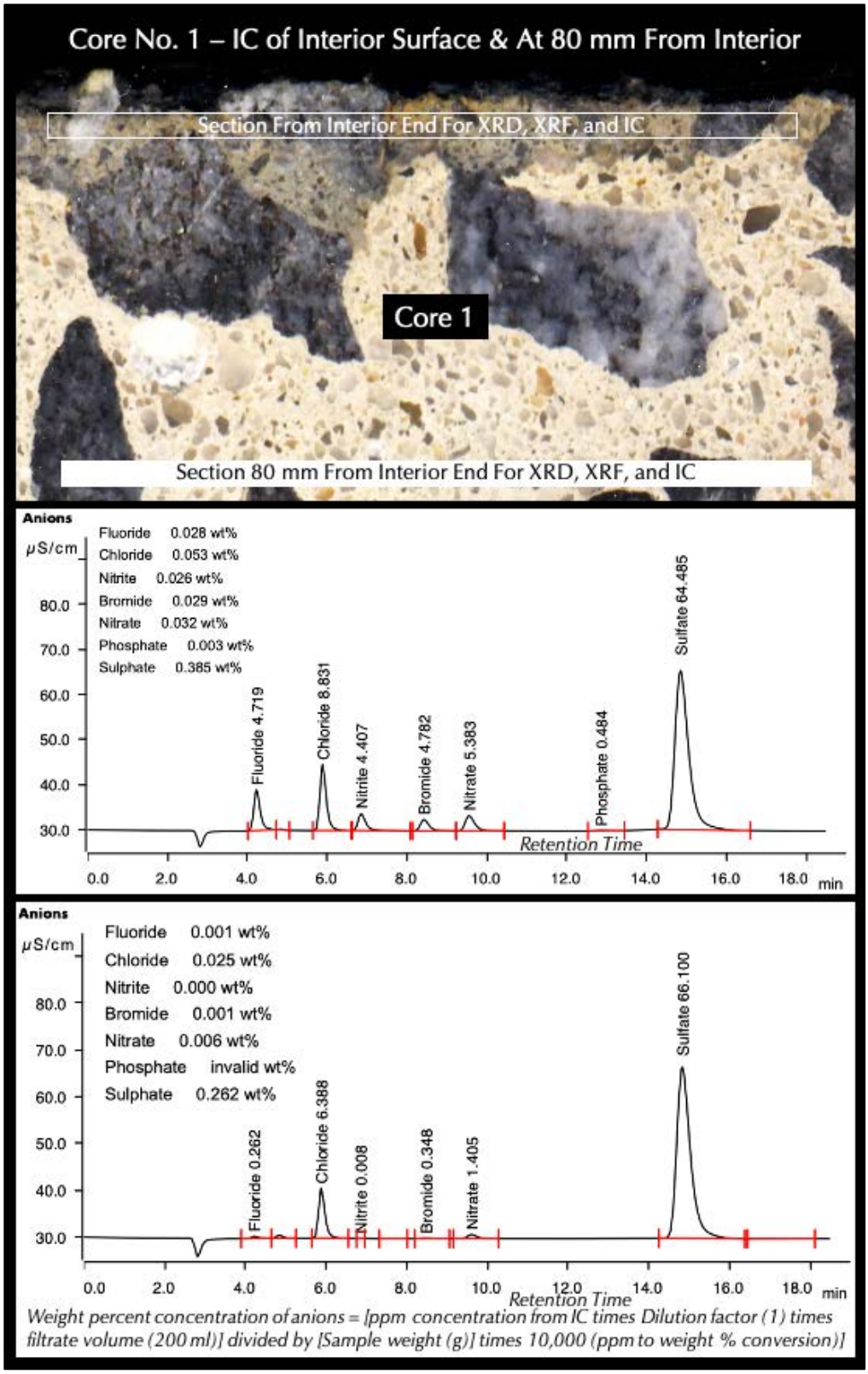

Figure 83: Anion chromatograms of water-soluble salts in the interior wall of tank and at mid-depth location in Core C1 after digesting about a gram of pulverized mortar from each sample in deionized water for 30 minutes at a temperature below boiling, followed by continued digestion in water at the ambient laboratory condition for 24 hours. The filtrate was analyzed by ion chromatography.

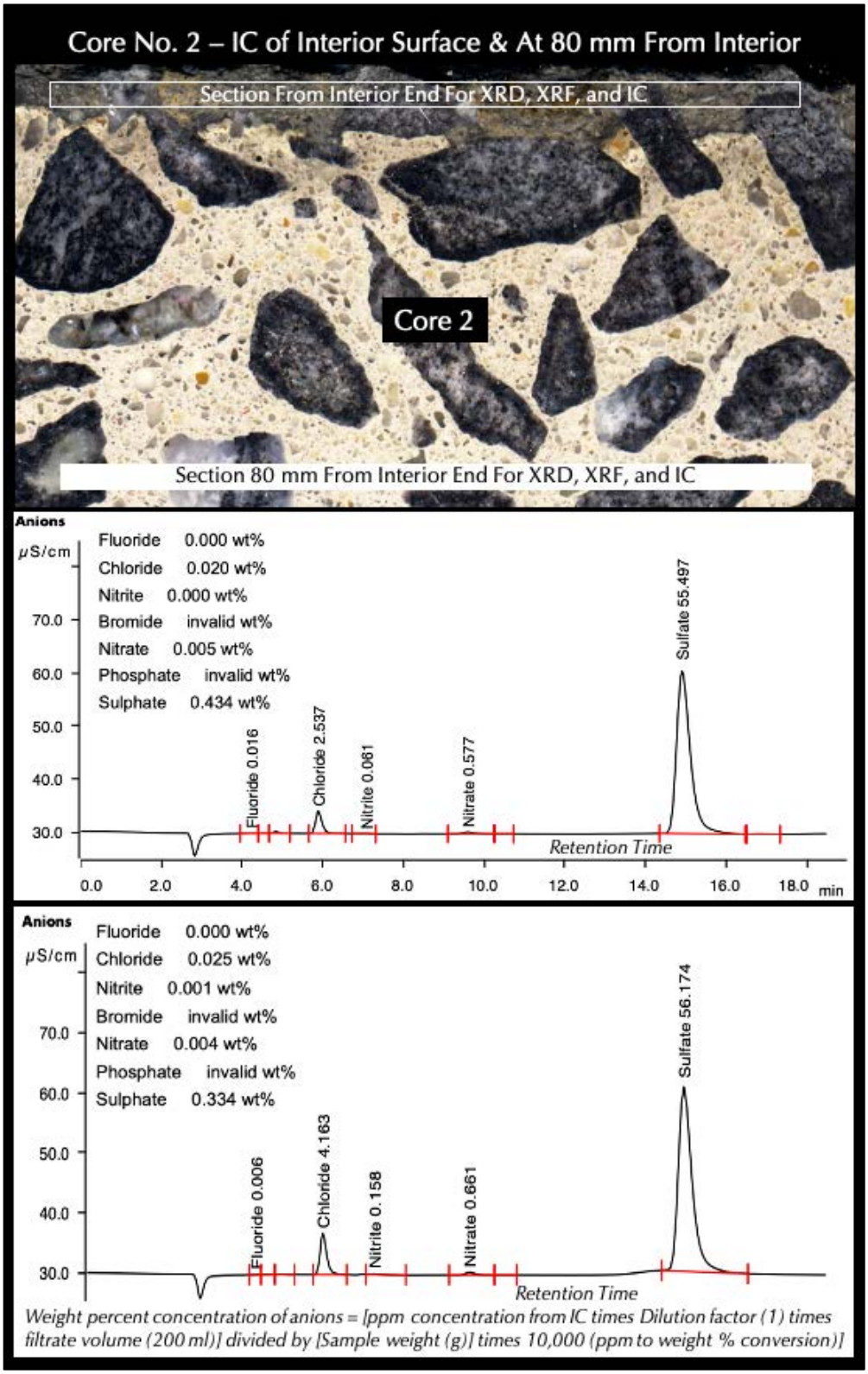

Figure 84: Anion chromatograms of water-soluble salts in the interior wall of tank and at mid-depth location in Core C2 after digesting about a gram of pulverized mortar from each sample in deionized water for 30 minutes at a temperature below boiling, followed by continued digestion in water at the ambient laboratory condition for 24 hours. The filtrate was analyzed by ion chromatography.

THERMAL ANALYSES OF ALTERED AND UNALTERED ZONES

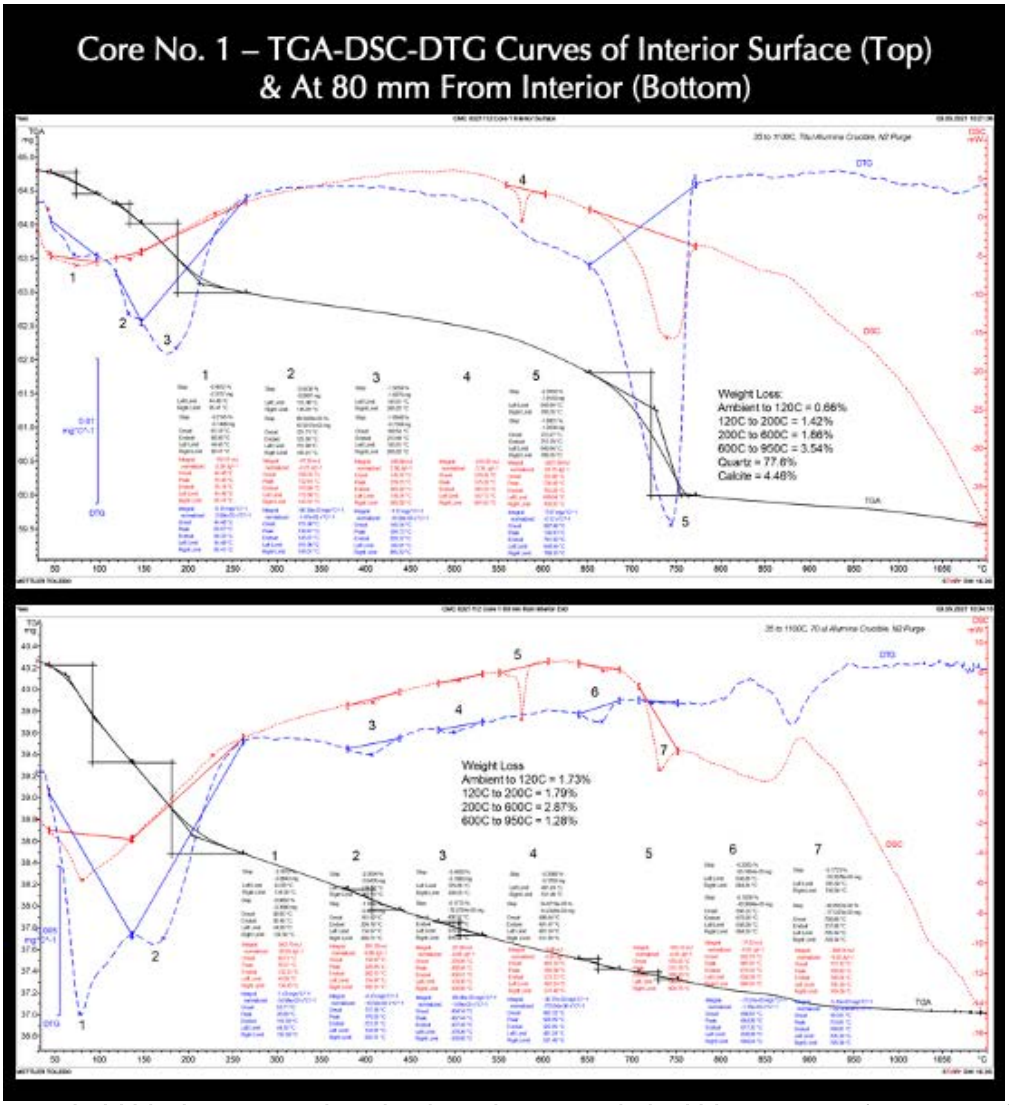

Figure 85: TGA (in bold black), DSC (in dotted red), and DTG (in dashed blue) curves of interior surface end (top) and at 80 mm depth from the interior surface end (bottom) in Core C1 showing losses in weights due to decompositions (loss of water and carbon dioxide) of various phases during controlled heating in a Mettler-Toledo's simultaneous TGA/DSC 1 unit from 30ºC to 1000ºC in a ceramic crucible (alumina 70µl, no lid) at a heating rate of 10ºC/min in a nitrogen purge at a rate of 75 mL/min. Dehydration and decarbonation reactions are marked as endothermic peaks in the DTG curve, whereas alpha to beta-form polymorphic transition of quartz is marked at the characteristic temperature of 573ºC in the DSC curve.

In the DTG curve, losses in weights are detected at (i) from the loss of free water (e.g., Peak #1 in both plots), (ii) loss of bound water (e.g., Peak #2 and 3 in top and Peak #2 in bottom), and (iii) dehydroxylation of hydrated phases (e.g., Peak #3 and 4 in bottom). DSC curve in Peak #4 in top and Peak #5 in bottom plot shows polymorphic transition from alpha to beta form of quartz around 575ºC from silica (quartz) sand.

Notice the difference in thermal plots of altered zone at the interior surface end in the top plot and mid-depth location away from the altered zone in the bottom plot where the bottom plot of more pristine unaltered concrete shows more hydrous phases appeared in the DTG curve than the altered zone.

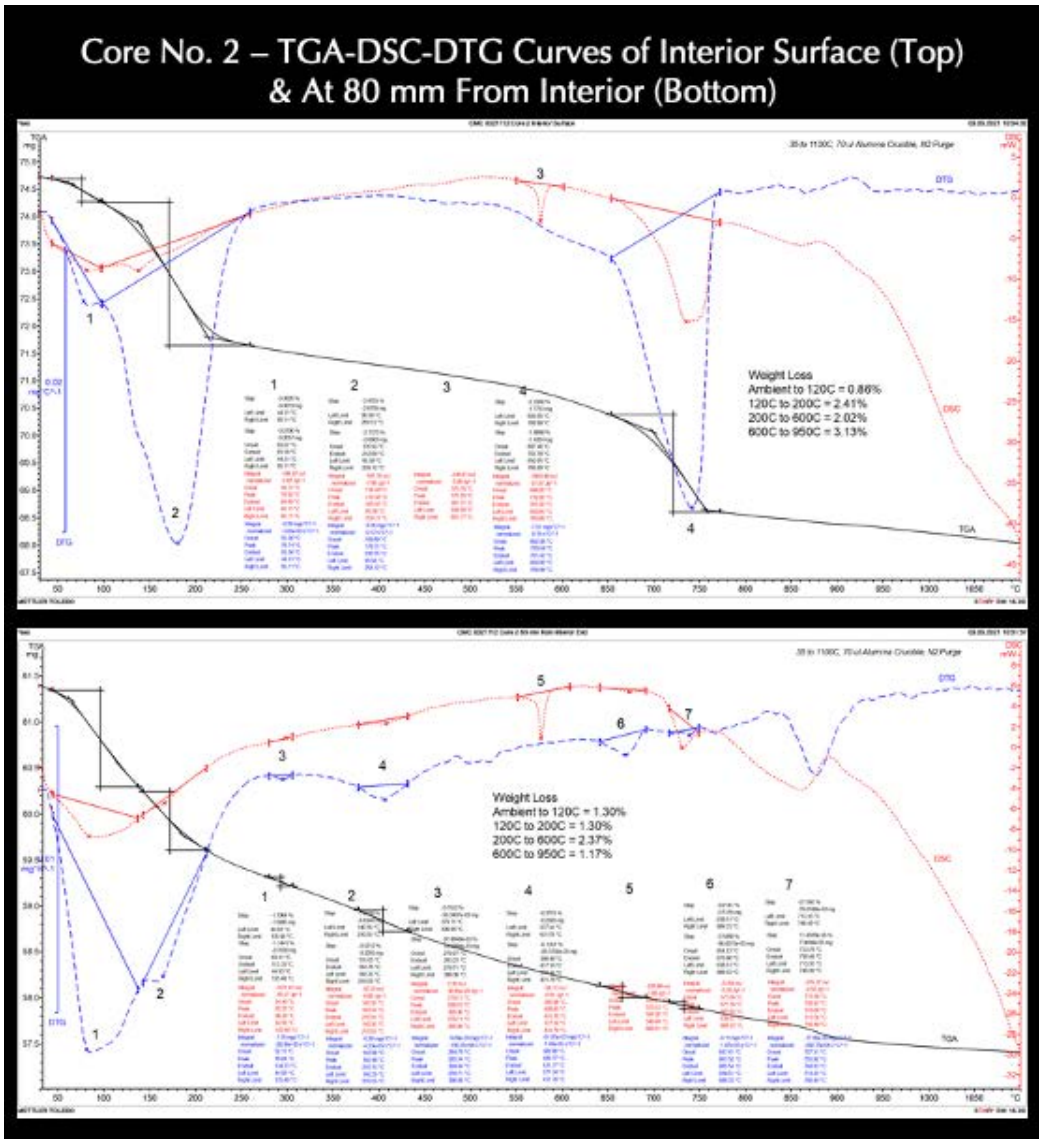

Figure 86: TGA (in bold black), DSC (in dotted red), and DTG (in dashed blue) curves of interior surface end (top) and at 80 mm depth from the interior surface end (bottom) in Core C2 showing losses in weights due to decompositions (loss of water and carbon dioxide) of various phases during controlled heating in a Mettler-Toledo's simultaneous TGA/DSC 1 unit from 30ºC to 1000ºC in a ceramic crucible (alumina 70µl, no lid) at a heating rate of 10ºC/min in a nitrogen purge at a rate of 75 mL/min. Dehydration and decarbonation reactions are marked as endothermic peaks in the DTG curve, whereas alpha to beta-form polymorphic transition of quartz is marked at the characteristic temperature of 573ºC in the DSC curve.

In the DTG curve, losses in weights are detected at (i) from the loss of free water (e.g., Peak #1 in both plots), (ii) loss of bound water (e.g., Peak #2 and 3 in top and Peak #2 in bottom), and (iii) dehydroxylation of hydrated phases (e.g., Peak #3 and 4 in bottom). DSC curve in Peak #4 in top and Peak #5 in bottom plot shows polymorphic transition from alpha to beta form of quartz around 575ºC from silica (quartz) sand.

Notice the difference in thermal plots of altered zone at the interior surface end in the top plot and mid-depth location away from the altered zone in the bottom plot where the bottom plot of more pristine unaltered concrete shows more hydrous phases appeared in the DTG curve than the altered zone.

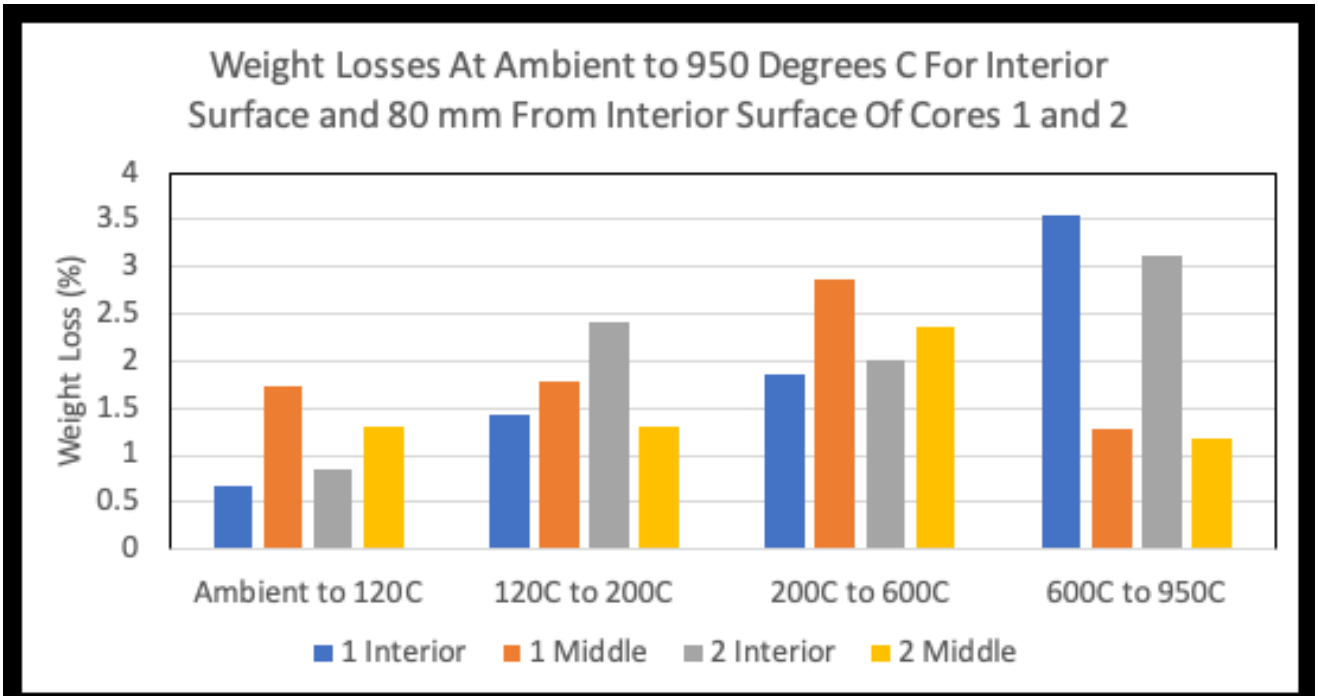

Core	Ambient to 120C	120C to 200C	200C to 600C	600C to 950C
1 Interior	0.66	1.42	1.86	3.54
1 Middle	1.73	1.79	2.87	1.28
2 Interior	0.86	2.41	2.02	3.13
2 Middle	1.3	1.3	2.37	1.17

Figure 87: The altered zones at the Interior ends of both cores show lower free water contents than the interior unaltered zones but the carbonate contents at the altered zones are noticeably higher from significantly greater loss of mass from decomposition of carbonates at 600ºC to 950ºC, which is consistent with overall carbonated nature of paste at the altered zones. The bound or structural water from calcium silicate hydrate phase of cement hydration is higher in the interior mid-depth unaltered zones in both cores than the altered ends due to decomposition of paste, which is consistent with observed alterations of paste from optical microscopy.

DISCUSSIONS

LIMITED DEPTHS OF ALTERATION OF CONCRETE AT THE INTERIOR TANK WALL

The interior tank wall surface in the four cores show clear evidence of alterations due to interactions with tank's containment solutions. Such interactions have created discoloration, softening of paste, sometimes microcracking, carbonation, leaching, oxidation (staining), etc., which are often present as bands of discolored altered pastes from black paste at the interior wall surface to reddish-brown oxidized and carbonated zone to gray and beige carbonated zone. Interfaces between the zones and between the altered and interior unaltered zones are sharp.

Depths of alteration of such zones, however, are shallow in all four cores, measured to be: (a) 5 to 7 mm in Core C1 occurring as a dark gray to black altered layer sometimes with an inner brown layer at the interior wall (Figures 24 to 27, 40); (b) 7 to 8 mm in Core C2, again occurring as a black to dark gray altered layer in the interior wall often with thin brown layer at the interior wall (Figures 30 to 33, 40); and (c) 7 mm from interior wall of Core C4 where instead of a black altered layer mostly beige to brown carbonated layer is seen (Figures 36 to 39, 40). Figure 40 summarizes variations in depths and appearances of these layered zones of concrete at the interior tank wall surface represented in Cores C1, C2, and C4 due to interactions with the containment solutions of the tank.

Evidence of interaction of containment solution with the altered zones in the interior tank wall is also reflected in chemical analyses where altered zones showed enrichment in sulfate both in XRF studies and in ion chromatography of water-solution sulfates from the altered zones.

Concrete beyond these maximum 10 mm of the altered interior surfaces of tank wall in Cores C1, C2, and C4 are sound and present in good conditions without any alteration.

NOTICEABLE DEPTHS OF CARBONATION OF CONCRETE AT THE EXTERIOR TANK WALL

By contrast the exterior tank wall surface represented in Cores C1, C2, and C4 show noticeable depths of carbonation, despite the presence of a thin (< 1 mm thickness) protective cementitious coating, indicating prolonged interaction of the tank's exterior wall with the atmospheric carbonation dioxide prior to the installation of the protective cementitious coat. Paste at the exterior surface ends of the cores show deep carbonation due to interaction with atmospheric carbon dioxide, which are measured to be 48 mm in Core C1 to 56 mm in Core C2 to only 14 mm in Core C4, whereas corresponding carbonation depths from the interior surfaces are only 5 mm in Core C1, 10 mm in Core C2, and 7 mm in Core C4.

SOUND INTERIOR CONCRETE OF THE TANK WALL

Sandwiched between the 10 mm altered interior tank wall and almost 56 mm carbonated exterior tank wall, the interior bodies of concrete in Cores C1, C2, and C4 are all present in sound and serviceable condition. Lack of air entrainment can cause some freezing-related issues, which is, however, absent probably due to the vertical orientation of the structure preventing any moisture saturation during freezing. Evidence of secondary ettringite

deposit in air voids, however, indicates prolonged presence of moisture in the concrete from penetration of containment solutions of tanks, which has not introduced any freezing-related deterioration of the non-air-entrained concrete in the tank wall.

FUTURE SERVICEABILITY OF THE TANK

Based on detailed petrographic examinations, determination of shallow depths of alterations of concrete from the interior tank wall especially for cores drilled from locations, which were in contact with the containment solutions, relatively sound conditions of concrete towards the exterior wall surface even in the deep carbonated portions, sound conditions of unaltered interior concrete, the tank wall is judged to be serviceable for its future intended purpose. Perhaps removal of the altered, discolored portions of interior wall with a fresh new repair coat will extend its life. The exterior cementitious coating is only 1 mm in thickness, with some peeling at some locations in the field photos but is important to mitigate future access of atmospheric carbonation especially since the concrete showed extensive carbonation from the exterior wall end which has happened prior to the placement of the protective coating. Deep carbonation from the exterior end can cause carbonation-induced corrosion of steel in concrete, where the importance of having such a protective coating as seen and its well adherence to the concrete wall are paramount.

REFERENCES

ASTM C 856 “Standard Practice for Petrographic Examination of Hardened Concrete,” Vol. 4.02, ASTM International, West Conshohocken, PA, 2017.

ASTM C 1218 “Standard Test Method for Water-Soluble Chloride in Mortar and Concrete,” Vol. 4.02, ASTM International, West Conshohocken, PA, 2017.

ASTM D 4327, “Standard Test Method for Anions in Water by Suppressed Ion Chromatography,” Vol. 11.01, ASTM International, West Conshohocken, PA, 2019.

Jana, D., “Sample Preparation Techniques in Petrographic Examinations of Construction Materials: A State-of-the-Art Review,” *Proceedings of the 28th Conference on Cement Microscopy (ICMA)*, 2006, pp. 23-70.

✪ ✪ ✪ END OF TEXT ✪ ✪ ✪

END OF REPORT[1]

[1] The CMC logo is made using a lapped polished section of a 1930's concrete from an underground tunnel in the U.S. Capitol.